



**TIM LINDEN**

**PULSARS ARE CRITICAL SOURCES OF COSMIC-  
RAYS AND TURBULENCE AT TEV ENERGIES**

**Astronomy Department Seminar  
Columbia University  
December 13, 2018**



**THE OHIO STATE UNIVERSITY**

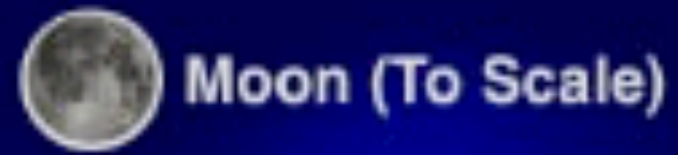
CENTER FOR COSMOLOGY AND  
ASTROPARTICLE PHYSICS







# HAWC OBSERVATIONS OF GEMINGA AND MONOGEM



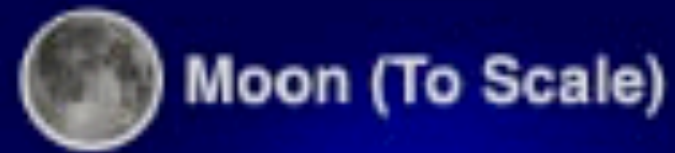
- Angular Resolution

Geminga

PSR B0656+14



# HAWC OBSERVATIONS OF GEMINGA AND MONOGEM



- Angular Resolution

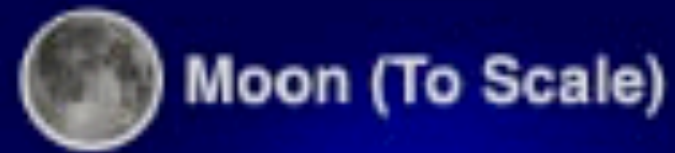
Geminga

PSR B0656+14

- Geminga
  - $4.9 \times 10^{-14} \text{ TeV}^{-1} \text{ cm}^{-2} \text{ s}^{-1}$  (7 TeV)
  - $1.4 \times 10^{31} \text{ TeV s}^{-1}$  (7 TeV)
  - 25 pc extension
  - 300 kyr



# HAWC OBSERVATIONS OF GEMINGA AND MONOGEM



- Angular Resolution

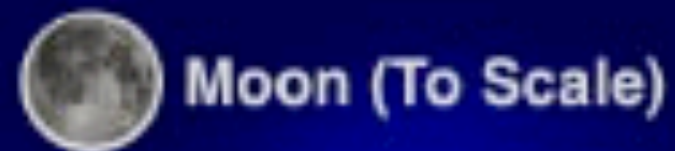
Geminga

PSR B0656+14

- Monogem
  - $2.3 \times 10^{-14} \text{ TeV}^{-1} \text{ cm}^{-2} \text{ s}^{-1}$  (7 TeV)
  - $1.1 \times 10^{31} \text{ TeV s}^{-1}$  (7 TeV)
  - 25 pc extension
  - 110 kyr !



# HAWC OBSERVATIONS OF GEMINGA AND MONOGEM



- Angular Resolution

Geminga

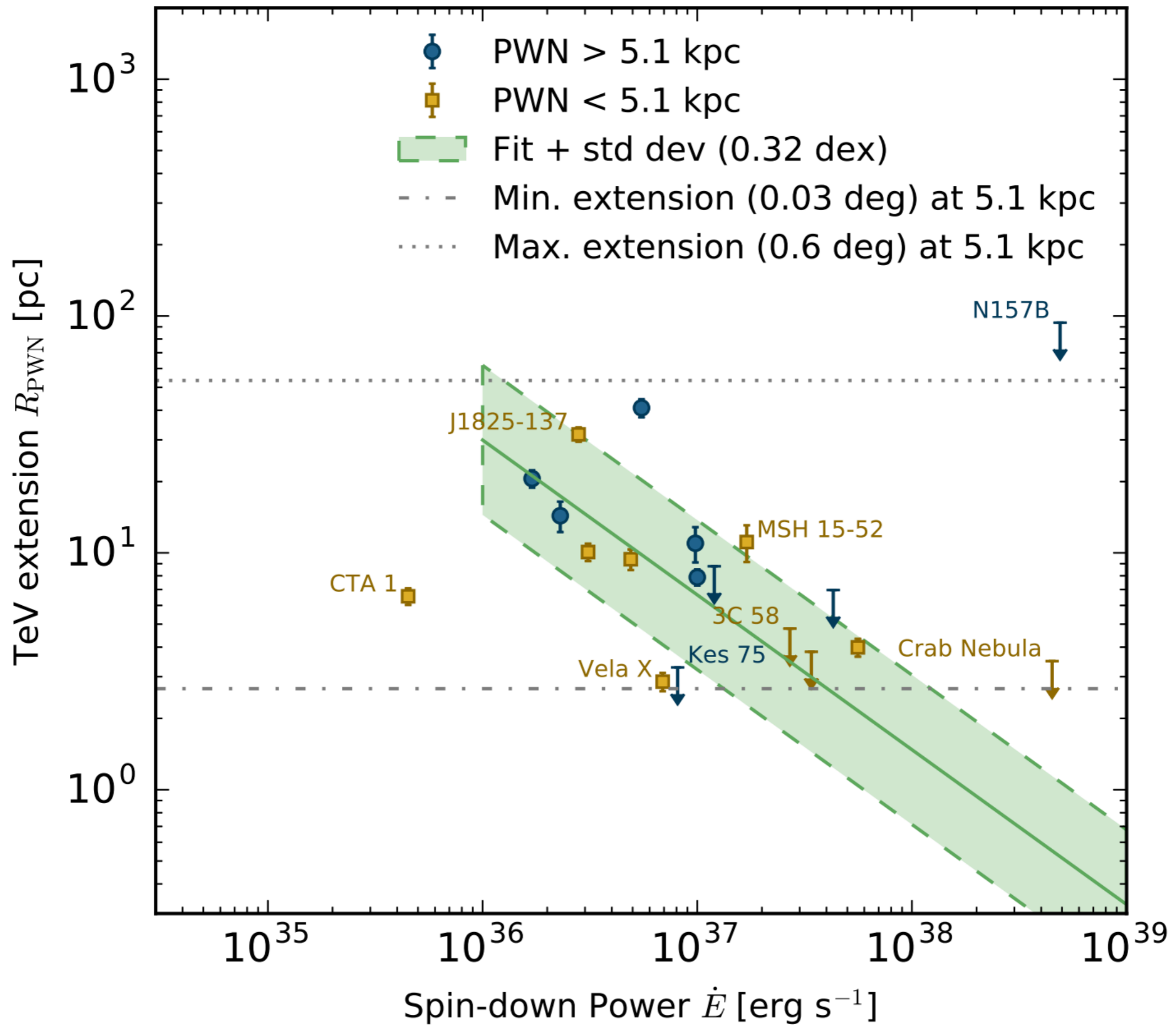
PSR B0656+14

- Emission is:
  - Very hard spectrum
  - Does not trace gas
  - **Almost certainly leptonic.**











# TeV HALOS



Moon (To Scale)

- Angular Resolution

———— 10 pc (Geminga distance)

Geminga

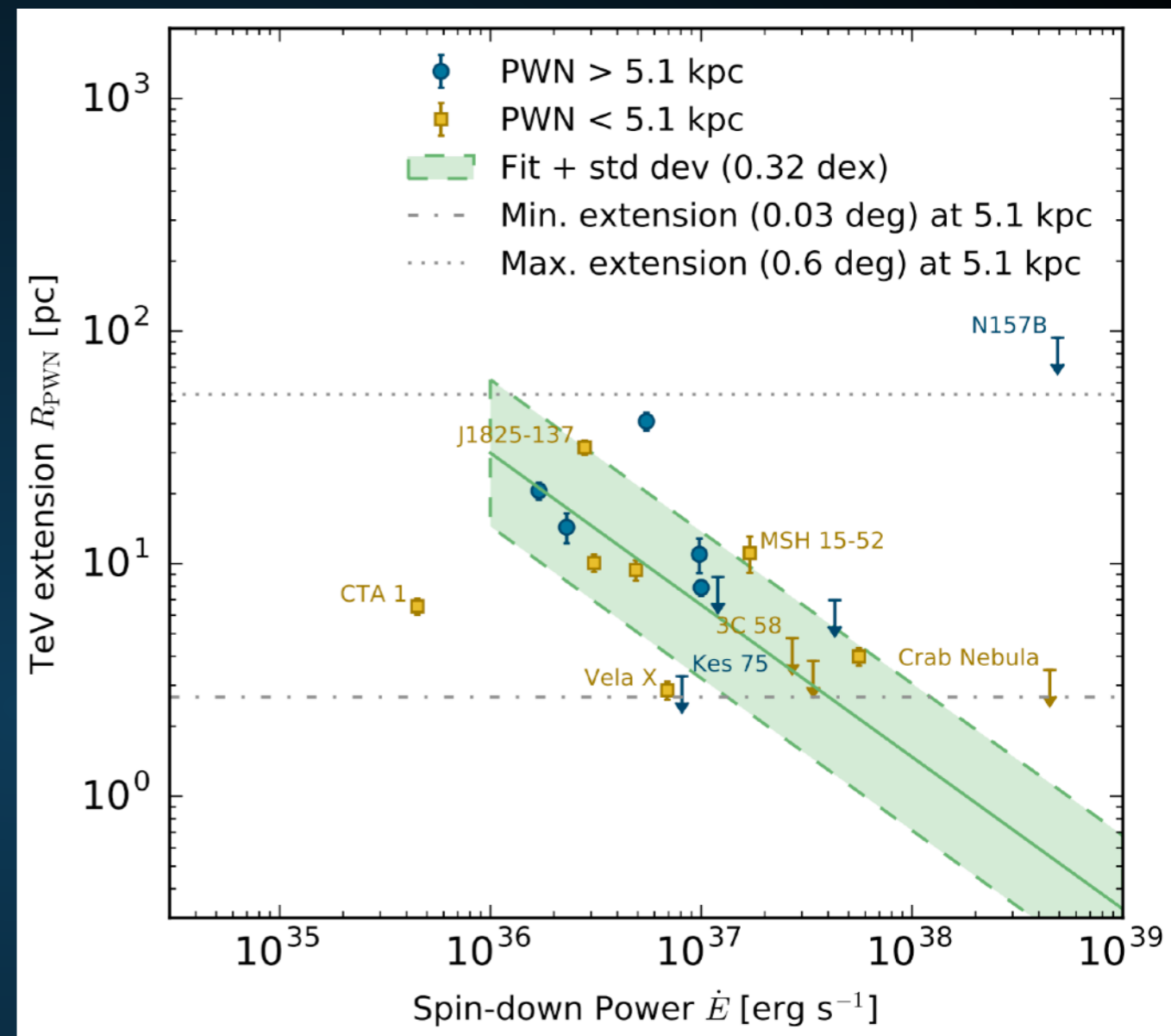
**I will call these sources "TeV halos"**

PSR B0656+14  
(Monogem)





- They are much larger than the PWN.
- Especially at low-energies.

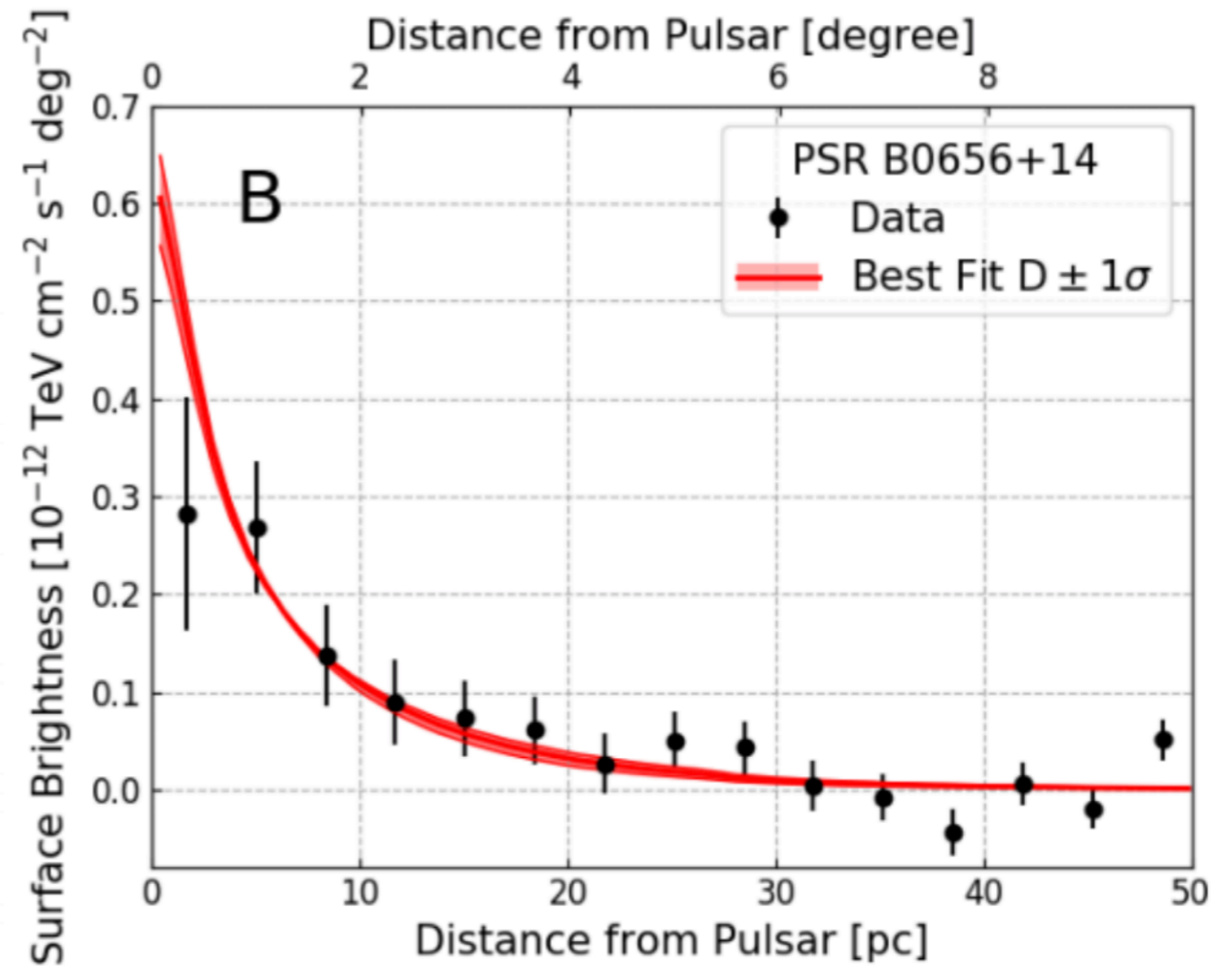
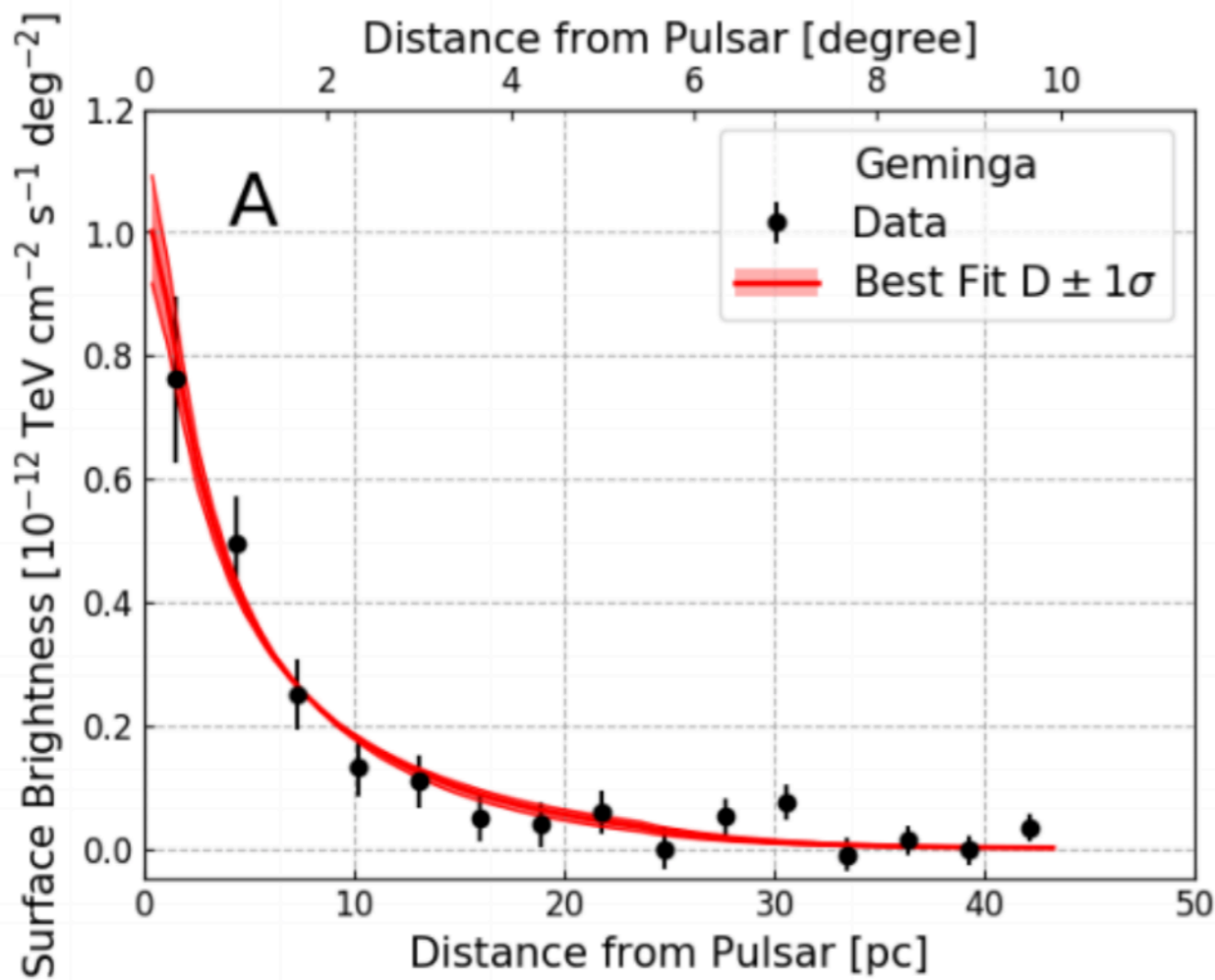


**NOTE: This has the opposite energy dependence as the X-Ray PWN.**

$$R_{\text{PWN}} \simeq 1.5 \left( \frac{\dot{E}}{10^{35} \text{ erg/s}} \right)^{1/2} \times \left( \frac{n_{\text{gas}}}{1 \text{ cm}^{-3}} \right)^{-1/2} \left( \frac{v}{100 \text{ km/s}} \right)^{-3/2} \text{ pc}$$



# TEV HALOS



- These sources are much smaller than expected via diffusion through the standard ISM.

$$\tau_{\text{loss}} \approx 30 \text{ Kyr} \quad D_0 \approx 5 \times 10^{28} \text{ cm}^2 \text{ s}^{-1}$$
$$L = \sqrt{Dt} \approx 2000 \text{ pc}$$





SNR  
 $\sim O(100)$  pc

TeV Halo  
 $\sim O(10)$  pc

PWN  
 $\sim O(1)$  pc



---

**Rule of Thumb for Audience:** Always consider the assumptions behind bold claims.

**Rule of Thumb for Speaker:** Don't remind the audience to consider the assumptions behind bold claims.



## TeV HALOS - AN EMPIRICAL MODEL

---

- **Assume that every pulsar converts an equivalent fraction of its spin down power into gamma-rays, with the same spectrum as Geminga.**

$$\phi_{\text{TeV halo}} = \left( \frac{\dot{E}_{\text{psr}}}{\dot{E}_{\text{Geminga}}} \right) \left( \frac{d_{\text{Geminga}}^2}{d_{\text{psr}}^2} \right) \phi_{\text{Geminga}}$$

- **This statement is well supported:**
  - **Observed because they are the two closest sources.**
  - **Many similar HESS Sources**



# TEV HALOS - AN EMPIRICAL MODEL

- Use a generic model for pulsar luminosities
- $B_0 = 10^{12.5} \text{ G}$  ( $\pm 10^{0.3} \text{ G}$ )
- $P_0 = 0.3 \text{ s}$  ( $\pm 0.15 \text{ s}$ )
- Spindown Timescale of  $\sim 10^4 \text{ yr}$  (depends on  $B_0$ )
- Galprop model for supernova distances

**PsrPopPy: An open-source package for pulsar population simulations**

D. Bates<sup>1,2</sup>, D. R. Lorimer<sup>1,3</sup>, A. Rane<sup>1</sup> and J. Swiggum<sup>1</sup>

<sup>1</sup>Department of Physics and Astronomy, West Virginia University, Morgantown, WV, 26506 USA  
<sup>2</sup>Centre for Astrophysics, School of Physics and Astronomy, The University of Manchester, Manchester M13 9PL, UK  
<sup>3</sup>Astronomy Observatory, PO Box 2, Green Bank, WV 24944, USA

software package for the simulation of pulsar populations. The codebase includes a series of modules, which remain in their original programming language, and improving the simulation support.

---

**Implication I:**

**Most TeV gamma-ray sources are TeV halos.**



# TeV HALO NUMEROLOGY

2HWC Name	ATNF Name	Distance (kpc)	Angular Separation	Projected Separation	Expected Flux ( $\times 10^{-15}$ )	Actual Flux ( $\times 10^{-15}$ )	Flux Ratio	Expected Extension	Actual Extension	Age (kyr)	Chance Overlap
J0700+143	B0656+14	0.29	0.18°	0.91 pc	43.0	23.0	1.87	2.0°	1.73°	111	0.0
J0631+169	J0633+1746	0.25	0.89°	3.88 pc	48.7	48.7	1.0	2.0°	2.0°	342	0.0
J1912+099	J1913+1011	4.61	0.34°	27.36 pc	13.0	36.6	0.36	0.11°	0.7°	169	0.30
J2031+415	J2032+4127	1.70	0.11°	3.26 pc	5.59	61.6	0.091	0.29°	0.7°	181	0.002
J1831-098	J1831-0952	3.68	0.04°	2.57 pc	7.70	95.8	0.080	0.14°	0.9°	128	0.006

2HWC Name	ATNF Name	Distance (kpc)	Angular Separation	Projected Separation	Expected Flux ( $\times 10^{-15}$ )	Actual Flux ( $\times 10^{-15}$ )	Flux Ratio	Expected Extension	Actual Extension	Age (kyr)	Chance Overlap
J1930+188	J1930+1852	7.0	0.03°	3.67 pc	23.2	9.8	2.37	0.07°	0.0°	2.89	0.002
J1814-173	J1813-1749	4.7	0.54°	44.30 pc	243	152	1.60	0.11°	1.0°	5.6	0.61
J2019+367	J2021+3651	1.8	0.27°	8.48 pc	99.8	58.2	1.71	0.28°	0.7°	17.2	0.04
J1928+177	J1928+1746	4.34	0.03°	2.27 pc	8.08	10.0	0.81	0.11°	0.0°	82.6	0.002
J1908+063	J1907+0602	2.58	0.36°	16.21 pc	40.0	85.0	0.47	0.2°	0.8°	19.5	0.26
J2020+403	J2021+4026	2.15	0.18°	6.75 pc	2.48	18.5	0.134	0.23°	0.0°	77	0.01
J1857+027	J1856+0245	6.32	0.12°	13.24 pc	11.0	97.0	0.11	0.08°	0.9°	20.6	0.06
J1825-134	J1826-1334	3.61	0.20°	12.66 pc	20.5	249	0.082	0.14°	0.9°	21.4	0.14
J1837-065	J1838-0655	6.60	0.38°	43.77 pc	12.0	341	0.035	0.08°	2.0°	22.7	0.48
J1837-065	J1837-0604	4.78	0.50°	41.71 pc	8.3	341	0.024	0.10°	2.0°	33.8	0.68
J2006+341	J2004+3429	10.8	0.42°	80.07 pc	0.48	24.5	0.019	0.04°	0.9°	18.5	0.08

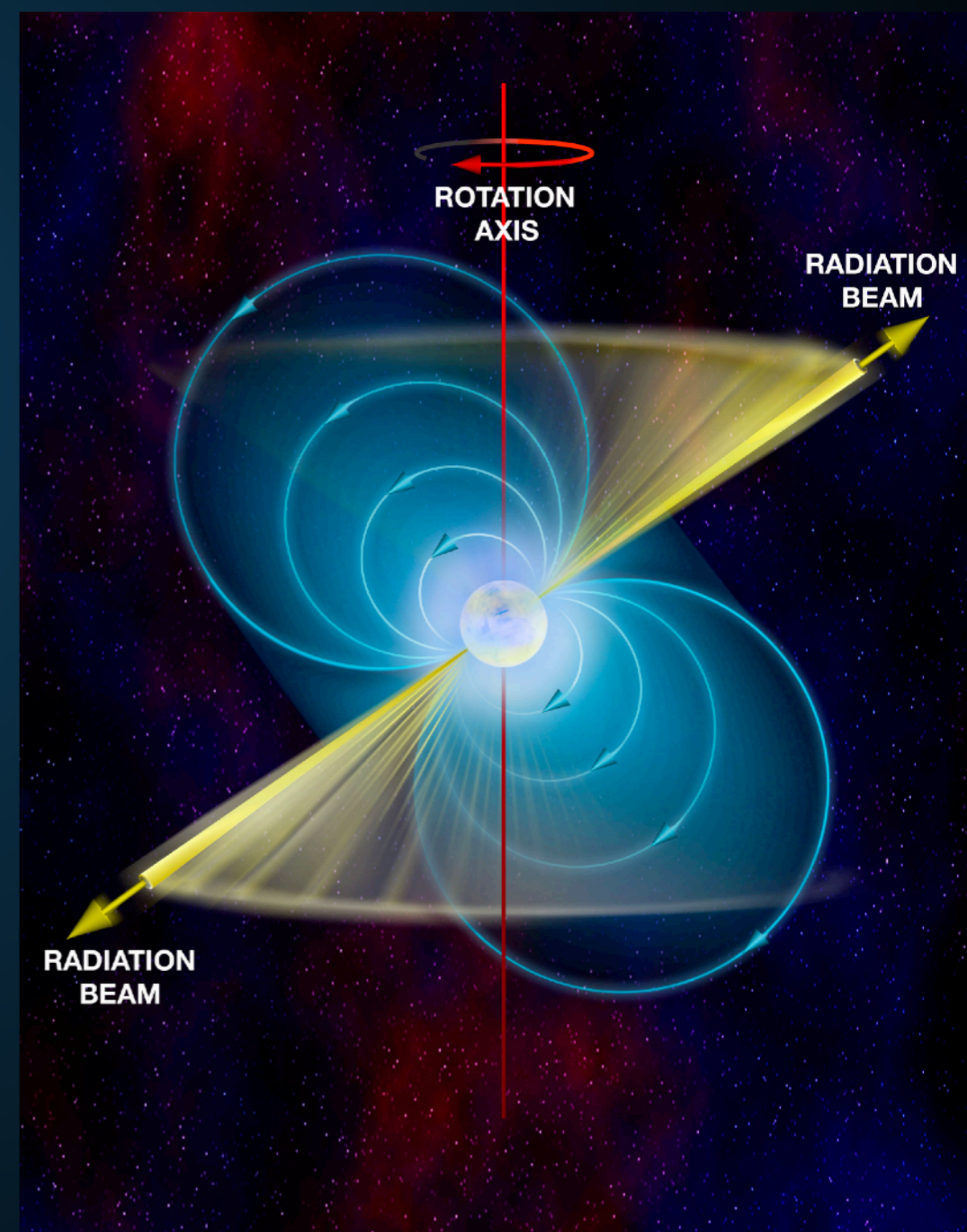
- **HAWC has observed 39 sources.**
- **5 are coincident with old ( $>100$  kyr) pulsars**
- **12 others coincident with young ( $<100$  kyr) pulsars**
  - **TeV emission may be contaminated by SNR**

- **Radio pulsars are beamed!**

- **Beaming fraction is small**

$$f = \left[ 1.1 \left( \log_{10} \left( \frac{\tau}{100 \text{ Myr}} \right) \right)^2 + 15 \right] \%$$

- **This varies between 15-30%.**
- **Most pulsars are unseen in radio!**





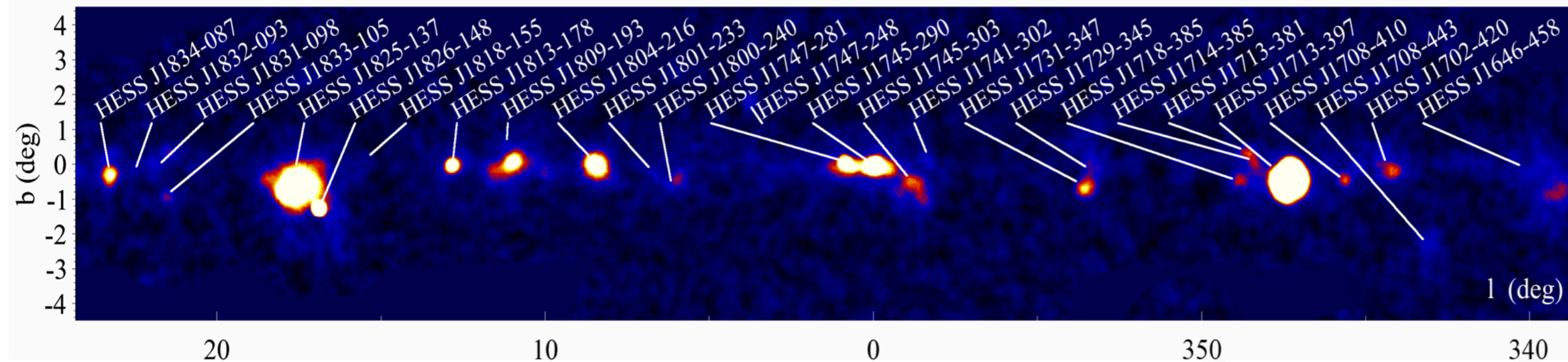
2HWC Name	ATNF Name	Distance (kpc)	Angular Separation	Projected Separation	Expected Flux ( $\times 10^{-15}$ )	Actual Flux ( $\times 10^{-15}$ )	Flux Ratio	Expected Extension	Actual Extension	Age (kyr)	Chance Overlap
J0700+143	B0656+14	0.29	0.18°	0.91 pc	43.0	23.0	1.87	2.0°	1.73°	111	0.0
J0631+169	J0633+1746	0.25	0.89°	3.88 pc	48.7	48.7	1.0	2.0°	2.0°	342	0.0
J1912+099	J1913+1011	4.61	0.34°	27.36 pc	13.0	36.6	0.36	0.11°	0.7°	169	0.30
J2031+415	J2032+4127	1.70	0.11°	3.26 pc	5.59	61.6	0.091	0.29°	0.7°	181	0.002
J1831-098	J1831-0952	3.68	0.04°	2.57 pc	7.70	95.8	0.080	0.14°	0.9°	128	0.006

2HWC Name	ATNF Name	Distance (kpc)	Angular Separation	Projected Separation	Expected Flux ( $\times 10^{-15}$ )	Actual Flux ( $\times 10^{-15}$ )	Flux Ratio	Expected Extension	Actual Extension	Age (kyr)	Chance Overlap
J1930+188	J1930+1852	7.0	0.03°	3.67 pc	23.2	9.8	2.37	0.07°	0.0°	2.89	0.002
J1814-173	J1813-1749	4.7	0.54°	44.30 pc	243	152	1.60	0.11°	1.0°	5.6	0.61
J2019+367	J2021+3651	1.8	0.27°	8.48 pc	99.8	58.2	1.71	0.28°	0.7°	17.2	0.04
J1928+177	J1928+1746	4.34	0.03°	2.27 pc	8.08	10.0	0.81	0.11°	0.0°	82.6	0.002
J1908+063	J1907+0602	2.58	0.36°	16.21 pc	40.0	85.0	0.47	0.2°	0.8°	19.5	0.26
J2020+403	J2021+4026	2.15	0.18°	6.75 pc	2.48	18.5	0.134	0.23°	0.0°	77	0.01
J1857+027	J1856+0245	6.32	0.12°	13.24 pc	11.0	97.0	0.11	0.08°	0.9°	20.6	0.06
J1825-134	J1826-1334	3.61	0.20°	12.66 pc	20.5	249	0.082	0.14°	0.9°	21.4	0.14
J1837-065	J1838-0655	6.60	0.38°	43.77 pc	12.0	341	0.035	0.08°	2.0°	22.7	0.48
J1837-065	J1837-0604	4.78	0.50°	41.71 pc	8.3	341	0.024	0.10°	2.0°	33.8	0.68
J2006+341	J2004+3429	10.8	0.42°	80.07 pc	0.48	24.5	0.019	0.04°	0.9°	18.5	0.08

- Correcting for the beaming fraction implies that  $56_{-11}^{+15}$  TeV halos are currently observed by HAWC.
- However, only 39 total HAWC sources.





## The H.E.S.S. Galactic plane survey

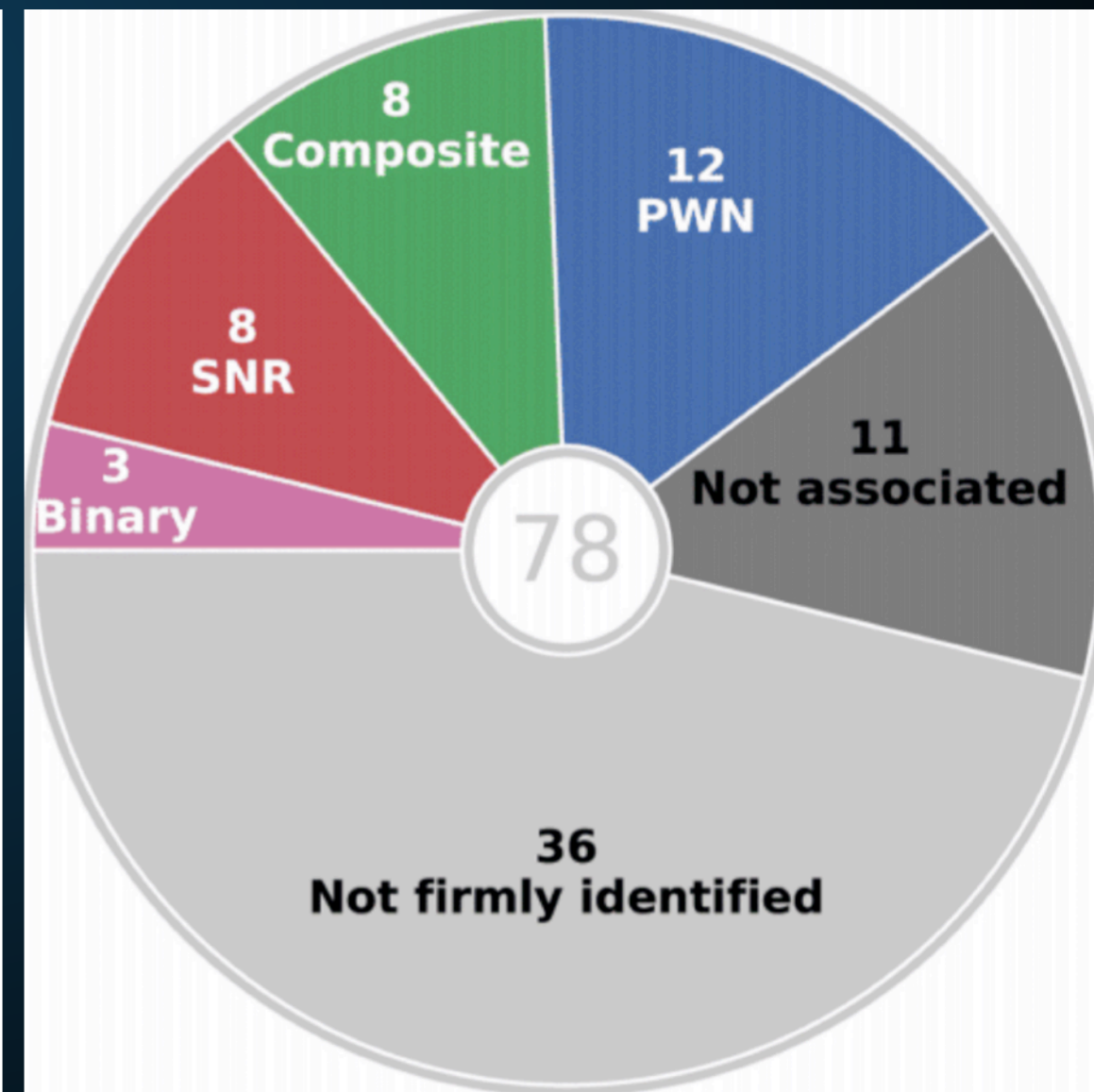
H.E.S.S. Collaboration, H. Abdalla<sup>1</sup>, A. Abramowski<sup>2</sup>, F. Aharonian<sup>3,4,5</sup>, F. Ait Benkhali<sup>3</sup>, E.O. Angüner<sup>21</sup>, M. Arakawa<sup>43</sup>, M. Arrieta<sup>15</sup>, P. Aubert<sup>24</sup>, M. Backes<sup>8</sup>, A. Balzer<sup>9</sup>, M. Barnard<sup>1</sup>, Y. Becherini<sup>10</sup>, J. Becker Tjus<sup>11</sup>, D. Berge<sup>12</sup>, S. Bernhard<sup>13</sup>, K. Bernlöhr<sup>3</sup>, R. Blackwell<sup>14</sup>, M. Böttcher<sup>1</sup>, C. Boisson<sup>15</sup>, J. Bolmont<sup>16</sup>, S. Bonnefoy<sup>37</sup>, P. Bordas<sup>3</sup>, J. Bregeon<sup>17</sup>, F. Brun<sup>18</sup>, P. Brun<sup>18</sup>, M. Bryan<sup>9</sup>, M. Büchele<sup>36</sup>, T. Bulik<sup>19</sup>, M. Capasso<sup>29</sup>, S. Carrigan<sup>3,48</sup>, S. Caroff<sup>30</sup>, A. Carosi<sup>24</sup>, S. Casanova<sup>21,3</sup>, M. Cerruti<sup>16</sup>, N. Chakraborty<sup>3</sup>, R.C.G. Chaves<sup>17,22</sup>, A. Chen<sup>23</sup>, J. Chevalier<sup>24</sup>, S. Colafrancesco<sup>23</sup>, B. Condon<sup>26</sup>, J. Conrad<sup>27,28</sup>, I.D. Davids<sup>8</sup>, J. Decock<sup>18</sup>, C. Deil<sup>3</sup>, J. Devin<sup>17</sup>, P. deWilt<sup>14</sup>, L. Dirson<sup>2</sup>, A. Djannati-Atai<sup>31</sup>, W. Domainko<sup>3</sup>, A. Donath<sup>3</sup>, L.O'C. Drury<sup>4</sup>, K. Dutson<sup>33</sup>, J. Dyks<sup>34</sup>, T. Edwards<sup>3</sup>, K. Egberts<sup>35</sup>, P. Eger<sup>3</sup>, G. Emery<sup>16</sup>, J.-P. Ernenwein<sup>20</sup>, S. Eschbach<sup>36</sup>, C. Farnier<sup>27,10</sup>, S. Fegan<sup>30</sup>, M.V. Fernandes<sup>2</sup>, A. Fiasson<sup>24</sup>, G. Fontaine<sup>30</sup>, A. Förster<sup>3</sup>, S. Funk<sup>36</sup>, M. Füßling<sup>37</sup>, S. Gabici<sup>31</sup>, Y.A. Gallant<sup>17</sup>, T. Garrigoux<sup>1</sup>, H. Gast<sup>3,49</sup>, F. Gaté<sup>24</sup>, G. Giavitto<sup>37</sup>, B. Giebels<sup>30</sup>, D. Glawion<sup>25</sup>, J.F. Glicenstein<sup>18</sup>, D. Gottschall<sup>29</sup>, M.-H. Grondin<sup>26</sup>, J. Hahn<sup>3</sup>, M. Haupt<sup>37</sup>, J. Hawkes<sup>14</sup>, G. Heinzlmann<sup>2</sup>, G. Henri<sup>32</sup>, G. Hermann<sup>3</sup>, J.A. Hinton<sup>3</sup>, W. Hofmann<sup>3</sup>, C. Hoischen<sup>35</sup>, T. L. Holch<sup>7</sup>, M. Holler<sup>13</sup>, D. Horns<sup>2</sup>, A. Ivascenko<sup>1</sup>, H. Iwasaki<sup>43</sup>, A. Jacholkowska<sup>16</sup>, M. Jamroz<sup>38</sup>, D. Jankowsky<sup>36</sup>, F. Jankowsky<sup>25</sup>, M. Jingo<sup>23</sup>, L. Jouvin<sup>31</sup>, I. Jung-Richardt<sup>36</sup>, M.A. Kastendieck<sup>2</sup>, K. Katarzyński<sup>39</sup>, M. Katsuragawa<sup>44</sup>, U. Katz<sup>36</sup>, D. Kerszberg<sup>16</sup>, D. Khangulyan<sup>43</sup>, B. Khélifi<sup>31</sup>, J. King<sup>3</sup>, S. Klepser<sup>37</sup>, D. Klochkov<sup>29</sup>, W. Kluźniak<sup>34</sup>, Nu. Komin<sup>23</sup>, K. Kosack<sup>11</sup>, S. Krakau<sup>11</sup>, M. Kraus<sup>36</sup>, P.P. Krüger<sup>1</sup>, H. Laffon<sup>26</sup>, G. Lamanna<sup>24</sup>, J. Lau<sup>14</sup>, J.-P. Lees<sup>24</sup>, J. Lefaucheur<sup>15</sup>, A. Lemièrre<sup>31</sup>, M. Lemoine-Goumard<sup>26</sup>, J.-P. Lenain<sup>16</sup>, E. Leser<sup>35</sup>, T. Lohse<sup>7</sup>, M. Lorentz<sup>18</sup>, R. Liu<sup>3</sup>, R. López-Coto<sup>3</sup>, I. Lypova<sup>37</sup>, V. Marandon<sup>43</sup>, D. Malyshev<sup>29</sup>, A. Marcowith<sup>17</sup>, C. Mariaud<sup>30</sup>, R. Marx<sup>3</sup>, G. Maurin<sup>24</sup>, N. Maxted<sup>14,45</sup>, M. Mayer<sup>7</sup>, P.J. Meintjes<sup>40</sup>, M. Meyer<sup>27</sup>, A.M.W. Mitchell<sup>3</sup>, R. Moderski<sup>34</sup>, M. Mohamed<sup>25</sup>, L. Mohrmann<sup>36</sup>, K. Morá<sup>27</sup>, E. Moulin<sup>18</sup>, T. Murach<sup>37</sup>, S. Nakashima<sup>44</sup>, M. de Naurois<sup>30</sup>, H. Ndiyavala<sup>1</sup>, F. Niederwanger<sup>13</sup>, J. Niemiec<sup>21</sup>, L. Oakes<sup>33</sup>, P. O'Brien<sup>37</sup>, H. Odaka<sup>44</sup>, S. Ohm<sup>37</sup>, M. Ostrowski<sup>38</sup>, I. Oya<sup>37</sup>, M. Padovani<sup>17</sup>, M. Panter<sup>3</sup>, R.D. Parsons<sup>3</sup>, M. Paz Arribas<sup>7</sup>, N.W. Pekeur<sup>1</sup>, G. Pelletier<sup>32</sup>, C. Perennes<sup>16</sup>, P.-O. Petrucci<sup>32</sup>, B. Peyaud<sup>18</sup>, Q. Piel<sup>24</sup>, S. Pita<sup>31</sup>, V. Poireau<sup>24</sup>, H. Poon<sup>3</sup>, D. Prokhorov<sup>10</sup>, H. Prokoph<sup>12</sup>, G. Pühlhofer<sup>29</sup>, M. Punch<sup>31,10</sup>, A. Quirrenbach<sup>25</sup>, S. Raab<sup>36</sup>, R. Rauth<sup>13</sup>, A. Reimer<sup>13</sup>, O. Reimer<sup>13</sup>, M. Renaud<sup>17</sup>, R. de los Reyes<sup>3</sup>, F. Rieger<sup>3,41</sup>, L. Rinchiuso<sup>18</sup>, C. Romoli<sup>4</sup>, G. Rowell<sup>14</sup>, B. Rudak<sup>34</sup>, C.B. Rulten<sup>15</sup>, S. Safi-Harb<sup>50</sup>, V. Sahakian<sup>6,5</sup>, S. Saito<sup>43</sup>, D.A. Sanchez<sup>24</sup>, A. Santangelo<sup>29</sup>, M. Sasaki<sup>36</sup>, M. Schandri<sup>36</sup>, R. Schlickeiser<sup>11</sup>, F. Schüssler<sup>18</sup>, A. Schulz<sup>37</sup>, U. Schwanke<sup>7</sup>, S. Schwemmer<sup>25</sup>, M. Seglar-Arroyo<sup>18</sup>, M. Settimo<sup>16</sup>, A.S. Seyffert<sup>1</sup>, N. Shafi<sup>23</sup>, I. Shilon<sup>36</sup>, K. Shiningayamwe<sup>8</sup>, R. Simoni<sup>9</sup>, H. Sol<sup>15</sup>, F. Spanier<sup>1</sup>, M. Spir-Jacob<sup>31</sup>, Ł. Stawarz<sup>38</sup>, R. Steenkamp<sup>8</sup>, C. Stegmann<sup>35,37</sup>, C. Steppa<sup>35</sup>, I. Sushch<sup>1</sup>, T. Takahashi<sup>44</sup>, J.-P. Tavernier<sup>16</sup>, T. Tavernier<sup>31</sup>, A.M. Taylor<sup>37</sup>, R. Terrier<sup>31</sup>, L. Tibaldo<sup>3</sup>, D. Tiziani<sup>36</sup>, M. Tluczykont<sup>2</sup>, C. Trichard<sup>20</sup>, M. Tsirou<sup>17</sup>, N. Tsuji<sup>43</sup>, R. Tufts<sup>3</sup>, Y. Uchiyama<sup>43</sup>, D.J. van der Walt<sup>1</sup>, C. van Eldik<sup>36</sup>, C. van Rensburg<sup>1</sup>, B. van Soelen<sup>40</sup>, G. Vasileiadis<sup>17</sup>, J. Veh<sup>36</sup>, C. Venter<sup>1</sup>, A. Viana<sup>3,46</sup>, P. Vincent<sup>16</sup>, J. Vink<sup>9</sup>, F. Voisin<sup>14</sup>, H.J. Völk<sup>3</sup>, T. Vuillaume<sup>24</sup>, Z. Wadiasingh<sup>1</sup>, S.J. Wagner<sup>25</sup>, P.M. Wagner<sup>27</sup>, R.M. White<sup>3</sup>, A. Wiercholska<sup>21</sup>, P. Willmann<sup>36</sup>, A. Würnlein<sup>36</sup>, D. Wouters<sup>18</sup>, R. Yang<sup>3</sup>, D. Zaborov<sup>30</sup>, M. Zacharias<sup>1</sup>, R. Zanin<sup>3</sup>, A.A. Zdziarski<sup>34</sup>, A. Zech<sup>15</sup>, F. Zefi<sup>30</sup>, A. Ziegler<sup>36</sup>, J. Zorn<sup>3</sup>, and N. Zywucka<sup>38</sup>

(Affiliations can be found after the references)

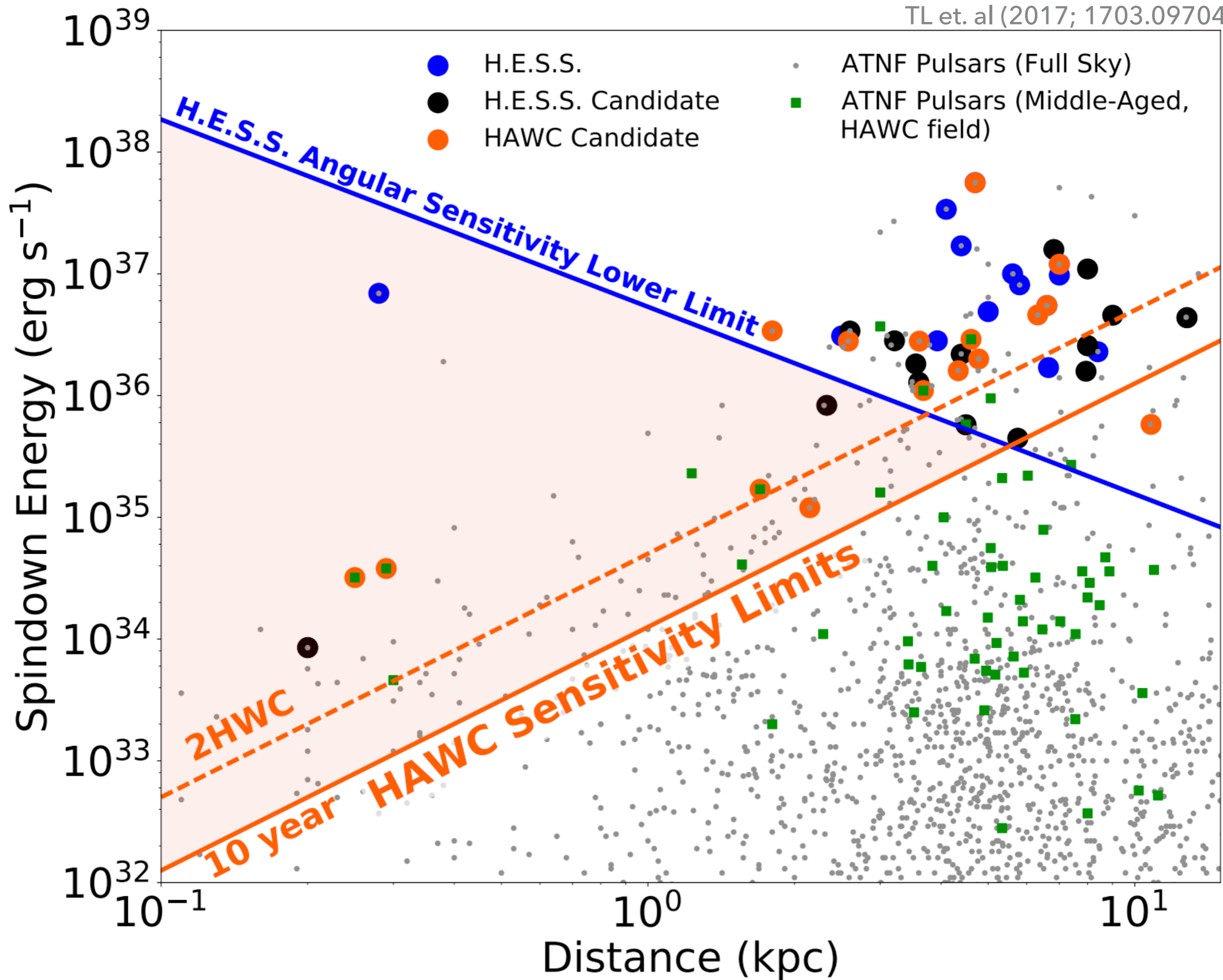
April 10, 2018

### ABSTRACT

We present the results of the most comprehensive survey of the Galactic plane in very high-energy (VHE)  $\gamma$ -rays, including a public release of Galactic sky maps, a catalog of VHE sources, and the discovery of 16 new sources of VHE  $\gamma$ -rays. The High Energy Spectroscopic System (H.E.S.S.) Galactic plane survey (HGPS) was a decade-long observation program carried out by the H.E.S.S. I array of Cherenkov telescopes in Namibia from 2004 to 2013. The observations amount to nearly 2700 h of quality-selected data, covering the Galactic plane at longitudes from  $l = 250^\circ$  to  $65^\circ$  and latitudes  $|b| \leq 3^\circ$ . In addition to the unprecedented spatial coverage, the HGPS also features a relatively high angular resolution ( $0.08^\circ \approx 5$  arcmin mean point spread function 68% containment radius), sensitivity ( $\lesssim 1.5\%$  Crab flux for point-like sources), and energy range (0.2 to 100 TeV). We constructed a catalog of VHE  $\gamma$ -ray sources from the HGPS data set with a systematic procedure for both source detection and characterization of morphology and spectrum. We present this likelihood-based method in detail, including the introduction of a model component to account for unresolved, large-scale emission along the Galactic plane. In total, the resulting HGPS catalog contains 78 VHE sources, of which 14 are not reanalyzed here, for example, due to their complex morphology, namely shell-like sources and the Galactic center region. Where possible, we provide a firm identification of the VHE source or plausible associations with sources in other astronomical catalogs. We also studied







# FIRST DETECTIONS!

[ [Previous](#) | [Next](#) | [ADS](#) ]

## HAWC detection of TeV emission near PSR B0540+23

ATel #10941; *Colas Riviere (University of Maryland), Henrike Fleischhack (Michigan Technological University), Andres Sandoval (Universidad Nacional Autonoma de Mexico) on behalf of the HAWC collaboration*

*on 9 Nov 2017; 23:11 UT*

*Credential Certification: Colas Riviere (riviere@umd.edu)*

Subjects: Gamma Ray, TeV, VHE, Pulsar

[Tweet](#) [Recommend 5](#)

The High Altitude Water Cherenkov (HAWC) collaboration reports the discovery of a new TeV gamma-ray source HAWC J0543+233. It was discovered in a search for extended sources of radius  $0.5^\circ$  in a dataset of 911 days (ranging from November 2014 to August 2017) with a test statistic value of 36 ( $6\sigma$  pre-trials), following the method presented in [Abeysekara et al. 2017, ApJ, 843, 40](#). The measured J2000.0 equatorial position is  $RA=85.78^\circ$ ,  $Dec=23.40^\circ$  with a statistical uncertainty of  $0.2^\circ$ . HAWC J0543+233 was close to passing the selection criteria of the 2HWC catalog ([Abeysekara et al. 2017, ApJ, 843, 40](#), see [HAWC J0543+233 in 2HWC map](#)), which it now fulfills with the additional data.

HAWC J0543+233 is positionally coincident with the pulsar PSR B0540+23 ( $\dot{E} = 4.1e+34$  erg  $s^{-1}$ ,  $dist = 1.56$  kpc,  $age = 253$  kyr). It is the third low  $\dot{E}$ , middle-aged pulsar announced to be detected with a TeV halo, along with Geminga and B0656+14. It was predicted to be one of the next such detection by HAWC by [Linden et al., 2017, arXiv:1703.09704](#).

Using a simple source model consisting of a disk of radius  $0.5^\circ$ , the measured spectral index is  $-2.3 \pm 0.2$  and the differential flux at 7 TeV is  $(7.9 \pm 2.3) \times 10^{-15}$  TeV $^{-1}$  cm $^{-2}$  s $^{-1}$ . The errors are statistical only. Further morphological and spectral analysis as well as studies of the systematic uncertainty are ongoing.

[ [Previous](#) | [Next](#) | [ADS](#) ]

## HAWC detection of TeV source HAWC J0635+070

ATel #12013; *Chad Brisbois (Michigan Technological University), Colas Riviere (University of Maryland), Henrike Fleischhack (Michigan Technological University), Andrew Smith (University of Maryland) on behalf of the HAWC collaboration*

*on 6 Sep 2018; 14:47 UT*

*Credential Certification: Colas Riviere (riviere@umd.edu)*

Subjects: Gamma Ray, TeV, VHE, Pulsar

[Tweet](#) [Recommend 2](#)

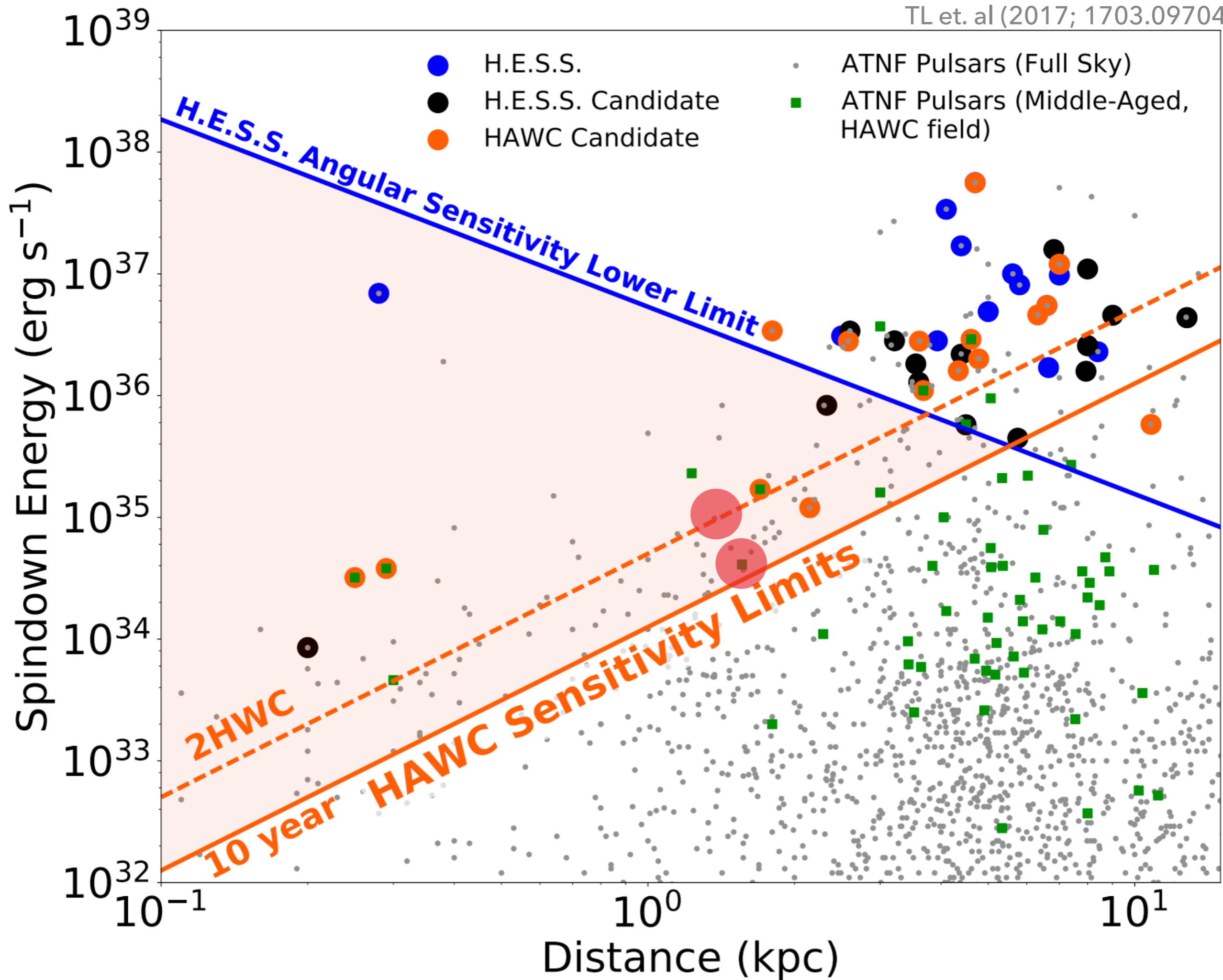
The High Altitude Water Cherenkov (HAWC) collaboration reports the discovery of a new TeV gamma-ray source HAWC J0635+070. It was discovered in a search for extended sources covering 1128 days of HAWC observations with a test statistic value of 27 ( $>5\sigma$  pre-trials), following the method presented in [[Abeysekara et al. 2017, ApJ, 843, 40](#)]. Its significance in the 2HWC data set excluded it from being included in the catalog ( $\sim 3.5\sigma$  pre-trials), but with the addition of  $\sim 600$  more days of data it now satisfies that criterion. The best-fit J2000.0 equatorial position is  $RA=98.71 \pm 0.20^\circ$ ,  $Dec=7.00 \pm 0.22^\circ$ , with a Gaussian 1-sigma extent of  $0.65^\circ \pm 0.18^\circ$ .

The spectral energy distribution is well-fit by a power law with spectral index  $-2.15 \pm 0.17$ . The differential flux at 10 TeV is  $(8.6 \pm 3.2) \times 10^{-15}$  TeV $^{-1}$  cm $^{-2}$  s $^{-1}$ . All errors are statistical only; further morphological and spectral analysis as well as studies of the systematic uncertainty are ongoing.

Given its spectrum and morphology, we believe HAWC J0635+070 may be the TeV halo of the pulsar PSR J0633+0632 ( $\dot{E} = 1.2e+35$  erg  $s^{-1}$ ,  $dist = 1.35$  kpc,  $age = 59$  kyr, unknown proper motion [[Manchester et al., 2005, AJ, 129](#)]). The gamma-ray spectrum and morphology is compatible with a "Geminga-like" TeV Halo [[Abeysekara et al. 2017, Science, 358, 911](#); [Linden et al., 2017, PRD, 96, 103016](#)]. We encourage follow-up observations at other wavelengths.

- **HAWC has detected two additional TeV halos**
- **Total Count:**
  - **Middle-Aged: 6**
  - **Younger: 13**





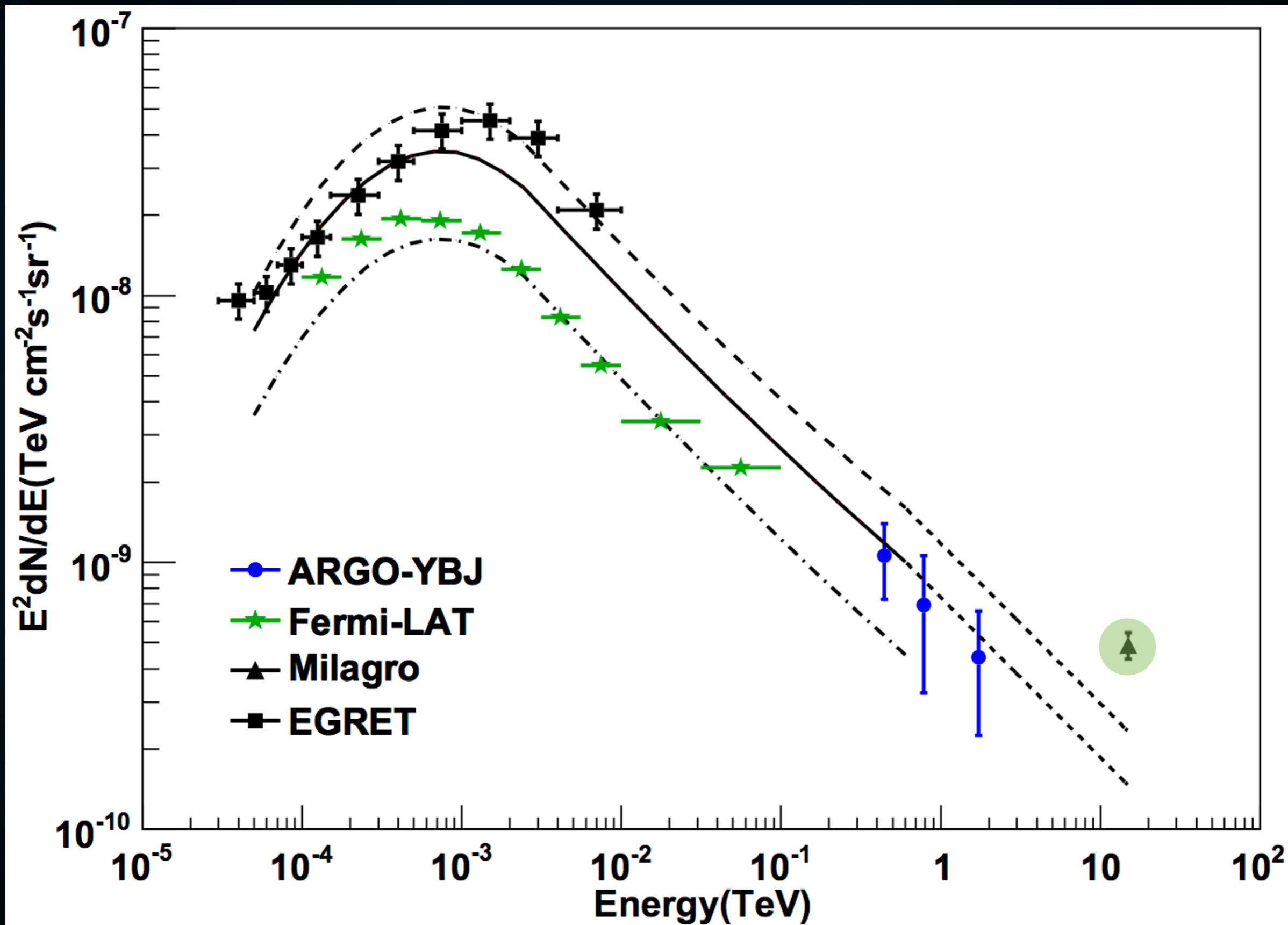
---

**Implication II:**

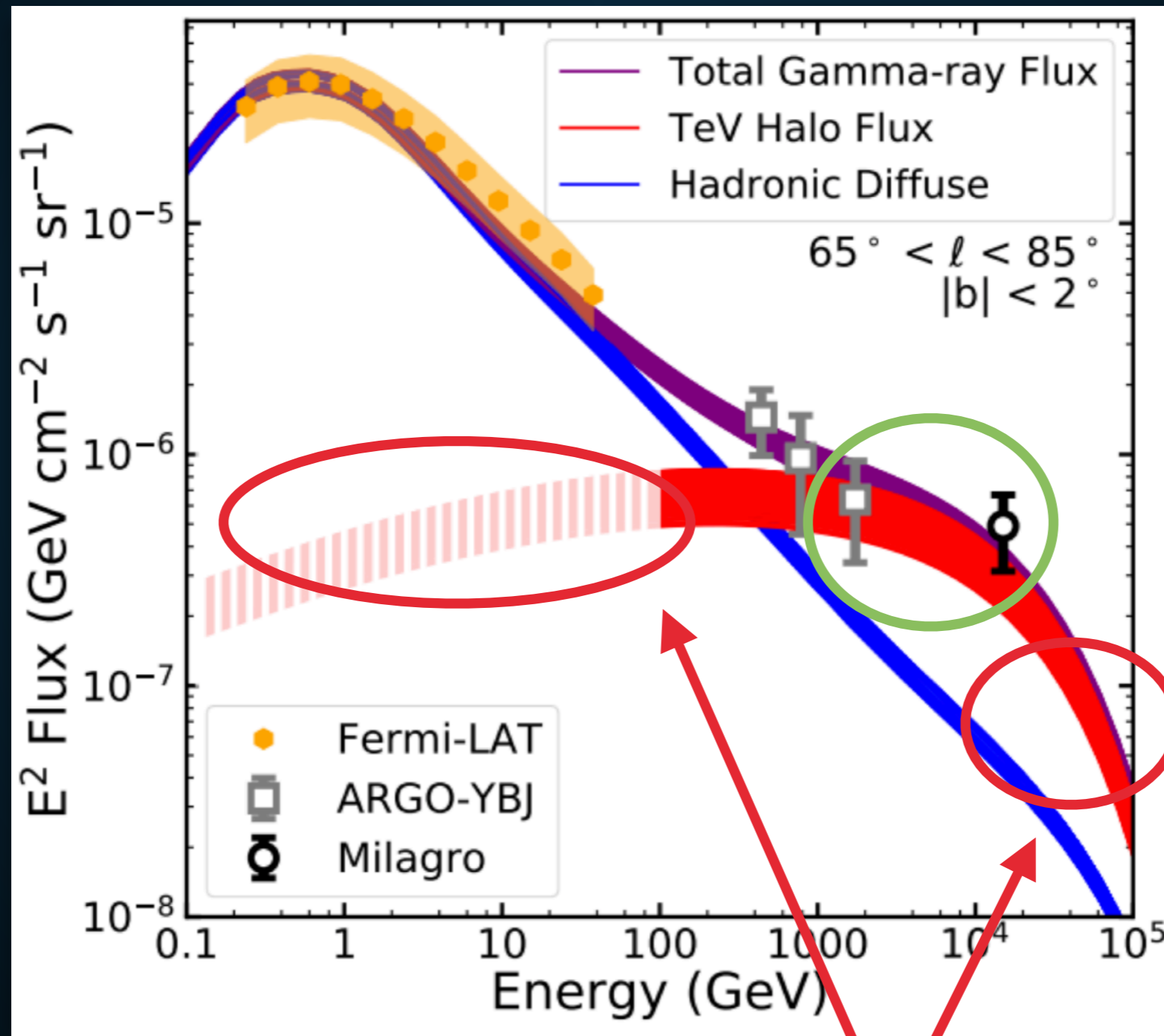
**TeV halos dominate the diffuse TeV sky**



# IMPLICATION I: THE TEV EXCESS



- TeV halos naturally explain the TeV excess!



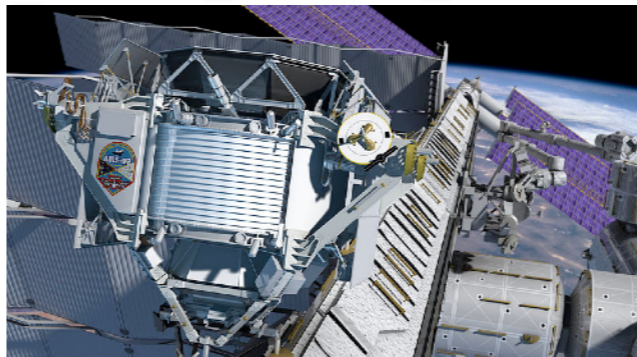
spectral assumption!



---

**Implication III: The positron excess is  
due to pulsar activity**

Positron fraction



$10^{-1}$

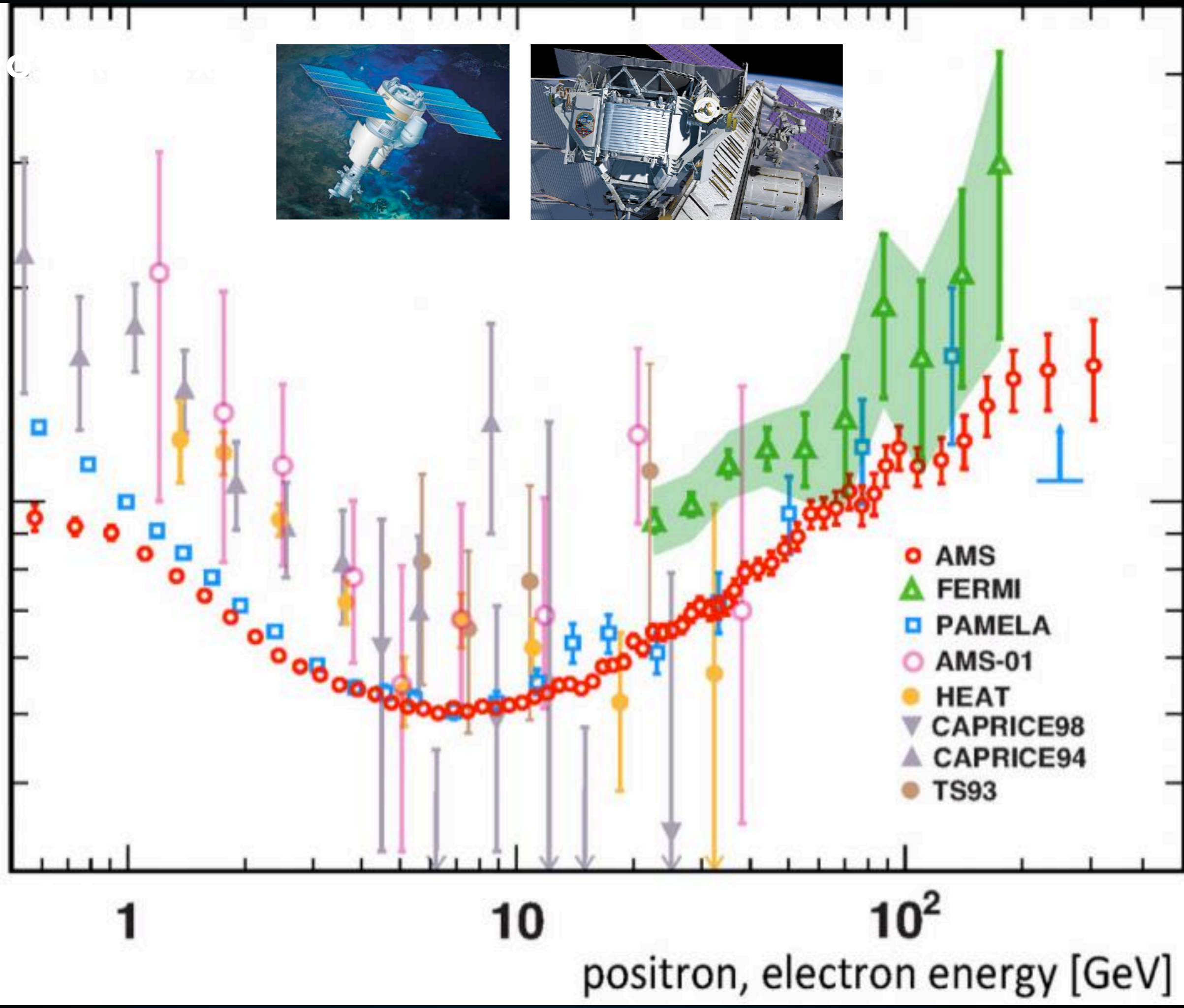
1

10

$10^2$

positron, electron energy [GeV]

- AMS
- △ FERMI
- PAMELA
- AMS-01
- HEAT
- ▽ CAPRICE98
- △ CAPRICE94
- TS93





# PULSARS PRODUCE THE POSITRON EXCESS

---

- **What were the uncertainties in pulsar models?**

- **I: The  $e^+e^-$  production efficiency?**

Profumo (0812.4457); Malyshev et al. (0903.1310)

%.

A quantitative discussion of plausible values for  $f_{e^\pm}$  was recently given in Ref. [38]. We shall not review their discussion here, but Ref. [38] argues (see in particular their very informative App. B and C) that in the context of a standard model for the pulsar wind nebulae, a reasonable range for  $f_{e^\pm}$  falls between 1% and 30%.

- **II: The  $e^+e^-$  spectrum.**

- **III: The propagation of  $e^+e^-$  to Earth.**

# PULSARS PRODUCE THE POSITRON EXCESS

---

- **What were the uncertainties in pulsar models?**

- **I: The  $e^+e^-$  production efficiency?**

- **II: The  $e^+e^-$  spectrum.**

Hooper et al. (0810.1527)

part of their energy adiabatically because of the expansion of the wind. The energy spectrum injected by a single pulsar depends on the environmental parameters of the pulsar, but some attempts to calculate the average spectrum injected by a population of mature pulsars suggest that the spectrum may be relatively hard, having a slope of  $\sim 1.5-1.6$  [18]. This spectrum, however, results from a complex interplay of individual pulsar spectra, of the spatial and age distributions of pulsars in the Galaxy, and on the assumption that the chief channel for pulsar spin down is magnetic dipole radiation. Due to the related uncertainties, variations from this injection spectra cannot be ruled out. Typically, one concentrates the attention on pulsars of age  $\sim 10^5$  years because younger pulsars are likely to still

- **III: The propagation of  $e^+e^-$  to Earth.**



# TEV HALOS ANSWER THE KEY QUESTIONS!

Name	Tested radius [ $^{\circ}$ ]	Index	$F_7 \times 10^{15}$ [ $\text{TeV}^{-1} \text{cm}^{-2} \text{s}^{-1}$ ]	TeVCat
2HWC J0631+169	-	$-2.57 \pm 0.15$	$6.7 \pm 1.5$	Geminga
"	2.0	$-2.23 \pm 0.08$	$48.7 \pm 6.9$	Geminga
2HWC J0635+180	-	$-2.56 \pm 0.16$	$6.5 \pm 1.5$	Geminga

- We assume a power-law electron injection spectrum with an exponential cutoff

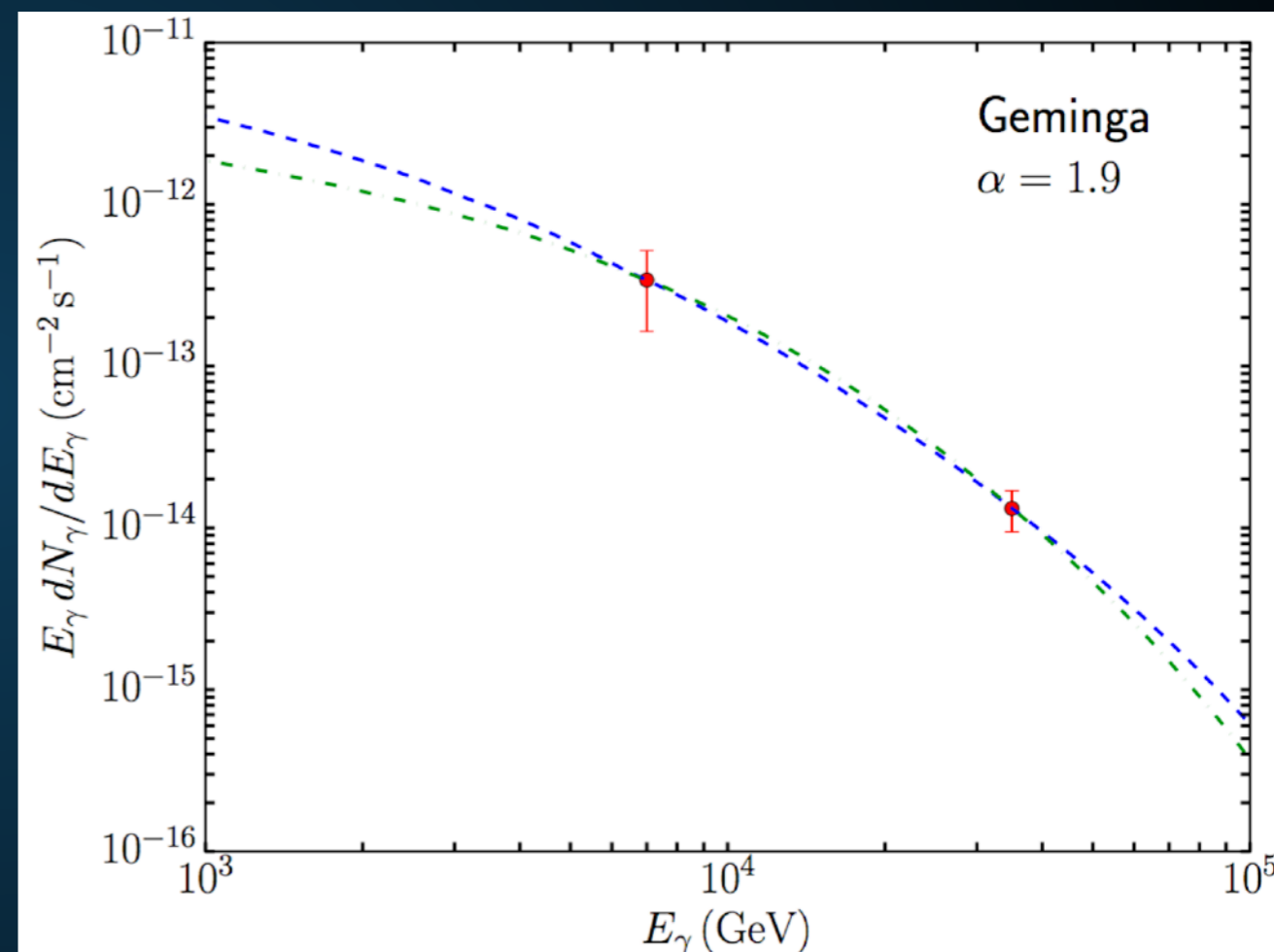
- Best Fit:

$$-1.9 < \alpha < -1.5$$

$$E_{\text{cut}} \cong 50 \text{ TeV}$$

$$\sim 3\text{-}9 \times 10^{33} \text{ erg s}^{-1} !$$

**9-27%** of the total pulsar spin-down power!



# PULSARS PRODUCE THE POSITRON EXCESS

---

- **What were the uncertainties in pulsar models?**

- **I: The  $e^+e^-$  production efficiency?**

- **II: The  $e^+e^-$  spectrum.**

- **III: The propagation of  $e^+e^-$  to Earth.**

Malyshev et al. (0903.1310)

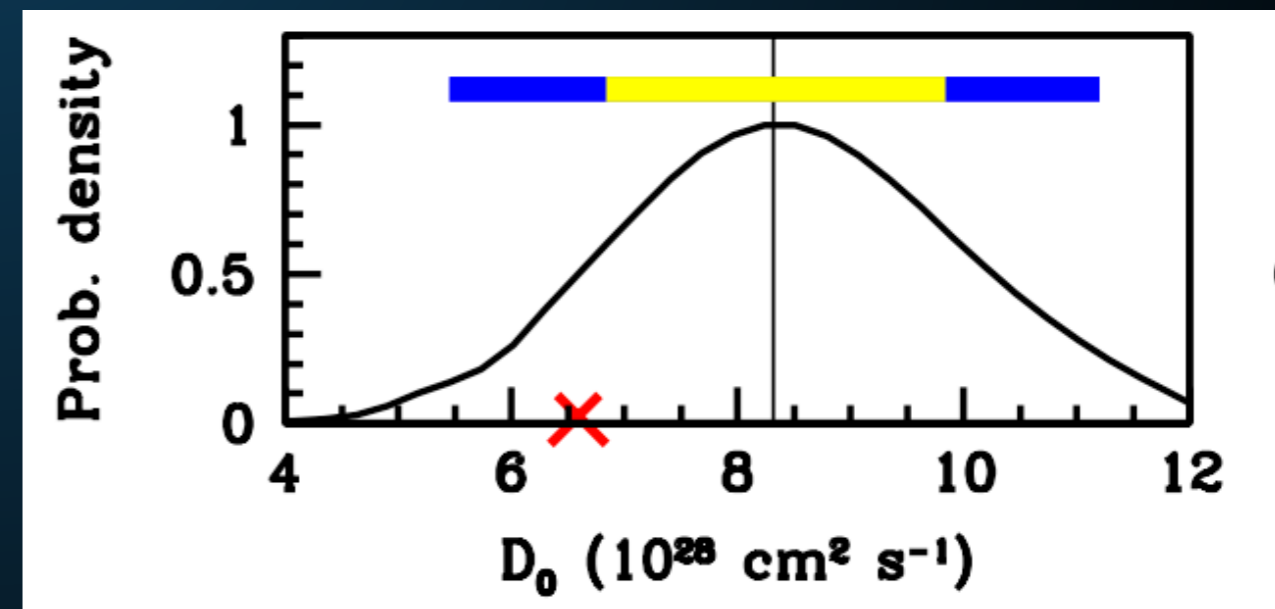
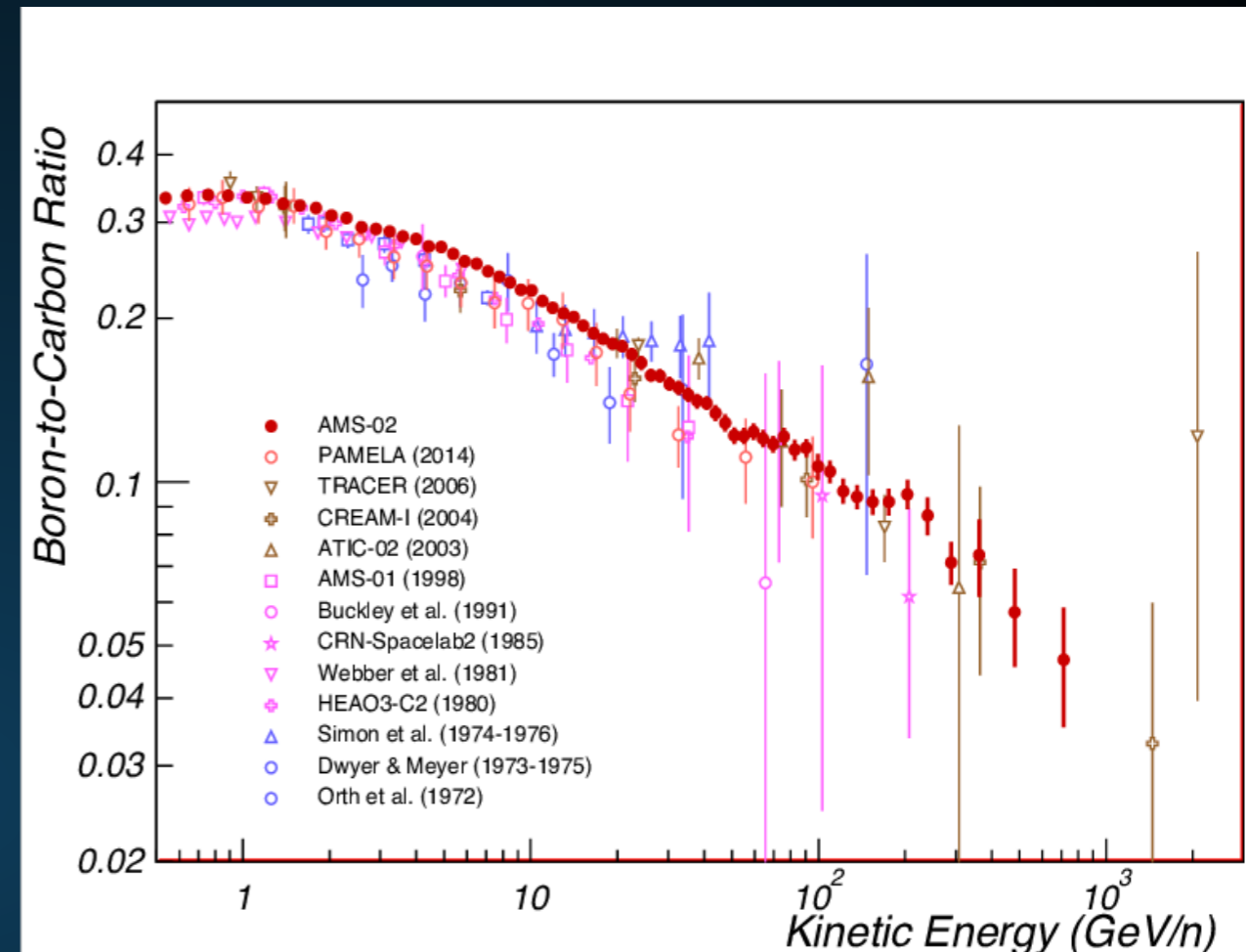
The observed spectrum on Earth of electrons and positrons injected by pulsars is also strongly dependent on propagation effects. In particular, the observed cutoff in the flux of electrons from a pulsar can be much smaller than the injection cutoff due to energy losses (“cooling”) during propagation. We define the cooling break,  $E_{br}(t)$ , as the maximal energy electrons can have after propagating for time  $t$ . Since – as stated above – the typical



---

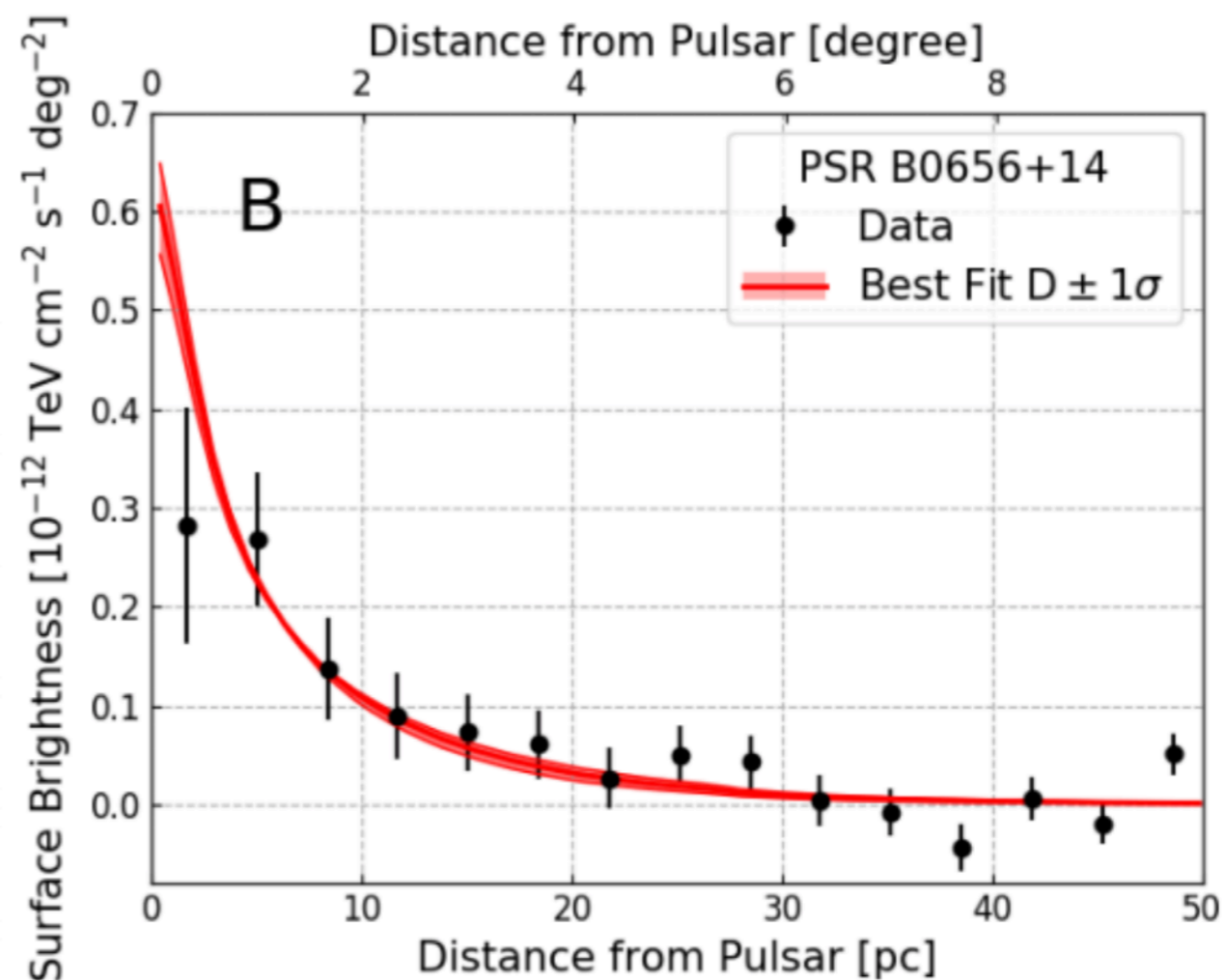
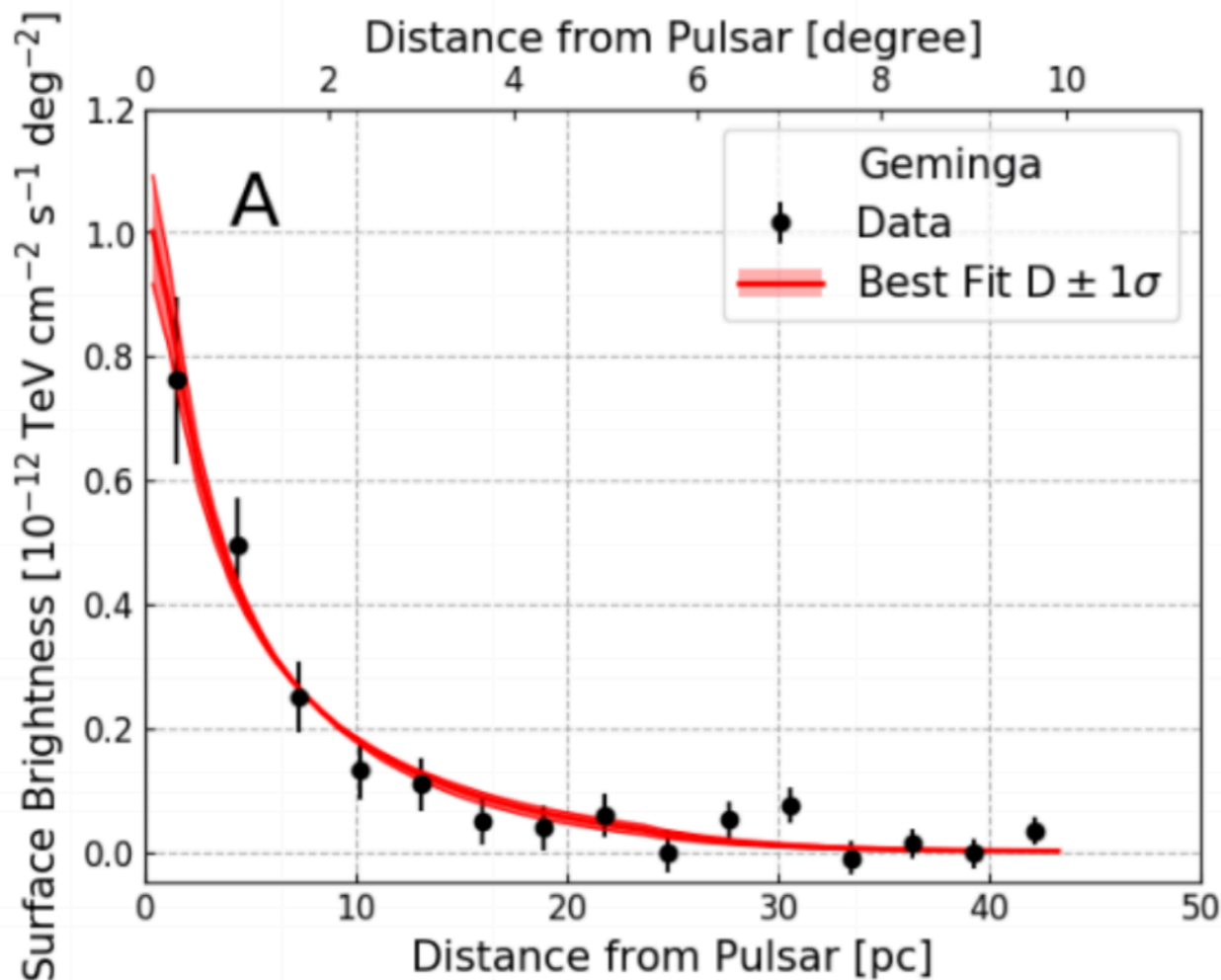
**Cosmic-ray propagation is the last key.**

- **Cosmic-Ray primary to secondary ratios tell us about:**
  - **The average grammage encountered by cosmic-rays before they escape the galaxy (e.g. B/C)**
  - **The average time cosmic-rays propagate before they escape (eg.  $^{10}\text{Be}/^9\text{Be}$ ).**
  - **Diffusion:  $5 \times 10^{28} \text{ cm}^2 \text{ s}^{-1}$ .**

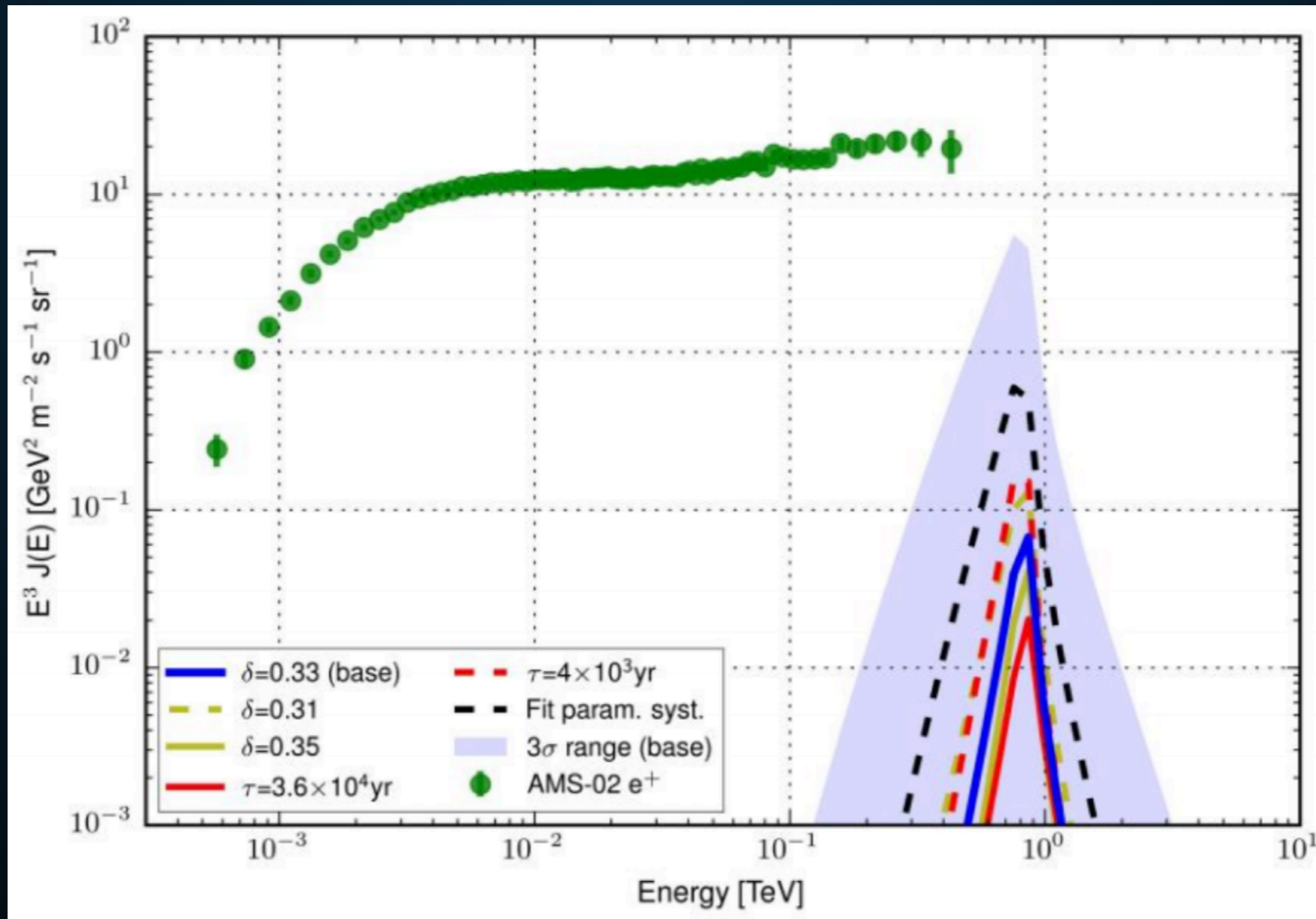




Pulsar Parameters		Geminga	PSR B0656+14
(Right ascension, declination) (J2000 source location)	[degrees]	(98.48, 17.77)	(104.95, 14.24)
$\tau_c$ (characteristic age)	[years]	342,000	110,000
$D_{100}$ (Diffusion coefficient of 100TeV electrons from joint fit of two PWNe)	[ $\times 10^{27}$ cm <sup>2</sup> /sec]	$4.5 \pm 1.2$	$4.5 \pm 1.2$

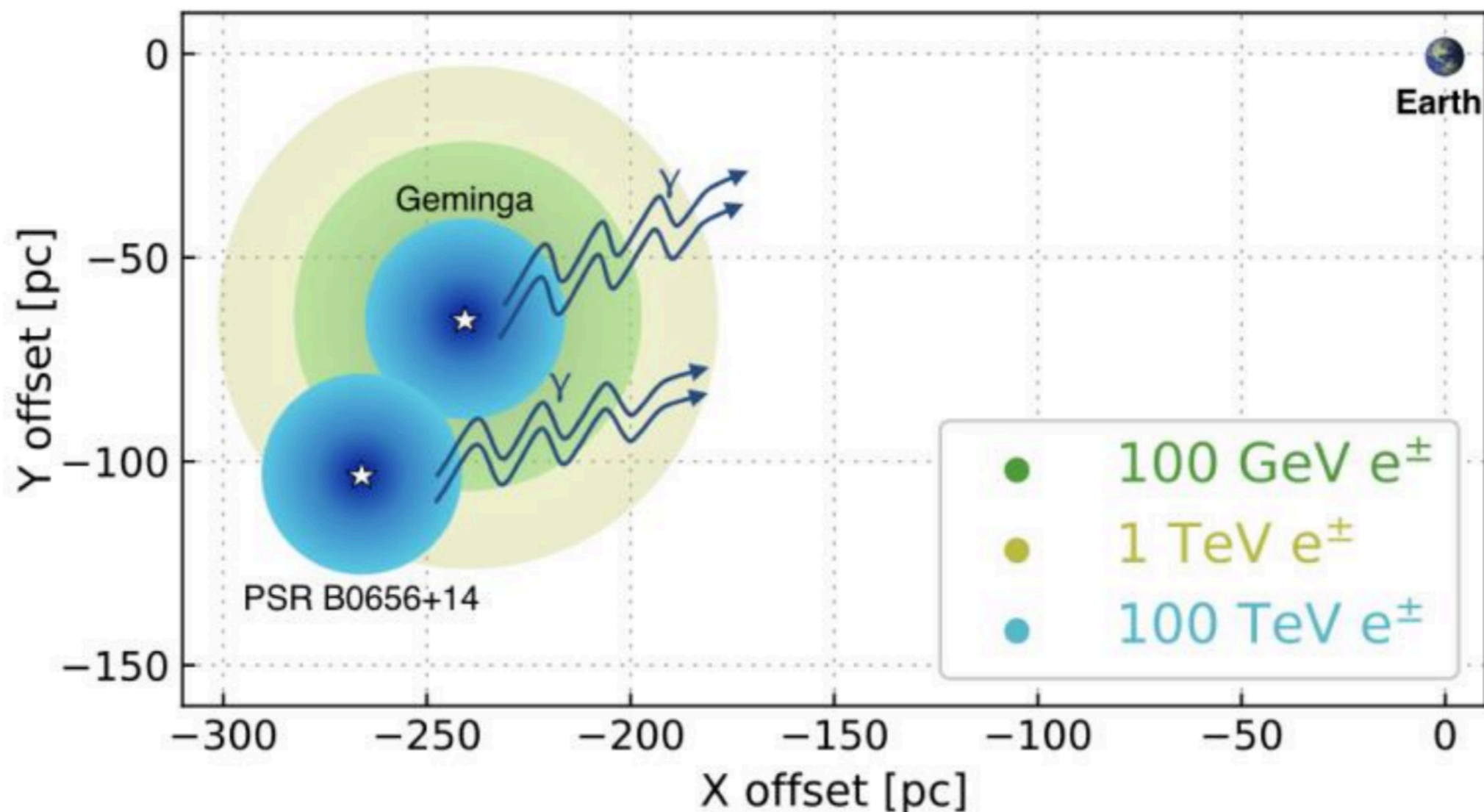


Pulsar Parameters		Geminga	PSR B0656+14
(Right ascension, declination) (J2000 source location)	[degrees]	(98.48, 17.77)	(104.95, 14.24)
$\tau_c$ (characteristic age)	[years]	342,000	110,000
$D_{100}$ (Diffusion coefficient of 100TeV electrons from joint fit of two PWNe)	$[ \times 10^{27} \text{ cm}^2/\text{sec} ]$	$4.5 \pm 1.2$	$4.5 \pm 1.2$



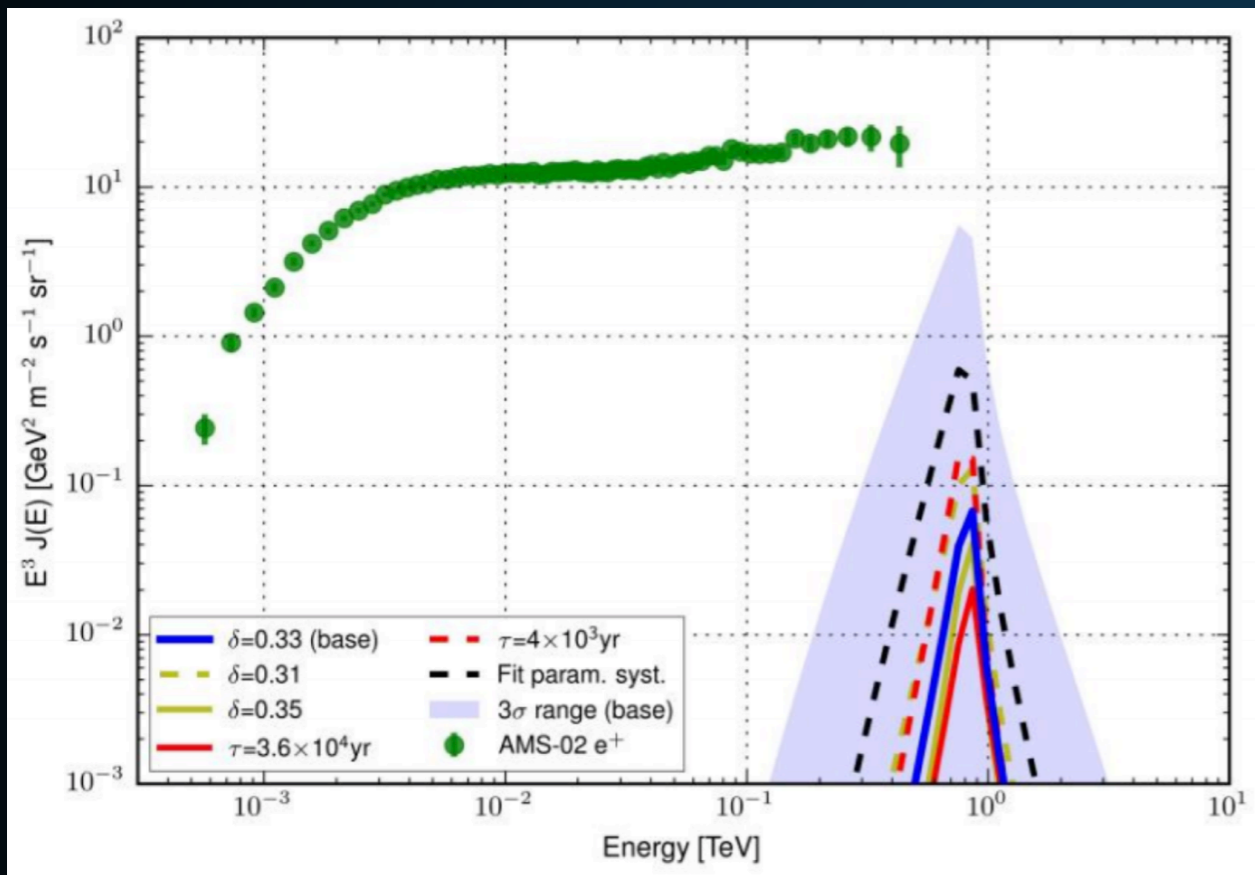


Pulsar Parameters		Geminga	PSR B0656+14
(Right ascension, declination) (J2000 source location)	[degrees]	(98.48, 17.77)	(104.95, 14.24)
$\tau_c$ (characteristic age)	[years]	342,000	110,000
$D_{100}$ (Diffusion coefficient of 100TeV electrons from joint fit of two PWNe)	$[ \times 10^{27} \text{ cm}^2/\text{sec} ]$	$4.5 \pm 1.2$	$4.5 \pm 1.2$



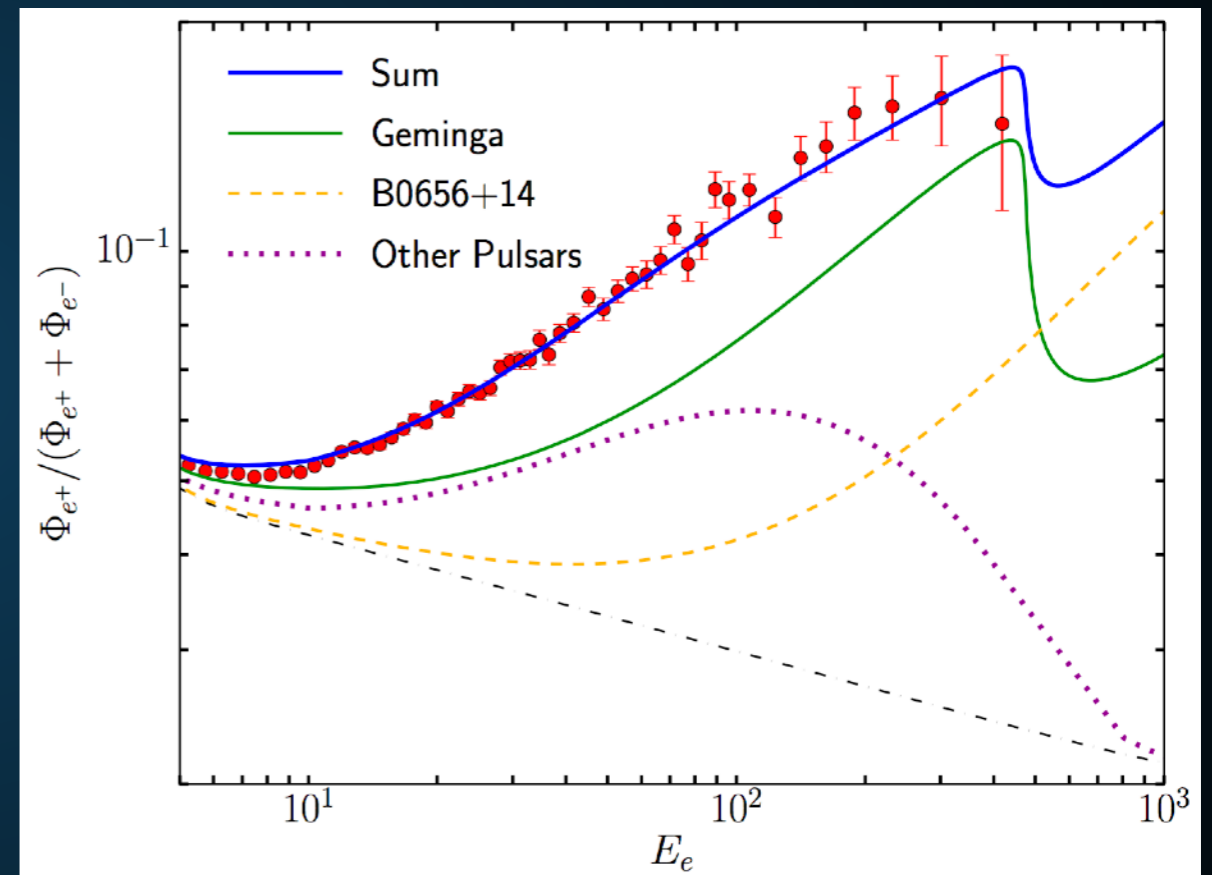
# TWO POSSIBLE ASSUMPTIONS

Extrapolate Low-Diffusion Constant  
UP to Earth:



100 GeV positrons do not make it to  
Earth

Extrapolate the High Diffusion  
Constant DOWN to Earth:



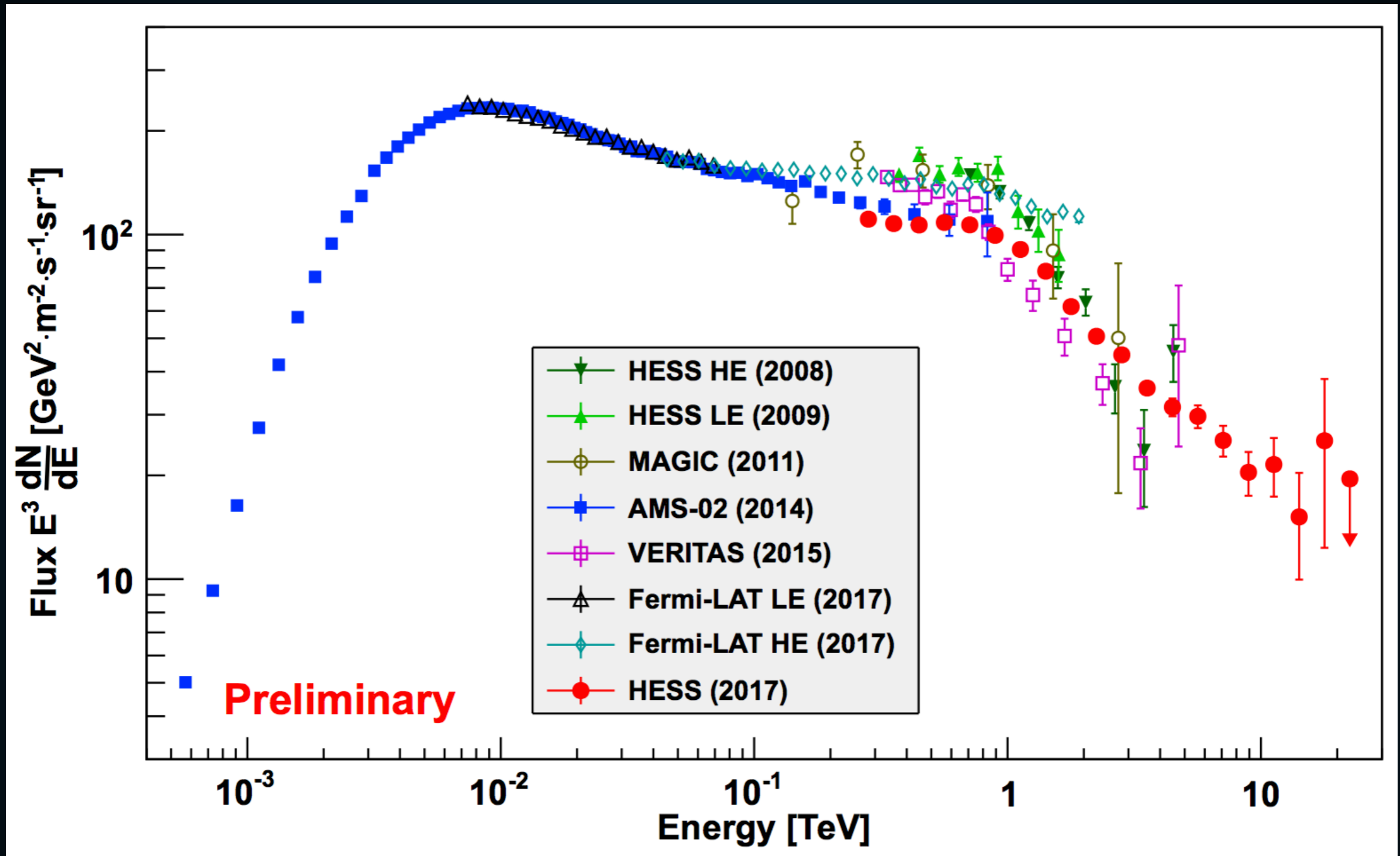
100 GeV positrons do make it to Earth

Hooper et al. (1702.08436)

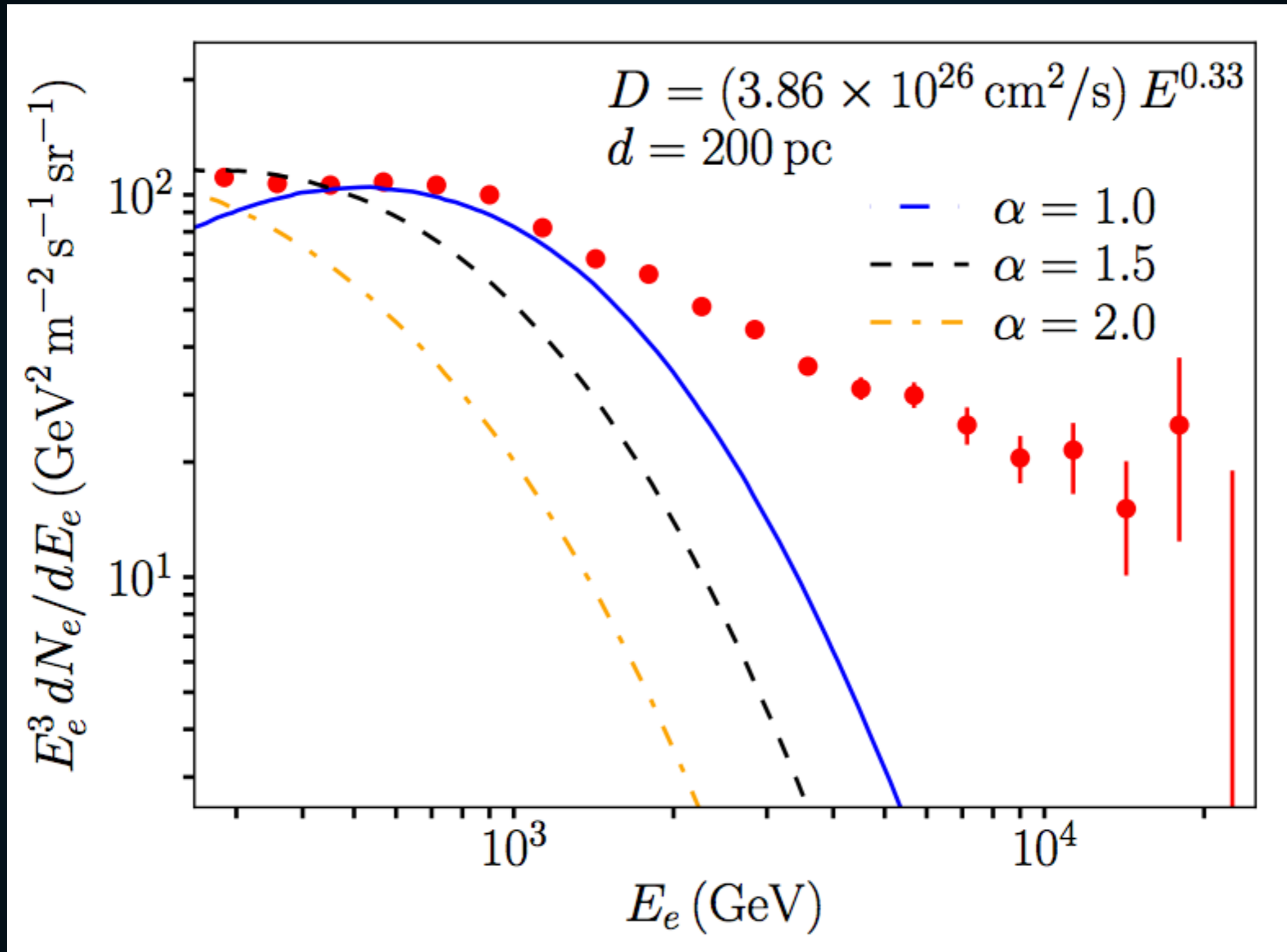
Profumo et al. (1803.09731)

Fang et al. (1803.02640)





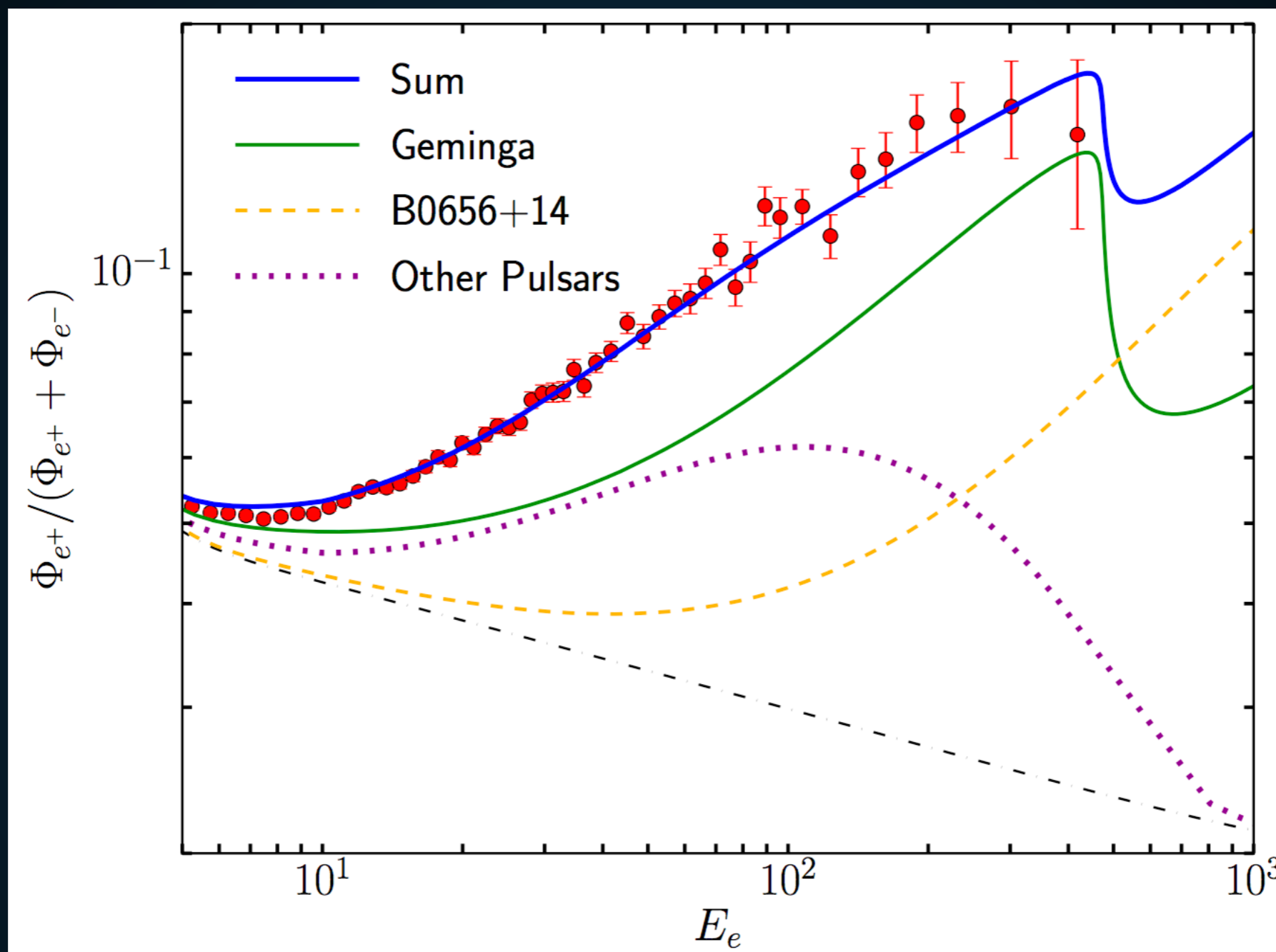
- Recently the HESS telescope detected 20 TeV electrons near Earth.



- If diffusion near Earth is low, then there is no source for these particles.



# THE POSITRON FRACTION FROM TEV HALOS



- Reasonable models can be exactly fit to the excess.

**\*Braking index slightly changed to fit model to data.**

## ASSUMPTIONS

TeV Gamma-Ray Luminosity Roughly Proportional to Spindown Power

= Pulsars explain the Milagro TeV Excess

+ High Energy  
electrons trapped in  
TeV halos

= HAWC Sources  
are TeV halos

+ Low energy  
electrons escape  
from TeV halos

= Pulsars explain  
the positron excess



---

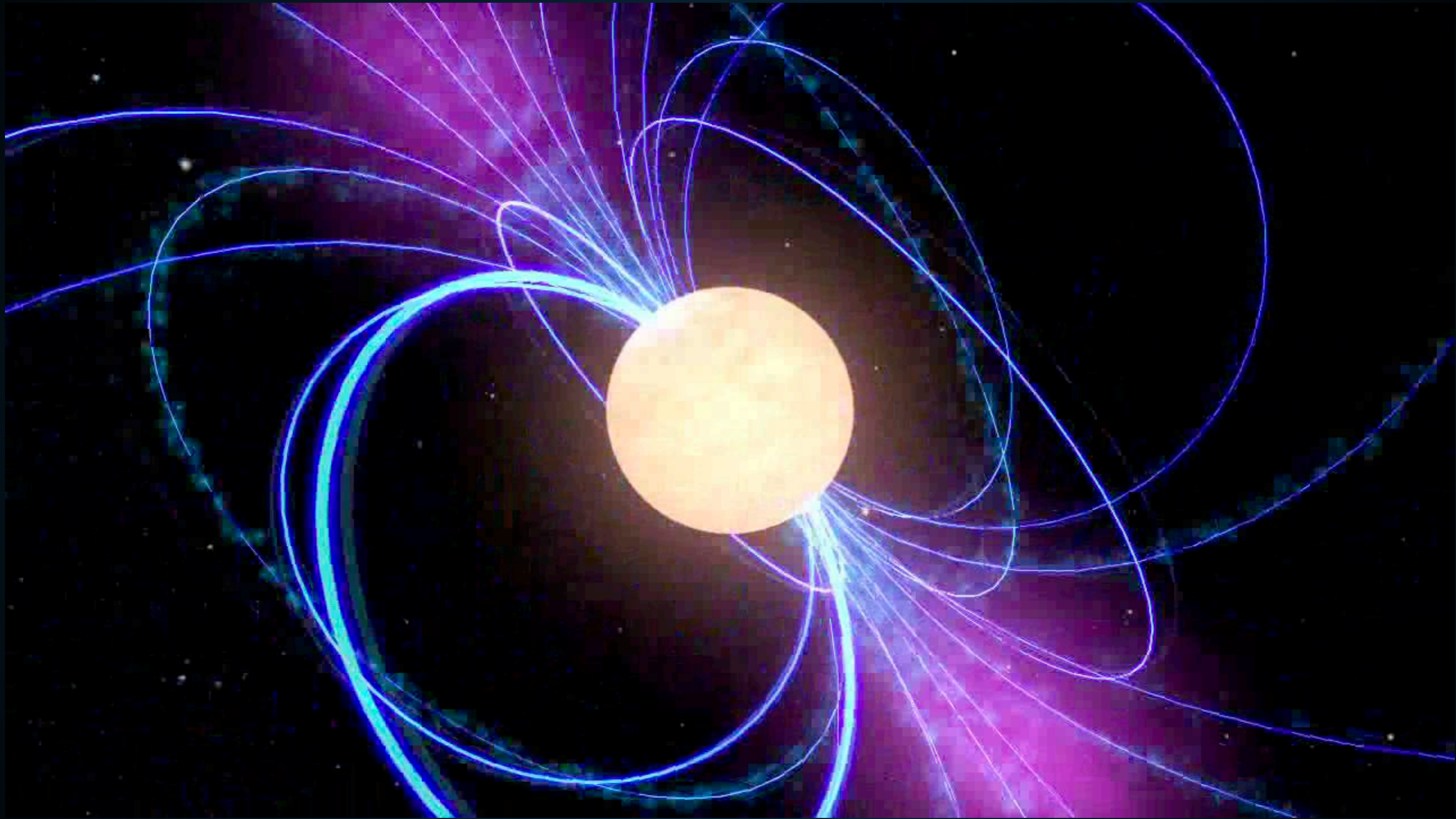
**What is a  
TeV halo?**

---

**What do we know about pulsars?**

## PULSARS AS ASTROPHYSICAL ACCELERATORS

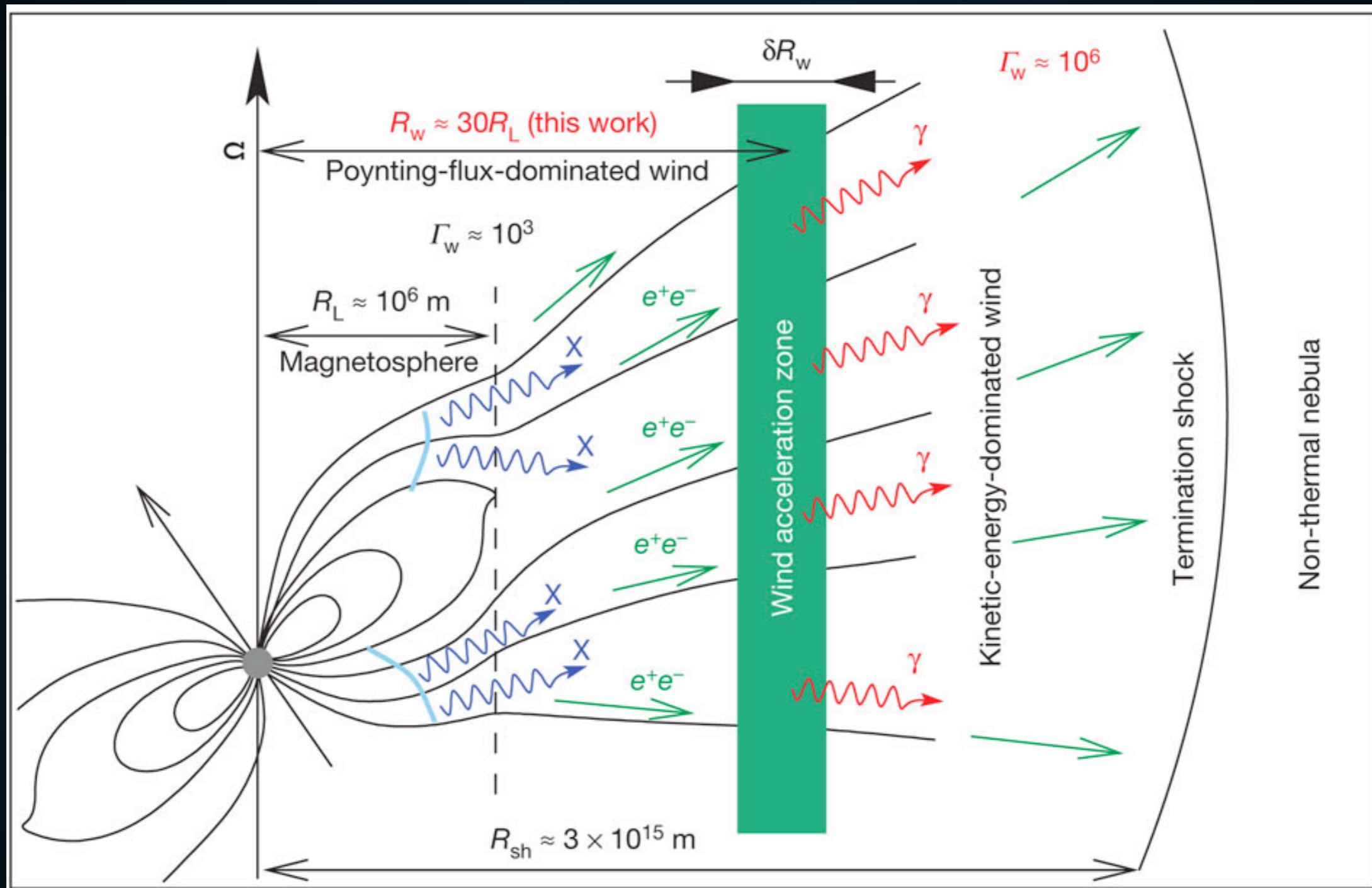
---



- **Rotational Kinetic Energy of the neutron star is the ultimate power source of all emission in this problem.**



# PRODUCTION OF ELECTRON AND POSITRON PAIRS



- **Electrons boiled off of the pulsar surface produce  $e^+e^-$  pairs.**
- **Final  $e^+e^-$  Spectrum is model dependent.**



# REACCELERATION IN THE PULSAR WIND NEBULA



Blandford & Ostriker (1978)  
Hoshino et al. (1992)  
Coroniti (1990)  
Sironi & Spitkovsky (2011)

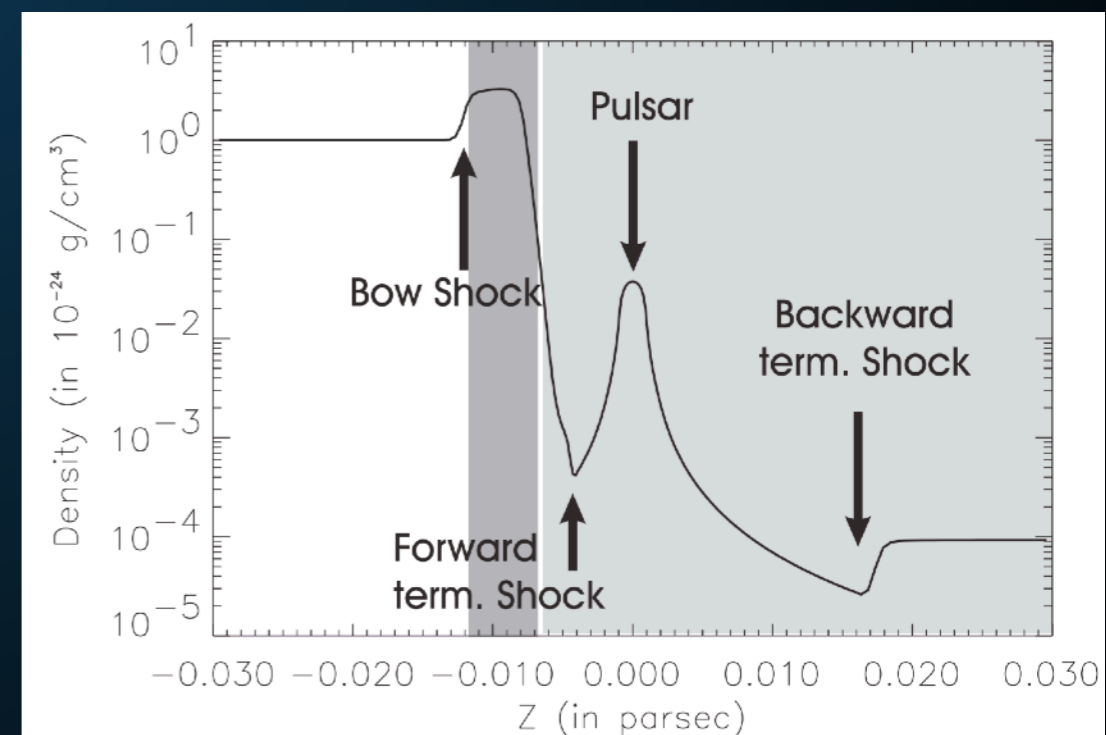
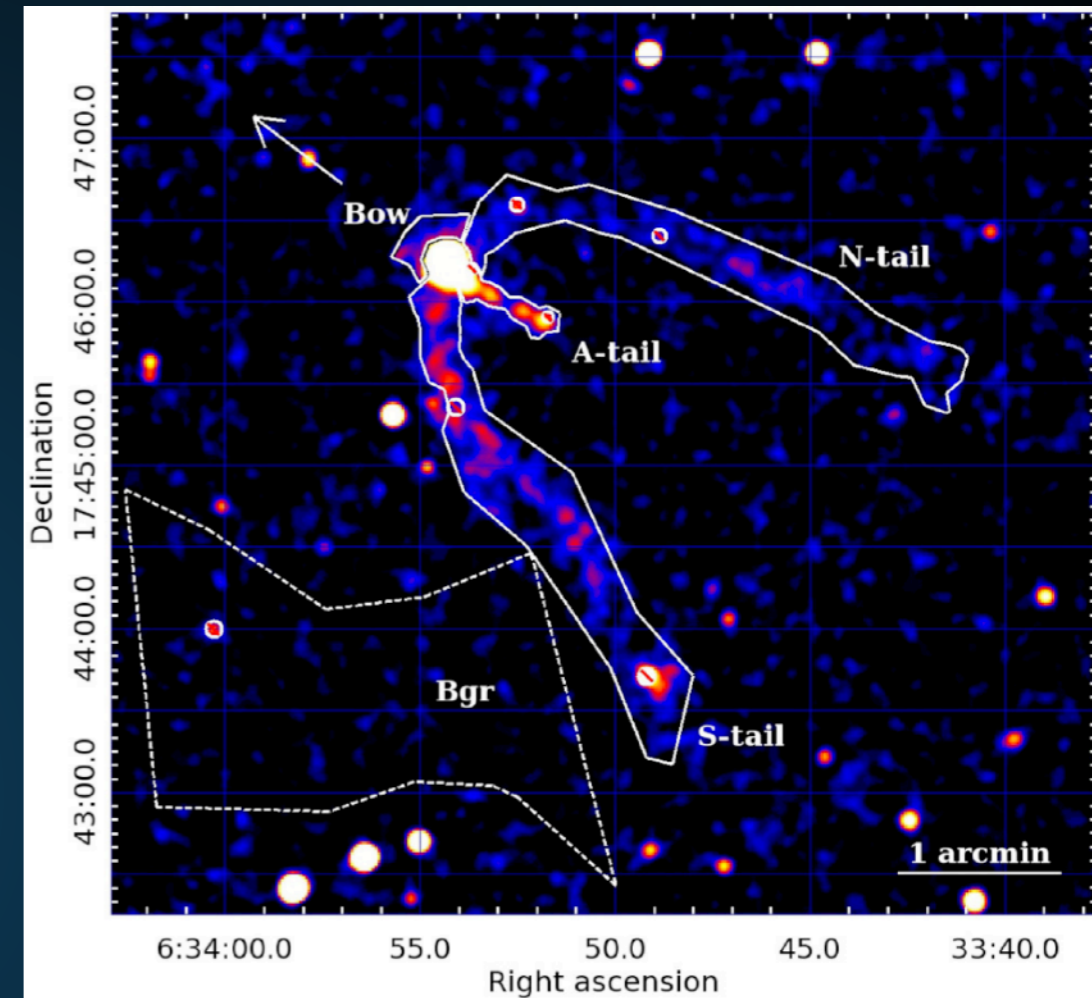
- **PWN termination shock:**
  - **Voltage Drop  $> 30$  PV**
  - **$e^+e^-$  energy  $> 1$  PeV**  
(known from synchrotron)
- **Resets  $e^+e^-$  spectrum.**
- **Many Possible Models:**
  - **1st Order Fermi-Acceleration**
  - **Magnetic Reconnection**
  - **Shock-Driven Reconnection**



- **Extent of radio and X-Ray PWN is approximately 1 pc.**
- **Termination shock produced when ISM energy density stops the relativistic pulsar wind.**

$$R_{\text{PWN}} \simeq 1.5 \left( \frac{\dot{E}}{10^{35} \text{ erg/s}} \right)^{1/2} \times \left( \frac{n_{\text{gas}}}{1 \text{ cm}^{-3}} \right)^{-1/2} \left( \frac{v}{100 \text{ km/s}} \right)^{-3/2} \text{ pc}$$

- **NOTE: The radial extent of PWN is explained by a known physical mechanism.**



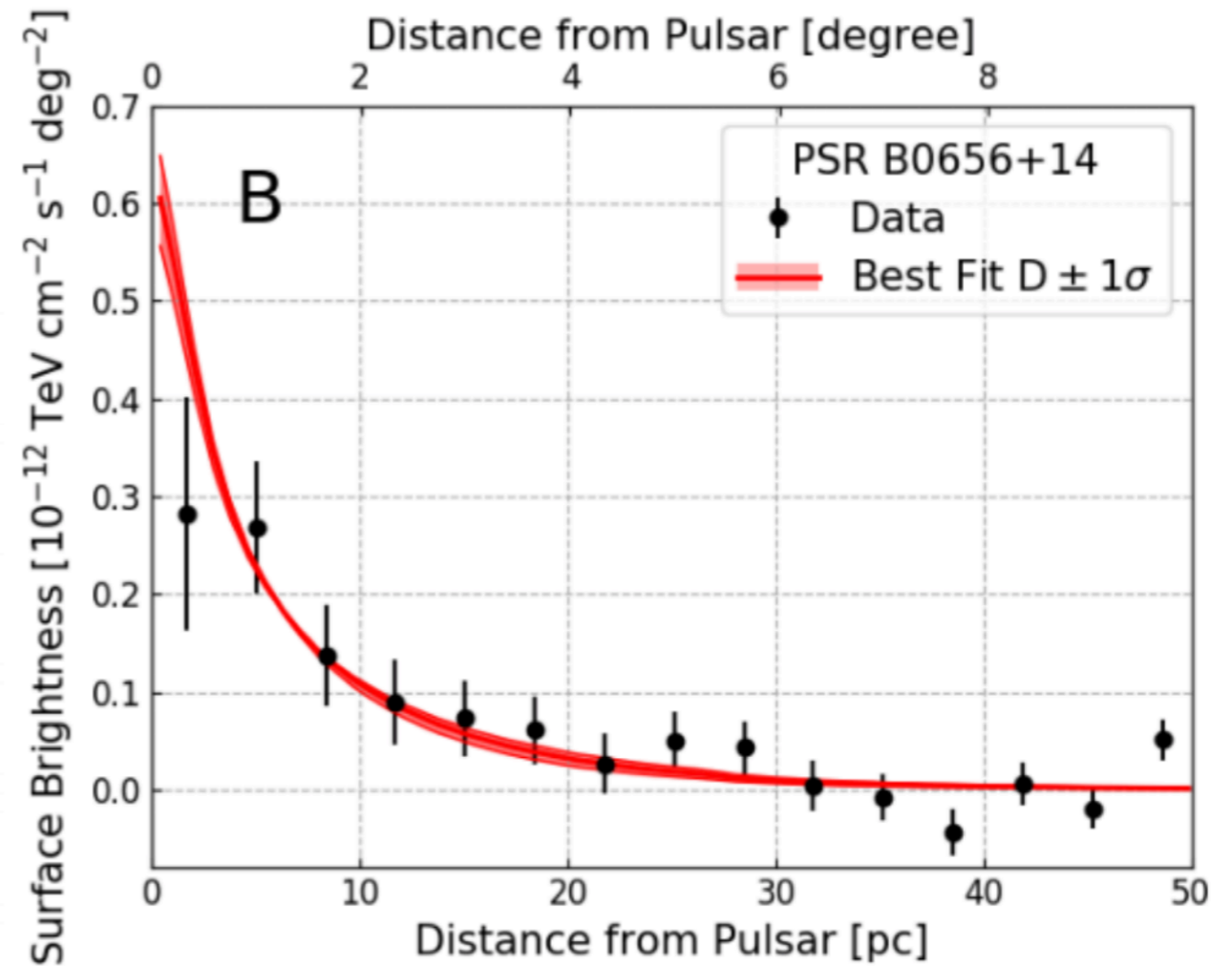
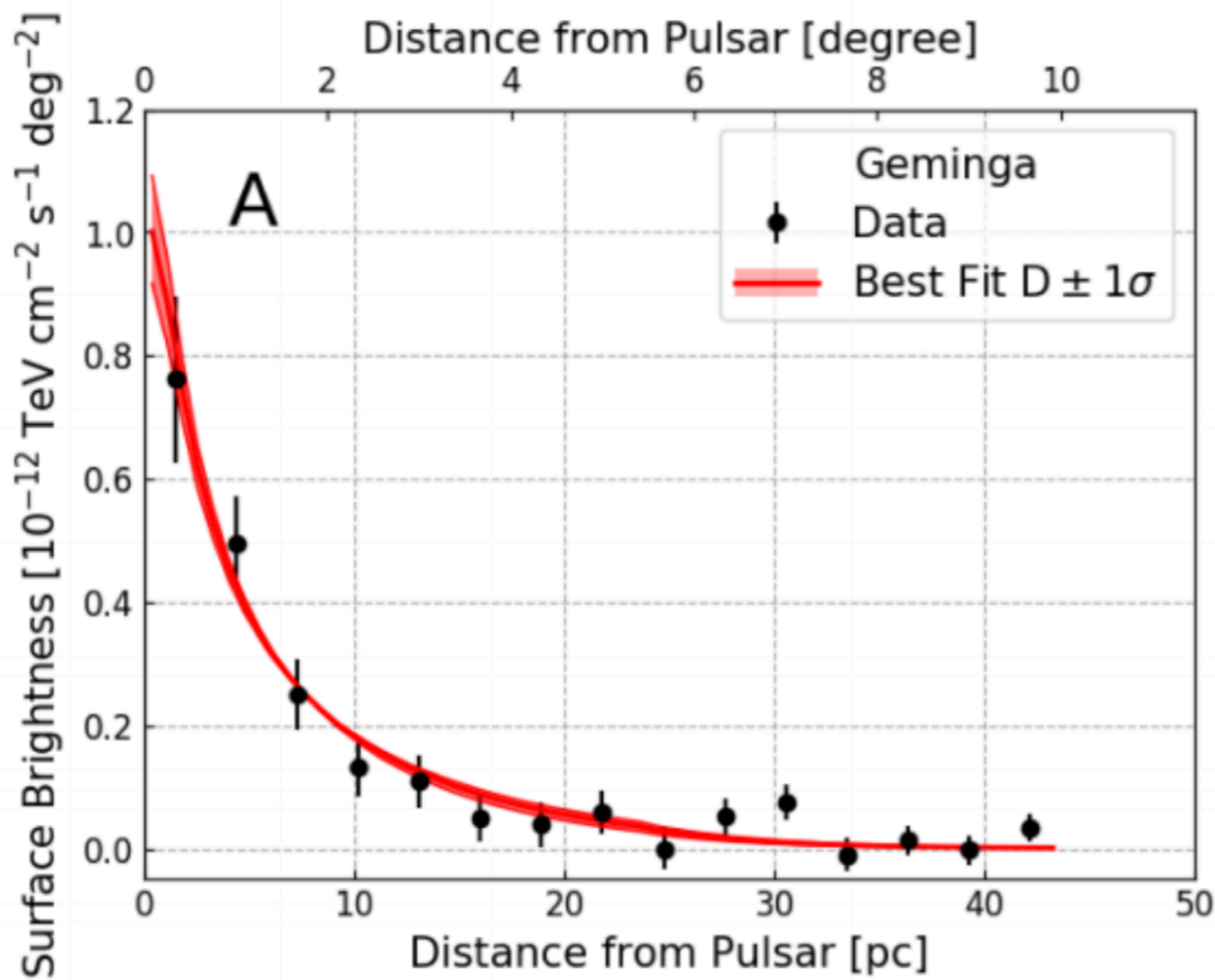


SNR  
 $\sim O(100)$  pc

TeV Halo  
 $\sim O(10)$  pc

PWN  
 $\sim O(1)$  pc

# TEV HALOS



- These sources are much smaller than expected via diffusion through the standard ISM.

$$\tau_{\text{loss}} \approx 30 \text{ Kyr} \quad D_0 \approx 5 \times 10^{28} \text{ cm}^2 \text{ s}^{-1}$$
$$L = \sqrt{Dt} \approx 2000 \text{ pc}$$



## COSMIC-RAY DIFFUSION

---

- **Diffusion equation controls the transport of cosmic rays**

$$\frac{\partial f}{\partial t} + u \frac{\partial f}{\partial z} - \frac{\partial}{\partial z} \left[ D(p, z, t) \frac{\partial f}{\partial z} \right] - \frac{du}{dz} \frac{p}{3} \frac{\partial f}{\partial p} + \frac{1}{p^2} \frac{\partial}{\partial p} \left[ p^2 \left( \frac{dp}{dt} \right)_e f \right] = Q_e(p, z, t),$$

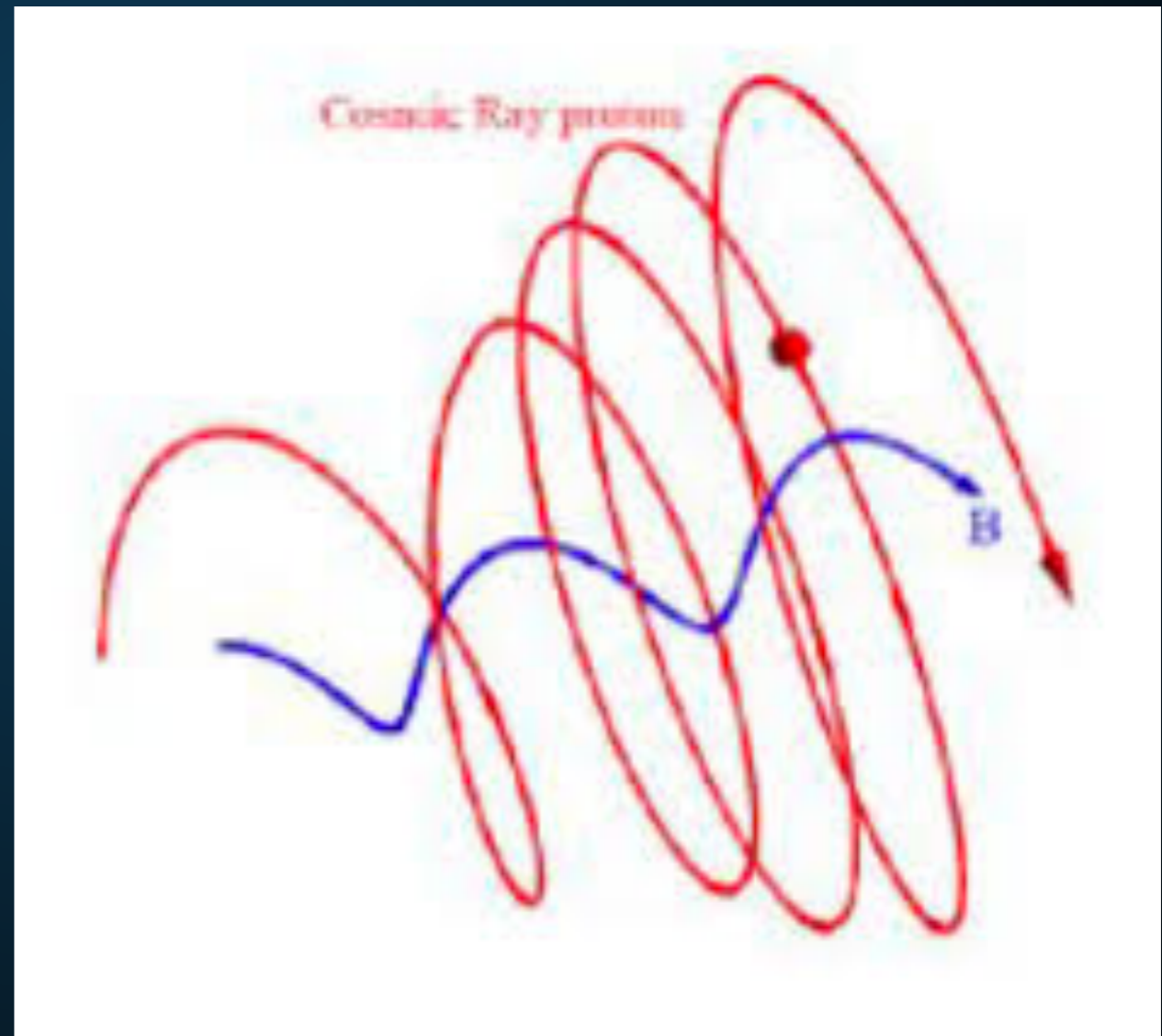
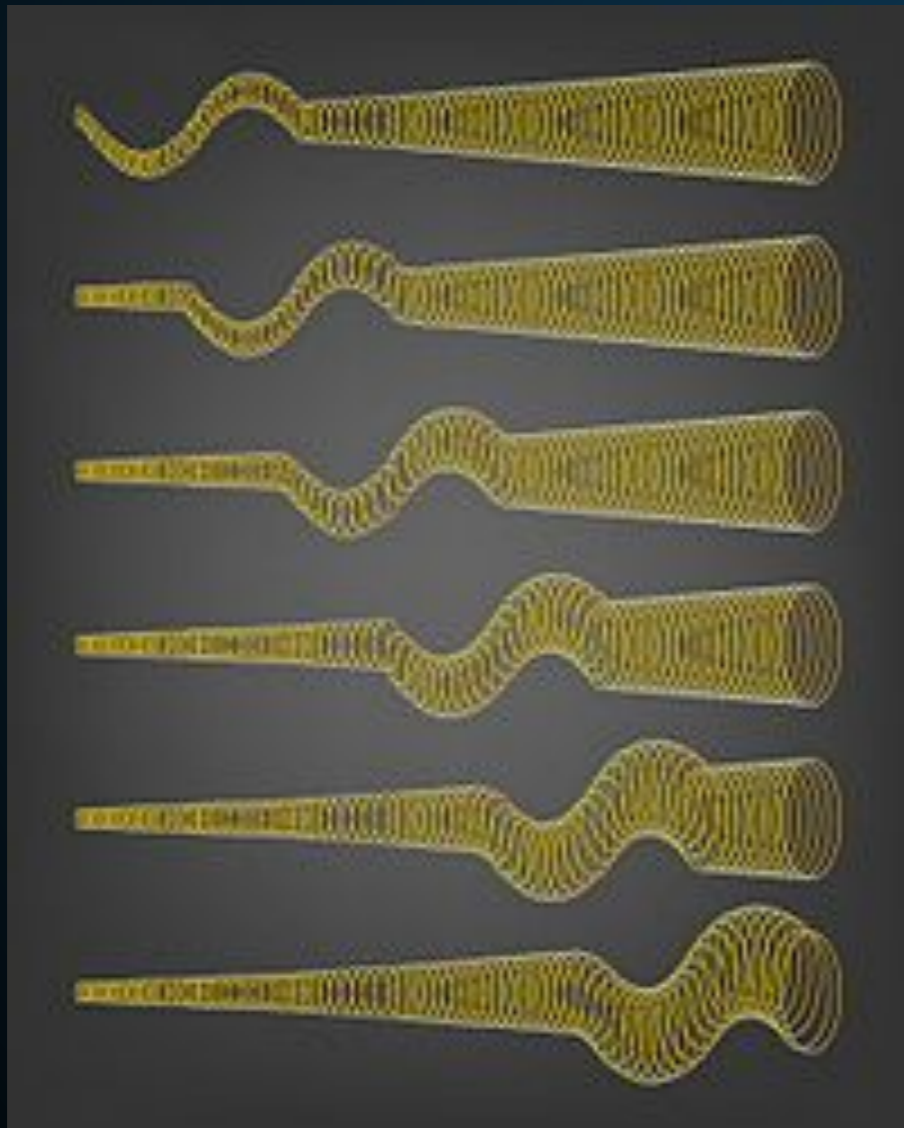
- **Diffusion is dominated by turbulence at a wavelength that is resonant with the particle gyroradius**

$$D(p, t) = \frac{4}{3\pi} \frac{c r_L(p)}{k_{\text{res}} \mathcal{W}(z, k_{\text{res}})}$$

## COSMIC-RAY DIFFUSION

---

- In regions with significant cosmic-ray anisotropies, the turbulence spectrum is dominated by self-generated turbulence produced by the streaming instability.



## COSMIC-RAY DIFFUSION

---

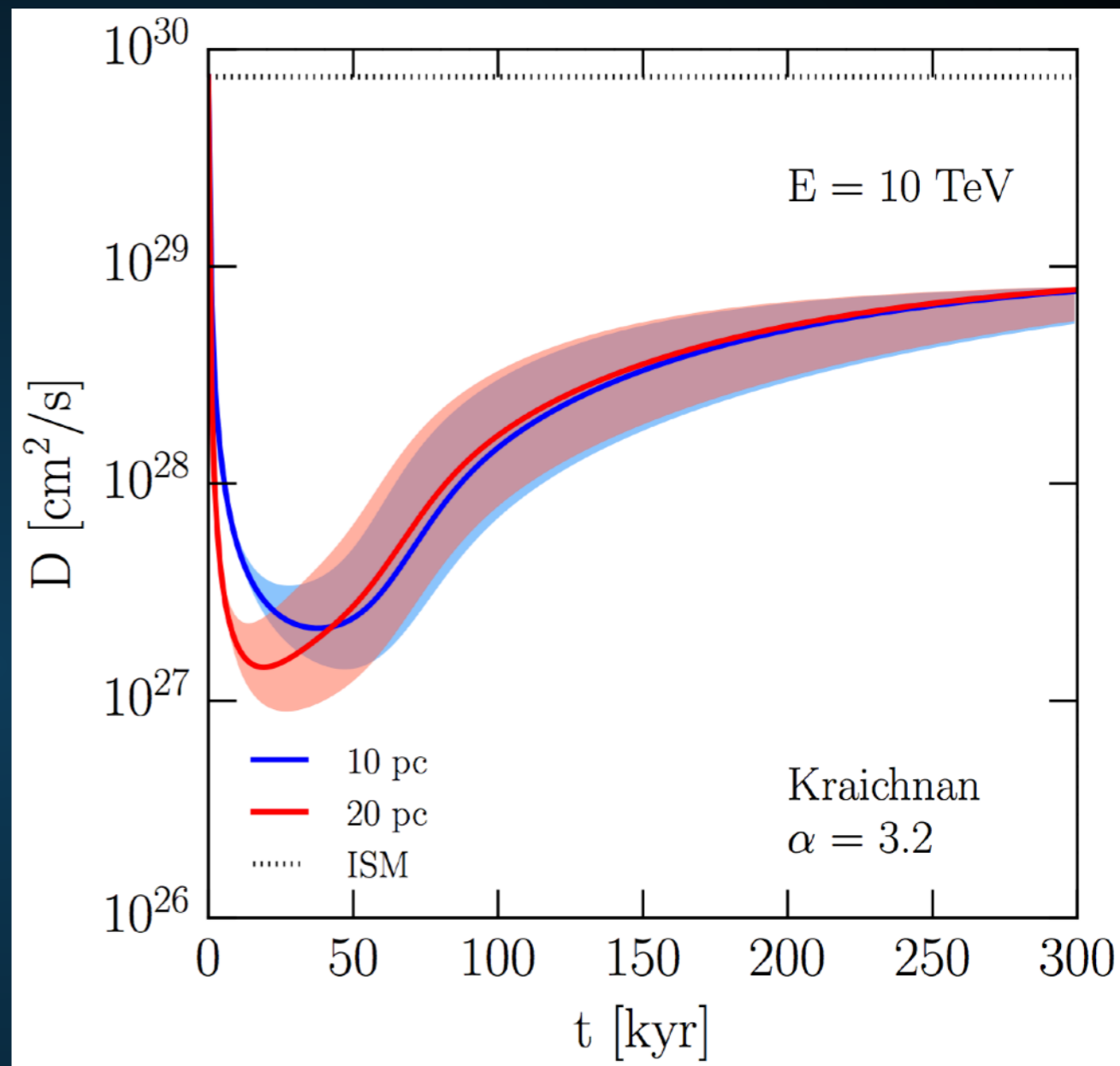
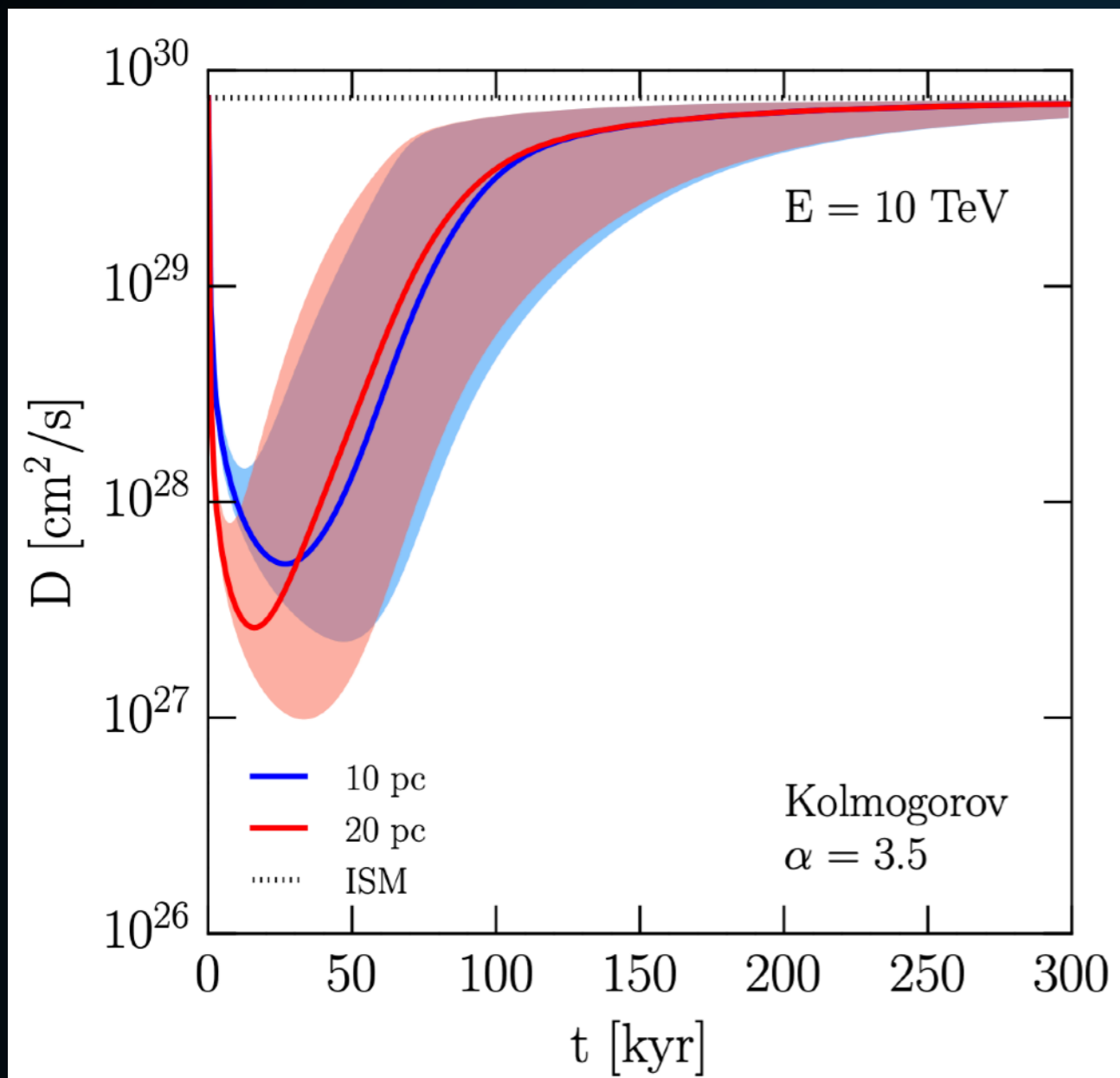
- **The turbulence spectrum at this wavenumber is controlled by a growth term depending on the streaming instability, and a damping term that depends on the background turbulence spectrum.**

$$\frac{\partial \mathcal{W}}{\partial t} + v_A \frac{\partial \mathcal{W}}{\partial z} = (\Gamma_{\text{CR}} - \Gamma_{\text{D}}) \mathcal{W}(k, z, t)$$

$$\Gamma_{\text{NLD}}(k) = c_k |v_A| \begin{cases} k^{3/2} \mathcal{W}^{1/2} & \text{(Kolmogorov)} \\ k^2 \mathcal{W} & \text{(Kraichnan)} \end{cases}$$

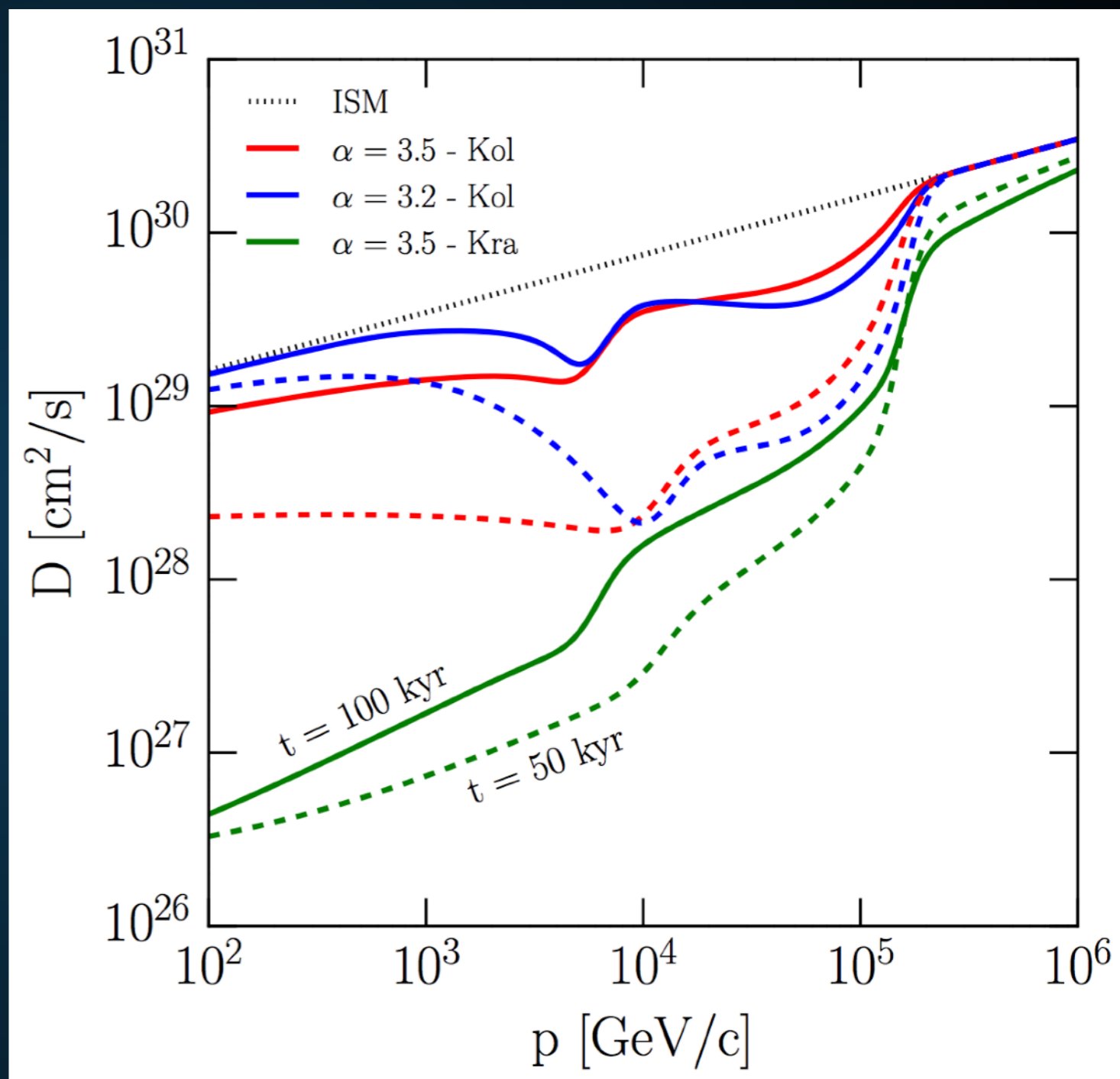
$$\Gamma_{\text{CR}}(k) = \frac{2\pi}{3} \frac{c |v_A|}{k \mathcal{W}(k) U_0} \left[ p^4 \frac{\partial f}{\partial z} \right]_{p_{\text{res}}}$$





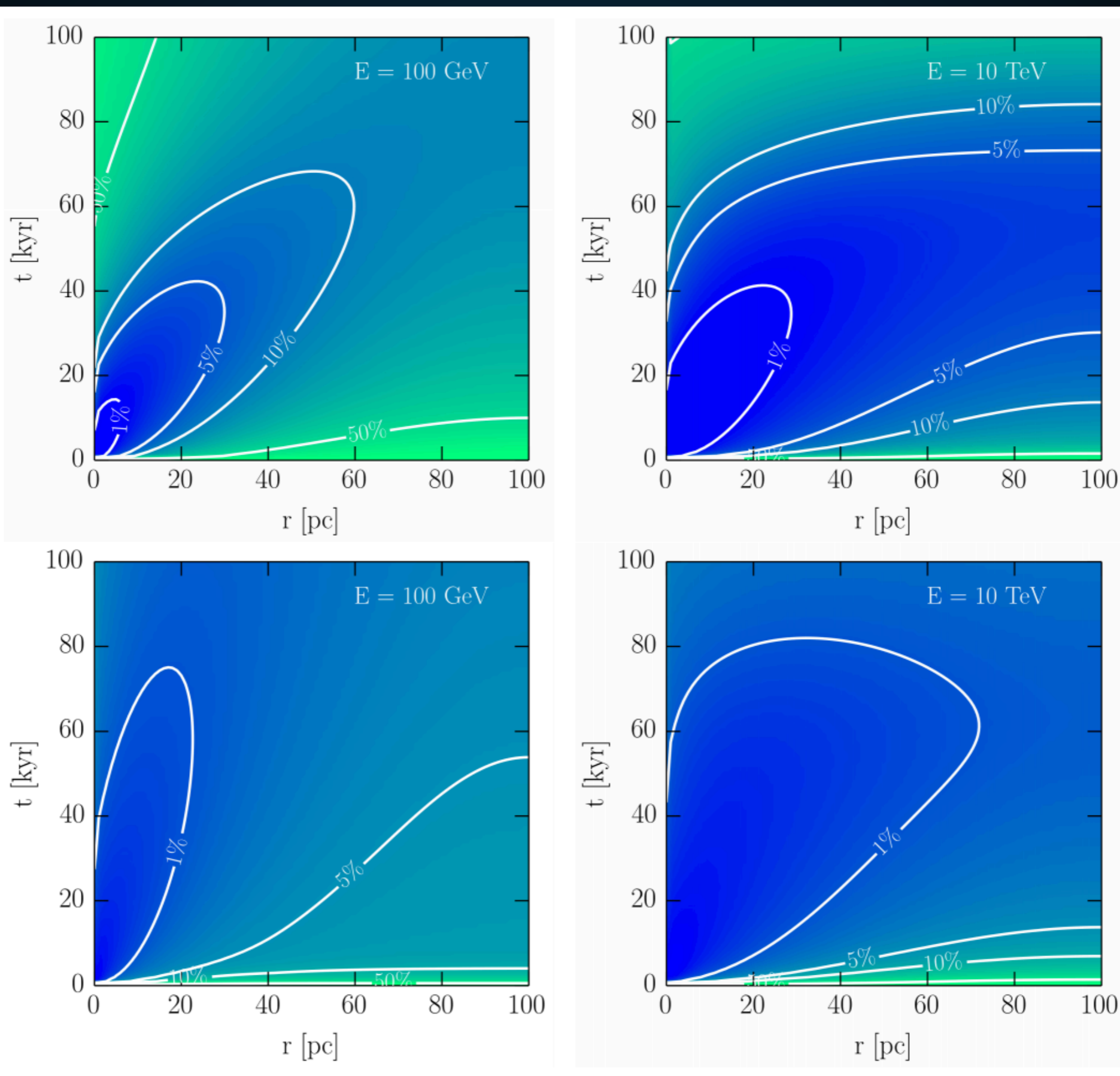
- **The effect is intense and time dependent.**
- **Relaxation rate strongly depends on turbulence spectrum.**

- Because most cosmic-rays are injected at high energies, high-energy diffusion is more inhibited.
- Can significantly affect the typical Kolmogorov or Kraichnan turbulence spectra.



# AN ANALYTIC MODEL FOR TEV HALOS

Evoli, TL, Morlino (2018; 1807.09263)





- **Implications for TeV Halos:**
  - **TeV halos take some time to form (earliest  $e^+e^-$  are not confined)**
  - **TeV halo parameters will depend on environment (to some extent)**
  - **Interference of multiple TeV halos can be destructive**
- **Early Stages:**
  - **Examined only single TeV halo in homogeneous ISM**
  - **Supernova Remnant not taken into account**

- **TeV observations open up a new window into understanding Milky Way pulsars.**
- **Early indications:**
  - **TeV halos power most TeV sources**
  - **TeV halos dominate the diffuse TeV emission**
  - **Positron Excess is due to pulsar activity**
  - **TeV halos produce regions of inhibited diffusion.**

- **Additional implications:**
  - **Young pulsar braking index**
  - **MSPs?**
  - **Source of IceCube neutrinos**
  - **TeV Dark Matter Constraints**

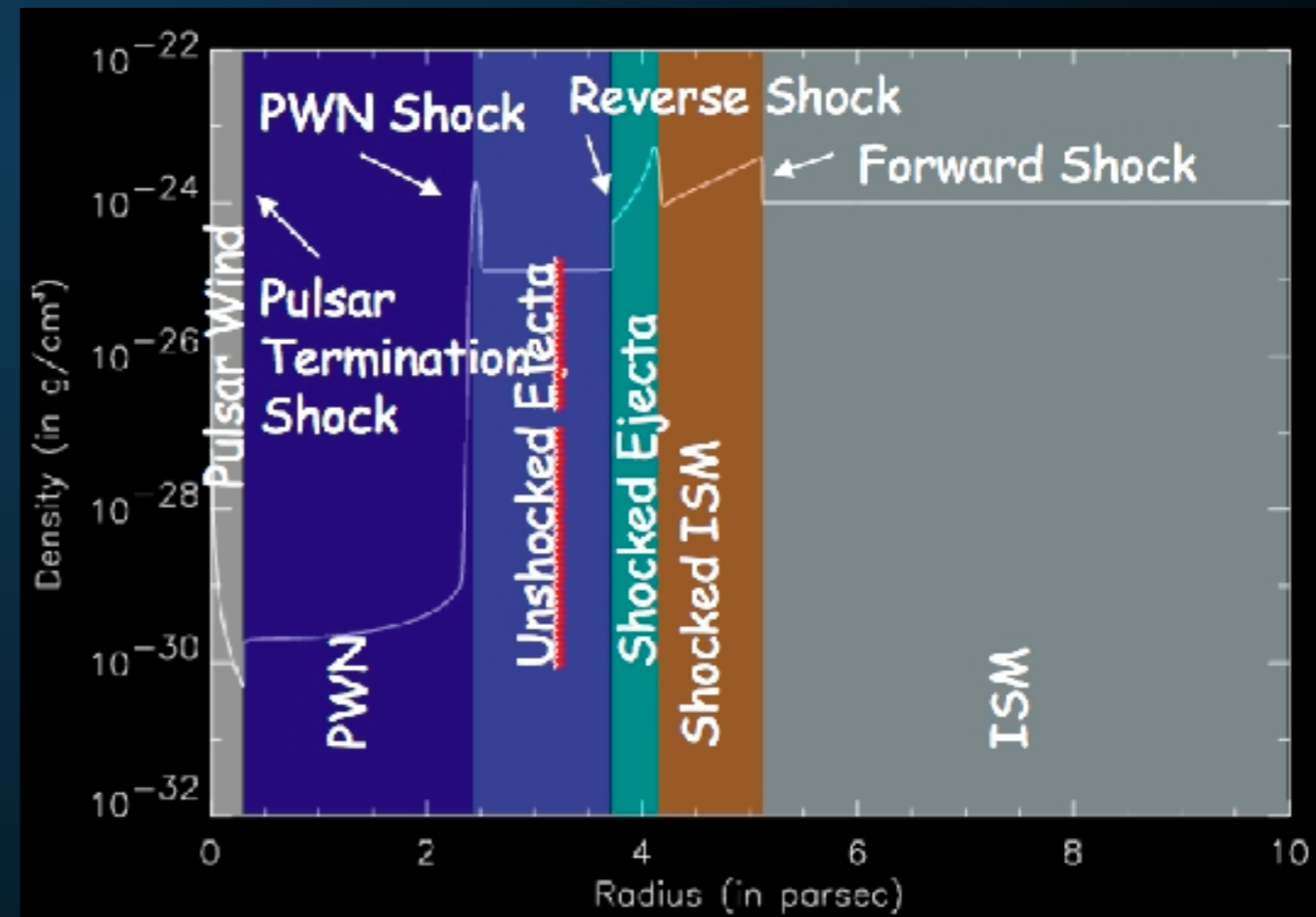


---

# Extra Slides

# WHAT ARE TEV HALOS

- **TeV halos are a new feature**
  - **3 orders of magnitude larger than PWN in volume**
  - **Opposite energy dependence**
- **PWN are morphologically connected to the physics of the termination shock**
- **TeV halos need a similar morphological description.**



---

**Strong evidence that Milky Way  
diffusion is extremely inhomogeneous!**



## CONFIRMING TEV HALOS

---

- **Several Methods to confirm TeV halo detections:**
  - **X-Ray PWN**
  - **X-Ray Halos**
  - **Thermal Pulsar Emission (see yesterday's talk)**

## X-RAY HALOS

---

- **An X-Ray halo with an identical morphology as the TeV halo must exist.**

$$E_{\text{sync,critical}} = 22 \text{ eV} \left( \frac{B}{5 \mu\text{G}} \right) \left( \frac{E_e}{10 \text{ TeV}} \right)^2$$

- **However, the signal has a low surface brightness and peaks at a low energy.**

## X-RAY PULSAR WIND NEBULAE

---



- **Larger magnetic fields make compact PWN easier to observe**
  - **Synchrotron dominated**
  - **Higher energy peak**
- **More distant sources easier to see.**
- **Significant observation times require careful HAWC analysis.**



# PULSARS PRODUCE THE POSITRON EXCESS

---

- **What were the uncertainties in pulsar models?**

- **I: The  $e^+e^-$  production efficiency?**

Profumo (0812.4457); Malyshev et al. (0903.1310)

%.

A quantitative discussion of plausible values for  $f_{e^\pm}$  was recently given in Ref. [38]. We shall not review their discussion here, but Ref. [38] argues (see in particular their very informative App. B and C) that in the context of a standard model for the pulsar wind nebulae, a reasonable range for  $f_{e^\pm}$  falls between 1% and 30%.

- **II: The  $e^+e^-$  spectrum.**

- **III: The propagation of  $e^+e^-$  to Earth.**

# PULSARS PRODUCE THE POSITRON EXCESS

---

- **What were the uncertainties in pulsar models?**

- **I: The  $e^+e^-$  production efficiency?**

- **II: The  $e^+e^-$  spectrum.**

Hooper et al. (0810.1527)

part of their energy adiabatically because of the expansion of the wind. The energy spectrum injected by a single pulsar depends on the environmental parameters of the pulsar, but some attempts to calculate the average spectrum injected by a population of mature pulsars suggest that the spectrum may be relatively hard, having a slope of  $\sim 1.5-1.6$  [18]. This spectrum, however, results from a complex interplay of individual pulsar spectra, of the spatial and age distributions of pulsars in the Galaxy, and on the assumption that the chief channel for pulsar spin down is magnetic dipole radiation. Due to the related uncertainties, variations from this injection spectra cannot be ruled out. Typically, one concentrates the attention on pulsars of age  $\sim 10^5$  years because younger pulsars are likely to still

- **III: The propagation of  $e^+e^-$  to Earth.**

# TEV HALOS ANSWER THE KEY QUESTIONS!

Name	Tested radius [°]	Index	$F_7 \times 10^{15}$ [TeV <sup>-1</sup> cm <sup>-2</sup> s <sup>-1</sup> ]	TeVCat
2HWC J0631+169	-	$-2.57 \pm 0.15$	$6.7 \pm 1.5$	Geminga
"	2.0	$-2.23 \pm 0.08$	$48.7 \pm 6.9$	Geminga
2HWC J0635+180	-	$-2.56 \pm 0.16$	$6.5 \pm 1.5$	Geminga

- We assume a power-law electron injection spectrum with an exponential cutoff

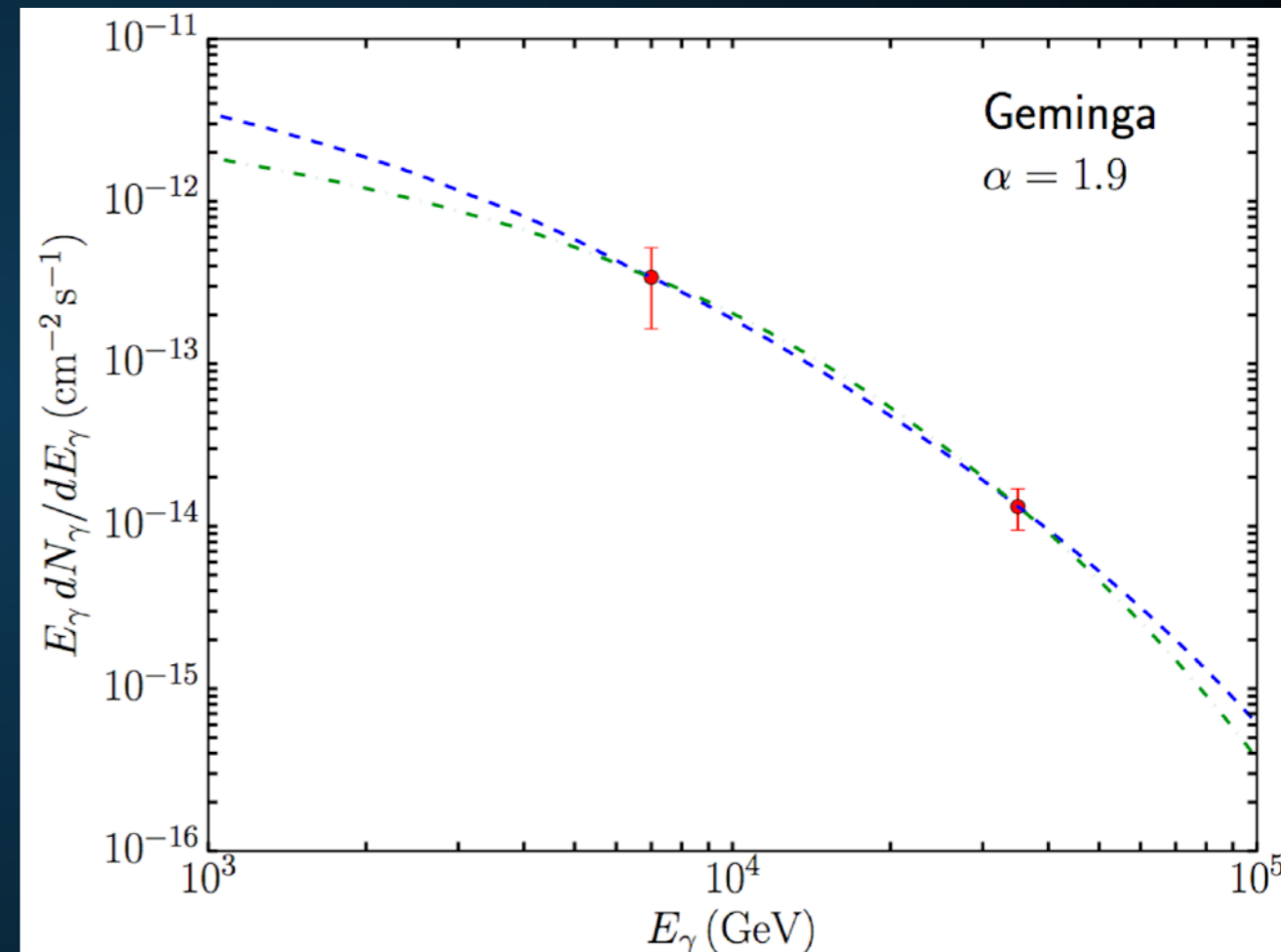
- Best Fit:

$$-1.9 < \alpha < -1.5$$

$$E_{\text{cut}} \cong 50 \text{ TeV}$$

$$\sim 3\text{-}9 \times 10^{33} \text{ erg s}^{-1} !$$

**9-27%** of the total pulsar spin-down power!





# PULSARS PRODUCE THE POSITRON EXCESS

---

- **What were the uncertainties in pulsar models?**

- **I: The  $e^+e^-$  production efficiency?**

- **II: The  $e^+e^-$  spectrum.**

- **III: The propagation of  $e^+e^-$  to Earth.**

Malyshev et al. (0903.1310)

The observed spectrum on Earth of electrons and positrons injected by pulsars is also strongly dependent on propagation effects. In particular, the observed cutoff in the flux of electrons from a pulsar can be much smaller than the injection cutoff due to energy losses (“cooling”) during propagation. We define the cooling break,  $E_{br}(t)$ , as the maximal energy electrons can have after propagating for time  $t$ . Since – as stated above – the typical

---

**Cosmic-ray propagation is the last key.**

---

**Fool me once.... shame on, shame on you...**

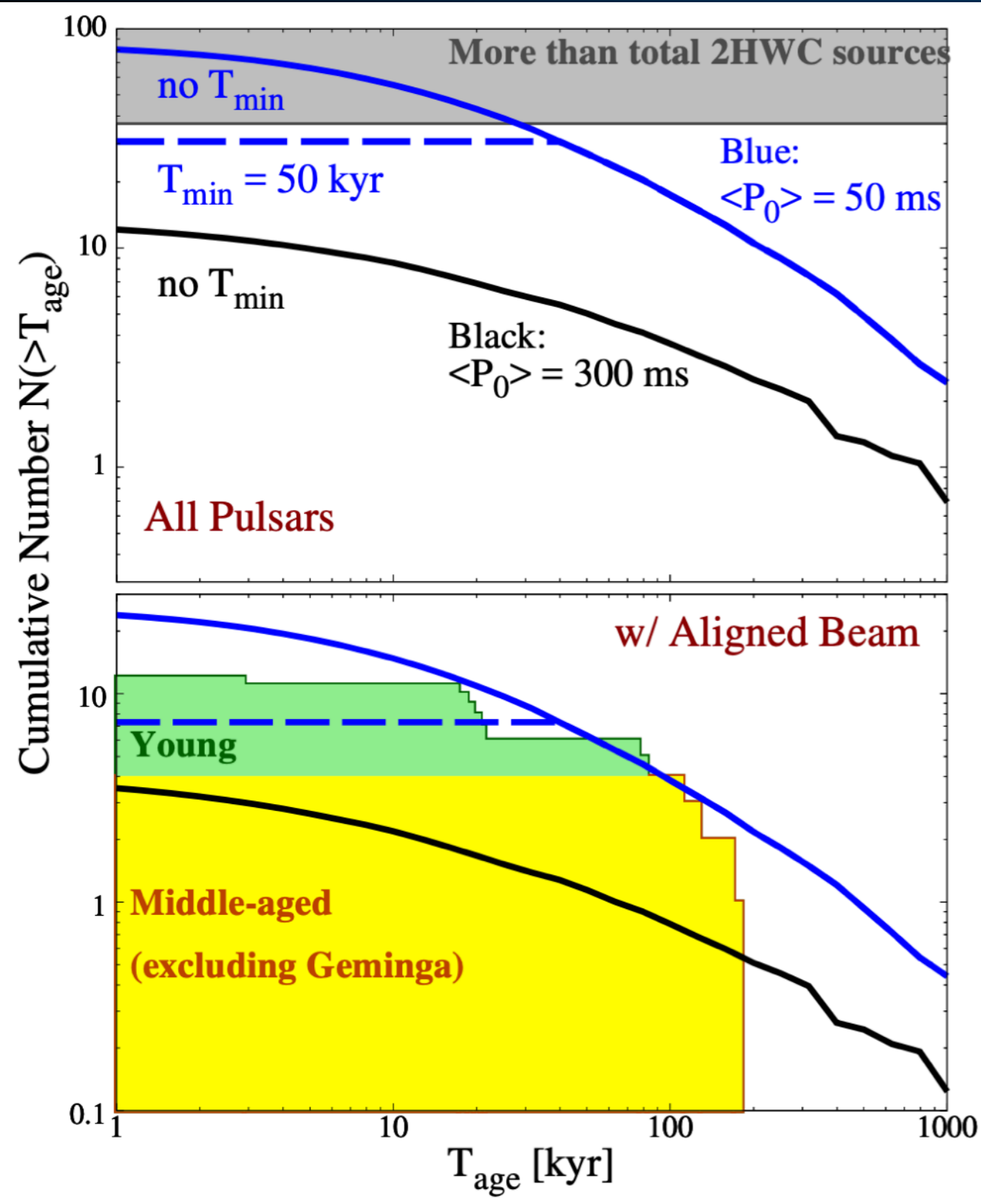
**Fool me..... you can't get fooled again!**



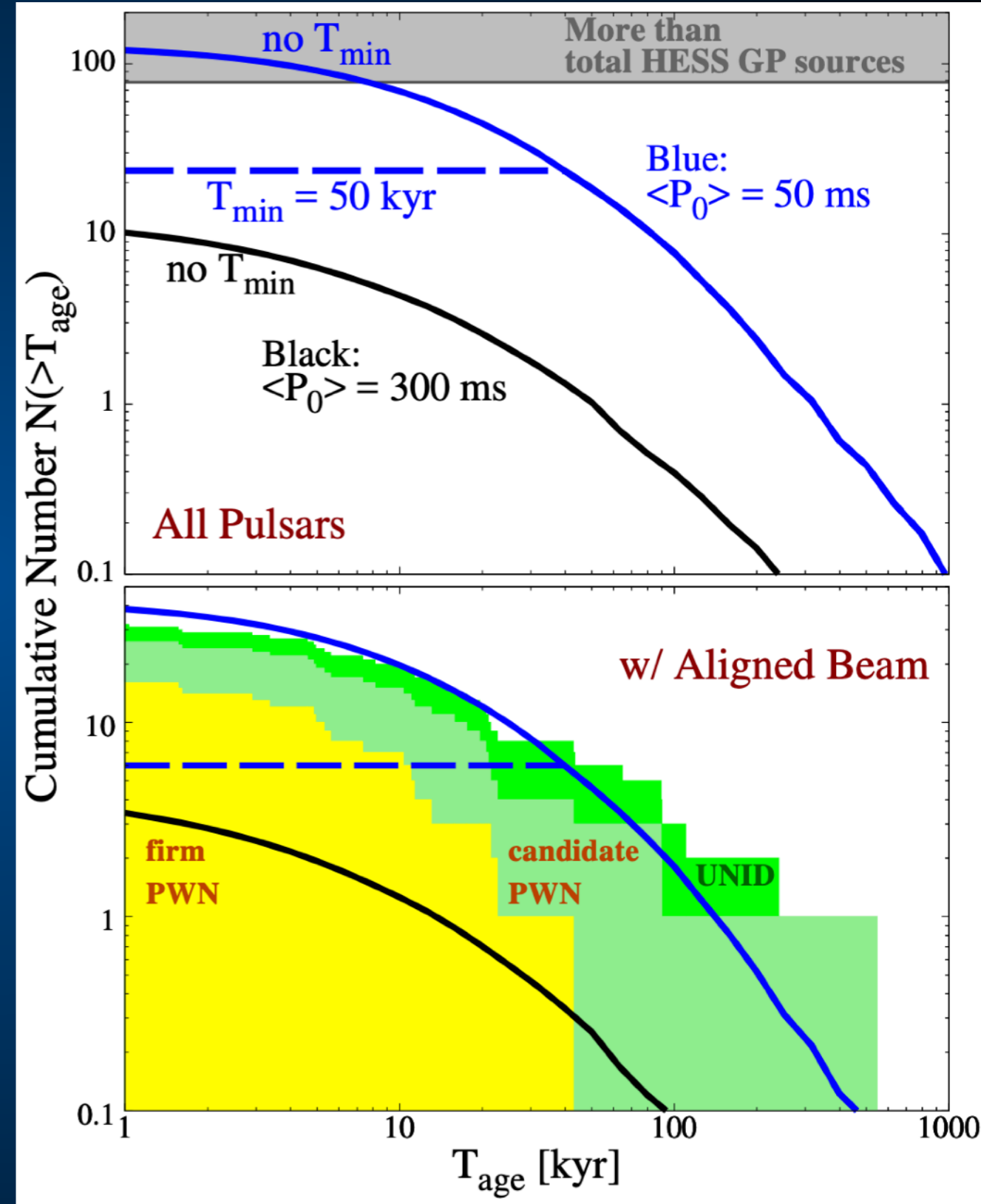




# Understanding Pulsars



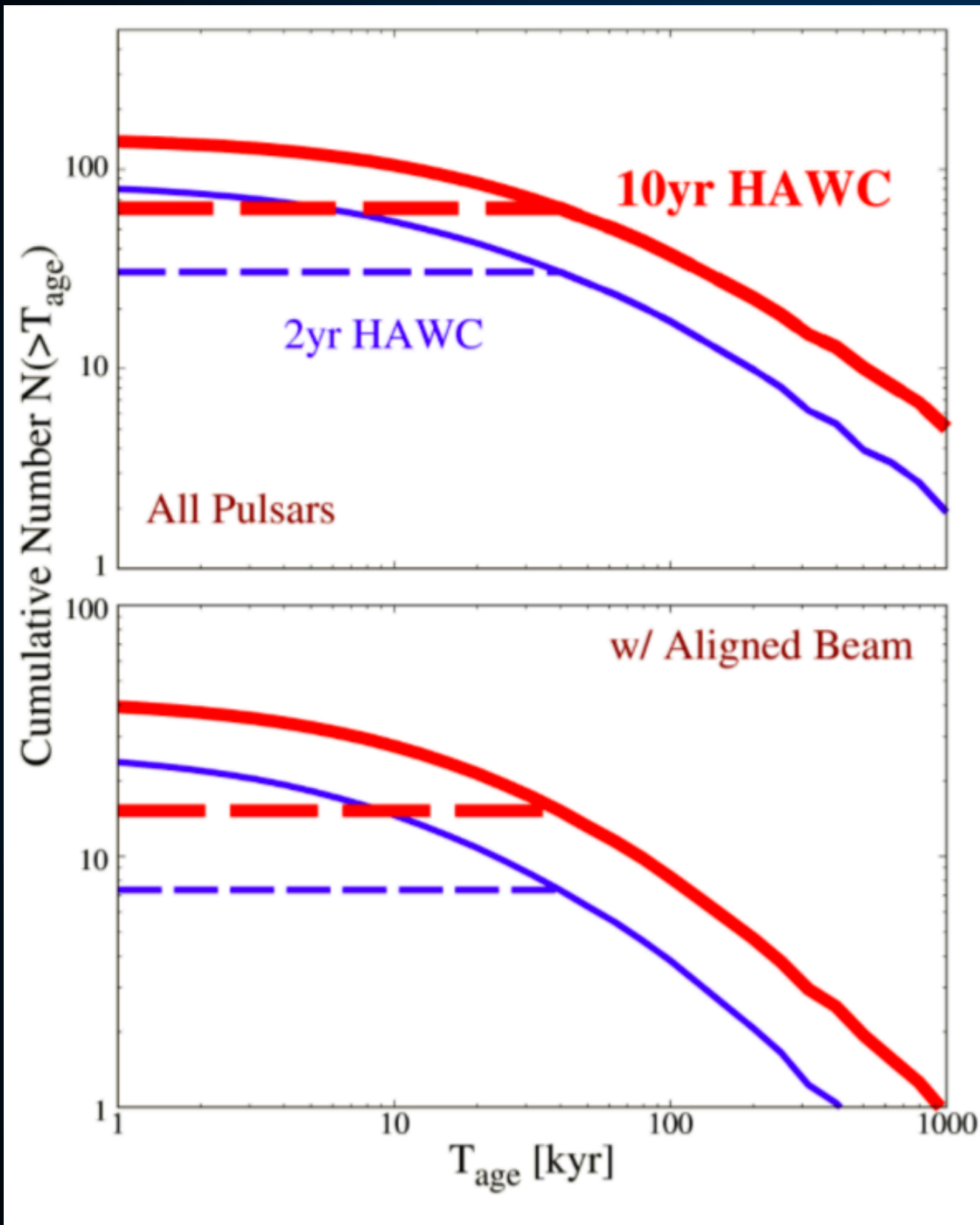
**HAWC**



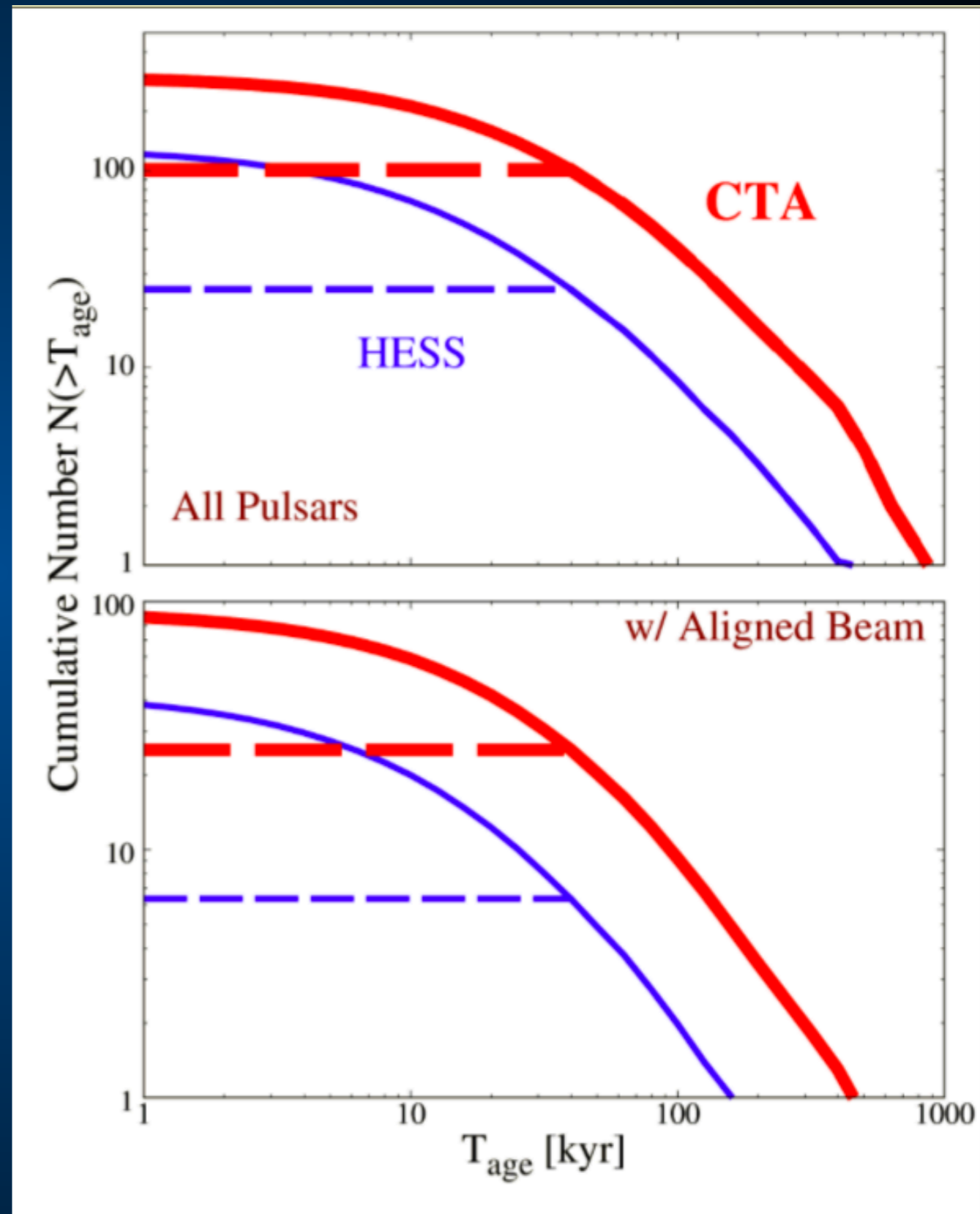
**HESS**

# Detecting New Pulsars

Sudoh, TL, Beacom (TBS)

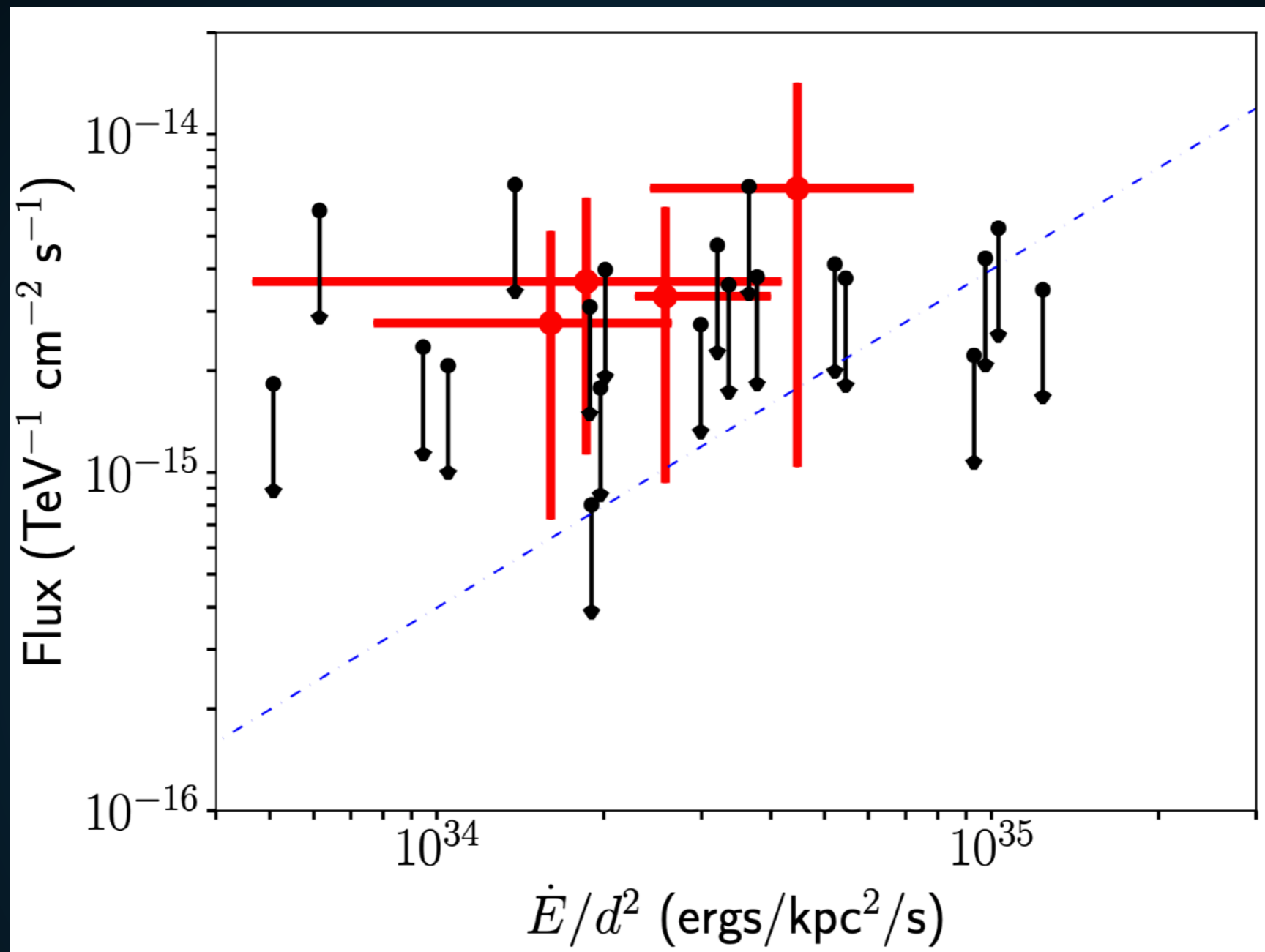


**HAWC (10 yr)**



**HESS/CTA**





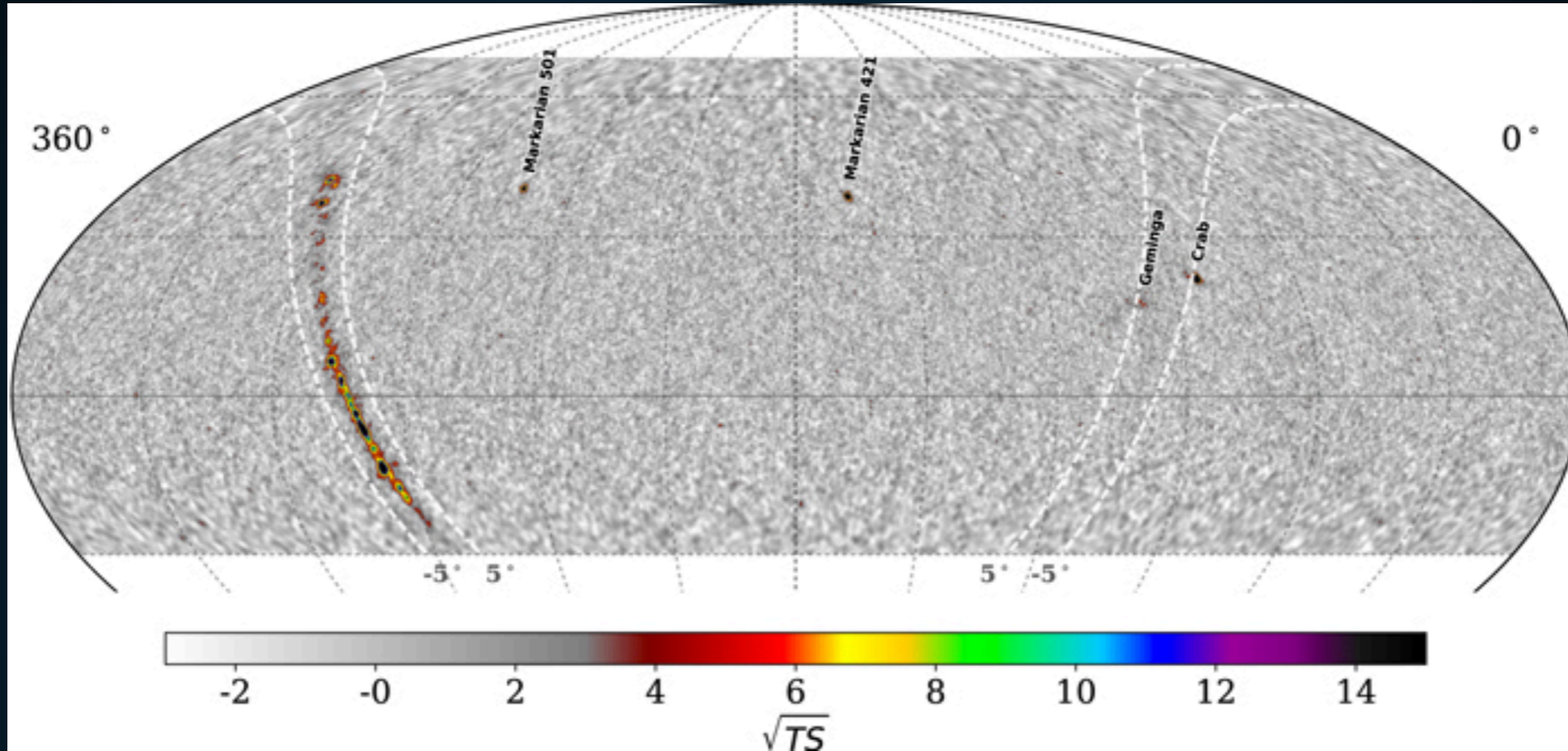
- Early evidence that millisecond pulsars also produce TeV halos.
- New opportunities to understand binary evolution.

- Should observe coincident synchrotron Halo
- Possible Detection! (G327-1.1)

	Region	Area (arcsec <sup>2</sup> )	Cts (1000)	N <sub>H</sub> (10 <sup>22</sup> cm <sup>-2</sup> )	Photon Index	Amplitude (10 <sup>-4</sup> )	kT (keV)	$\tau$ (10 <sup>12</sup> s cm <sup>-3</sup> )	Norm. (10 <sup>-3</sup> )	F <sub>1</sub> (10 <sup>-12</sup> )	F <sub>2</sub>	Red. $\chi^2$
1	Compact Source	84.657	6.34	1.93 <sup>+0.08</sup> <sub>-0.08</sub>	1.61 <sup>+0.08</sup> <sub>-0.07</sub>	1.05 <sup>+0.11</sup> <sub>-0.10</sub>	...	...	...	0.45	...	0.80
2	Cometary PWN	971.22	7.75	1.93	1.62 <sup>+0.08</sup> <sub>-0.07</sub>	1.47 <sup>+0.16</sup> <sub>-0.14</sub>	...	...	...	1.09	...	...
3	Trail East	537.42	2.13	1.93	1.84 <sup>+0.12</sup> <sub>-0.12</sub>	0.44 <sup>+0.07</sup> <sub>-0.06</sub>	...	...	...	0.27	...	...
4	Trail West	766.56	3.12	1.93	1.80 <sup>+0.11</sup> <sub>-0.11</sub>	0.61 <sup>+0.09</sup> <sub>-0.08</sub>	...	...	...	0.39	...	...
5	Trail 1	424.45	1.98	1.93	1.76 <sup>+0.12</sup> <sub>-0.12</sub>	0.39 <sup>+0.05</sup> <sub>-0.05</sub>	...	...	...	0.26	...	...
6	Trail 2	588.19	2.13	1.93	1.95 <sup>+0.11</sup> <sub>-0.11</sub>	0.49 <sup>+0.07</sup> <sub>-0.06</sub>	...	...	...	0.28	...	...
7	Trail 3	994.92	2.99	1.93	2.09 <sup>+0.10</sup> <sub>-0.10</sub>	0.78 <sup>+0.09</sup> <sub>-0.08</sub>	...	...	...	0.42	...	...
8	Trail 4	839.48	2.38	1.93	2.28 <sup>+0.12</sup> <sub>-0.12</sub>	0.74 <sup>+0.09</sup> <sub>-0.09</sub>	...	...	...	0.37	...	...
9	Prong East	828.58	1.66	1.93	1.72 <sup>+0.14</sup> <sub>-0.14</sub>	0.30 <sup>+0.06</sup> <sub>-0.05</sub>	...	...	...	0.27	...	...
10	Prong West	971.22	2.06	1.93	1.85 <sup>+0.14</sup> <sub>-0.14</sub>	0.44 <sup>+0.08</sup> <sub>-0.07</sub>	...	...	...	1.09	...	...
11	Diffuse PWN*	20007	27.7	1.93	2.11 <sup>+0.04</sup> <sub>-0.05</sub>	6.91 <sup>+0.37</sup> <sub>-0.74</sub>	0.23 <sup>+0.14</sup> <sub>-0.05</sub>	0.21 <sup>+0.88</sup> <sub>-0.16</sub>	6.0 <sup>+16</sup> <sub>-4.0</sub>	3.68	17.7	0.82
12	Relic PWN*	26787	17.2	1.93	2.58 <sup>+0.07</sup> <sub>-0.10</sub>	6.51 <sup>+0.53</sup> <sub>-0.71</sub>	0.23	0.21	6.9 <sup>+18</sup> <sub>-5.5</sub>	3.14	20.3	...

- New opportunities for studying TeV halo morphologies!

# TEV HALO NUMEROLOGY

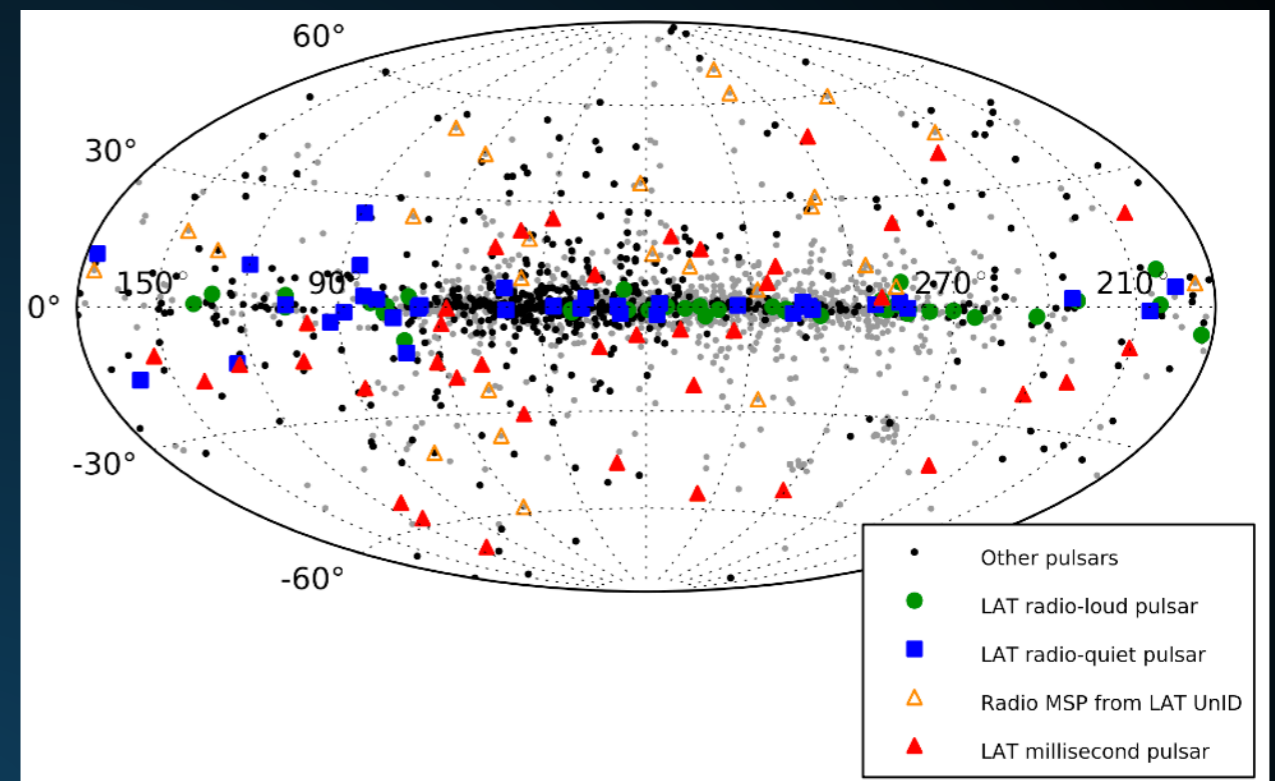


ATNF Name	Dec. ( $^{\circ}$ )	Distance (kpc)	Age (kyr)	Spindown Lum. ( $\text{erg s}^{-1}$ )	Spindown Flux ( $\text{erg s}^{-1} \text{kpc}^{-2}$ )	2HWC
J0633+1746	17.77	0.25	342	$3.2\text{e}34$	$4.1\text{e}34$	2HWC J0631+169
B0656+14	14.23	0.29	111	$3.8\text{e}34$	$3.6\text{e}34$	2HWC J0700+143
B1951+32	32.87	3.00	107	$3.7\text{e}36$	$3.3\text{e}34$	—
J1740+1000	10.00	1.23	114	$2.3\text{e}35$	$1.2\text{e}34$	—
J1913+1011	10.18	4.61	169	$2.9\text{e}36$	$1.1\text{e}34$	2HWC J1912+099
J1831-0952	-9.86	3.68	128	$1.1\text{e}36$	$6.4\text{e}33$	2HWC J1831-098
J2032+4127	41.45	1.70	181	$1.7\text{e}35$	$4.7\text{e}33$	2HWC J2031+415
B1822-09	-9.58	0.30	232	$4.6\text{e}33$	$4.1\text{e}33$	—
B1830-08	-8.45	4.50	147	$5.8\text{e}35$	$2.3\text{e}33$	—
J1913+0904	9.07	3.00	147	$1.6\text{e}35$	$1.4\text{e}33$	—
B0540+23	23.48	1.56	253	$4.1\text{e}34$	$1.4\text{e}33$	—



# MISSING TEV HALOS

- Fermi-LAT has 5 middle-aged pulsars in the HAWC field.



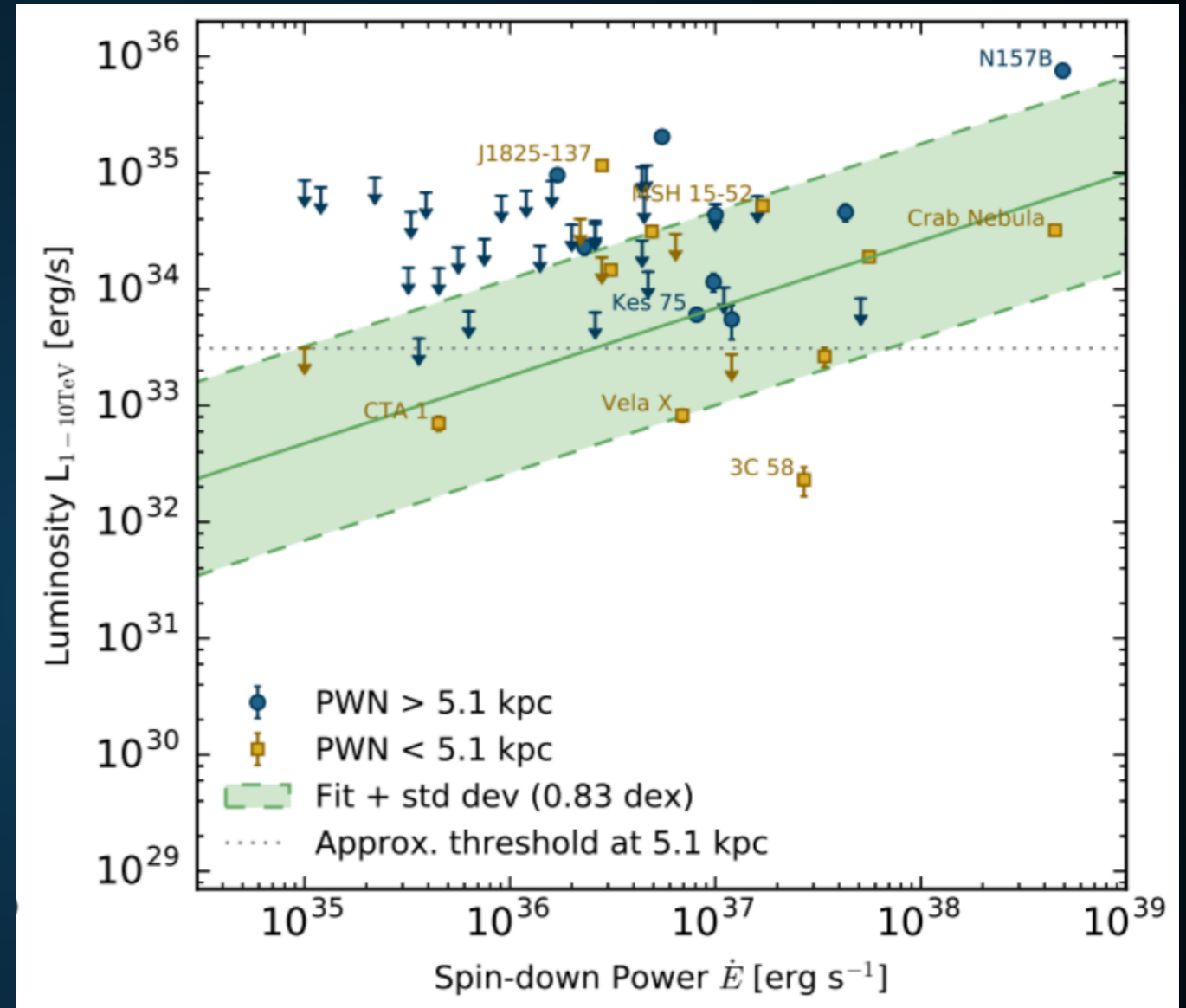
- X-Ray studies have only reported 6 X-Ray PWN without pulsars in the HAWC field of view.

PWNe With No Detected Pulsar						
Gname	other name(s)	R	X	O	G	
G0.13-0.11					?	notes
G0.9+0.1					N	notes
G7.4-2.0	GeV J1809-2327, Tazzie				Y	notes
G16.7+0.1					N	notes
G18.5-0.4	GeV J1825-1310, Eel				Y	notes
G20.0-0.2					N	notes
G24.7+0.6					N	notes
G27.8+0.6					N	notes
G39.2-0.3	3C 396				Y	notes
G63.7+1.1					N	notes
G74.9+1.2	CTB 87				Y	notes
G119.5+10.2	CTA 1				Y	notes
G189.1+3.0	IC 443				?	notes
G279.8-35.8	B0453-685				N	notes
G291.0-0.1	MSH 11-62				Y	notes
G293.8+0.6					N	notes
G313.3+0.1	Rabbit				Y	notes
G318.9+0.4					N	notes
G322.5-0.1					N	notes
G326.3-1.8	MSH 15-56				N	notes
G327.1-1.1					N	notes
G328.4+0.2	MSH 15-57				N	notes
G358.6-17.2	RX J1856.5-3754	N	N		N	notes
G359.89-0.08					Y	notes

**What if the “Geminga”-like  
model is wrong?**

- ▶ Alternatively can utilize HESS results which find:

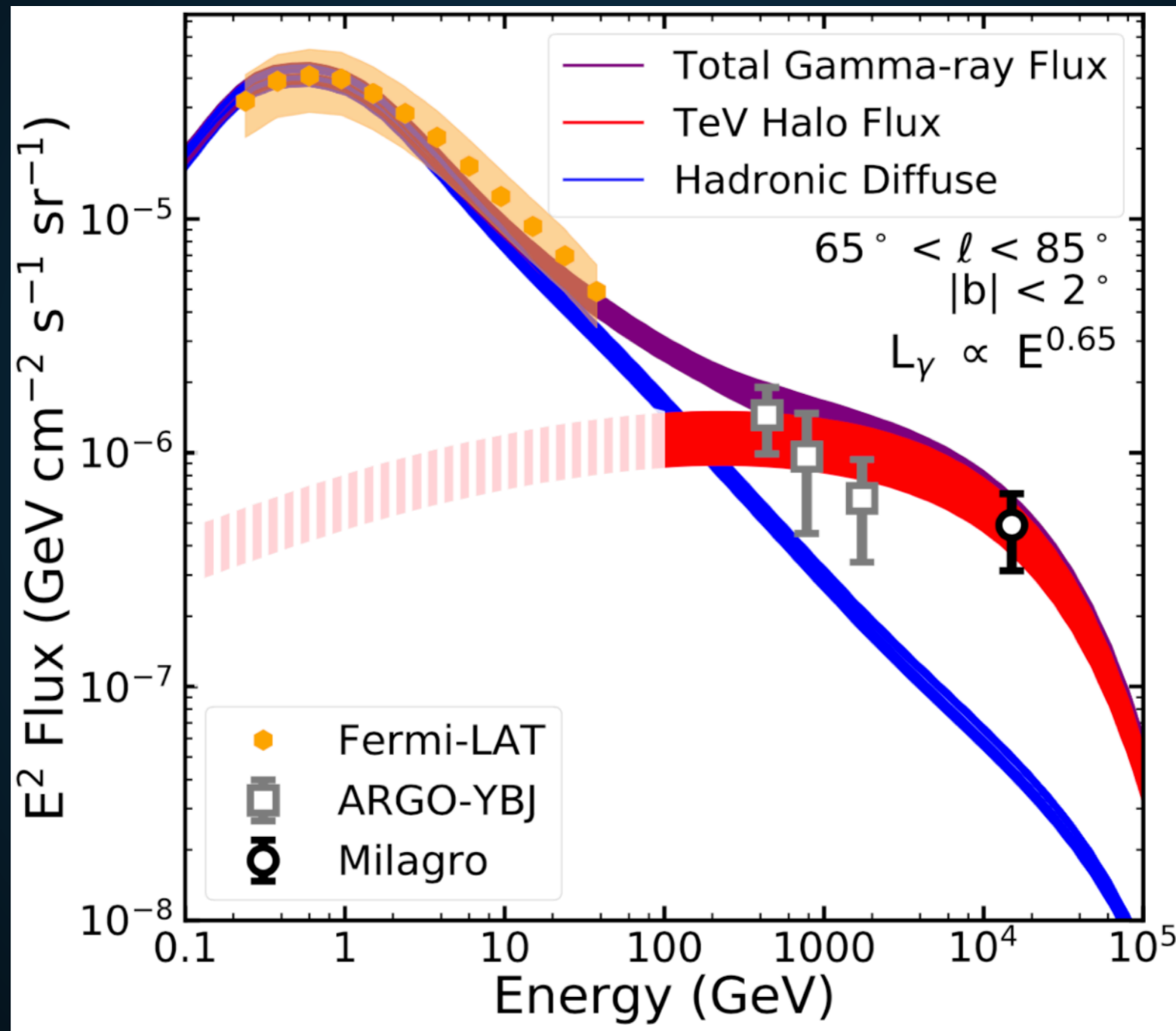
$$L = \dot{E}_{\text{dot}}^{0.59}$$



$$\phi_{\text{TeV halo}} = \left( \frac{\dot{E}_{\text{psr}}}{\dot{E}_{\text{Geminga}}} \right) \left( \frac{d_{\text{Geminga}}^2}{d_{\text{psr}}^2} \right) \phi_{\text{Geminga}}$$

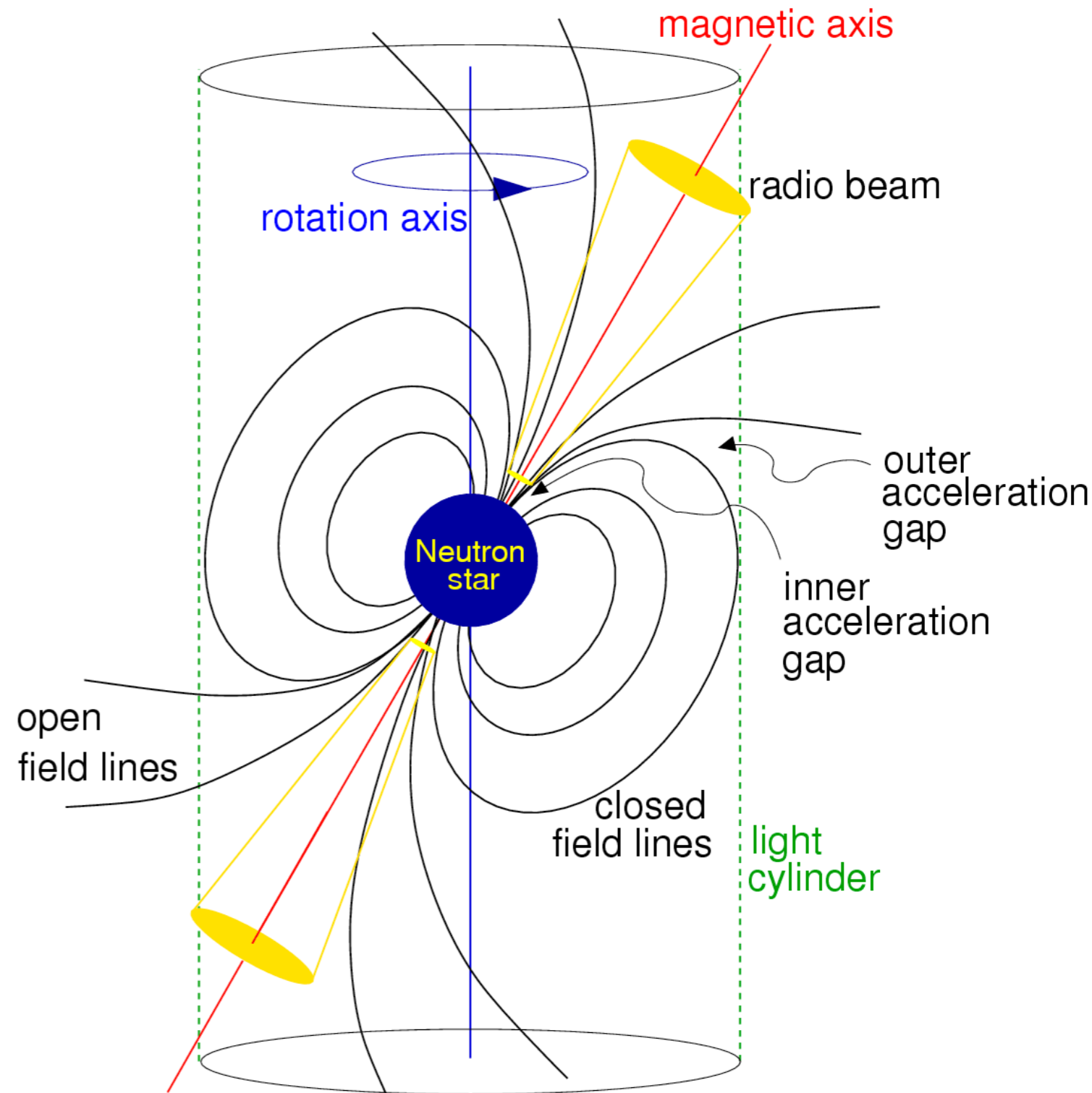


▶ TeV halos naturally explain the TeV excess!

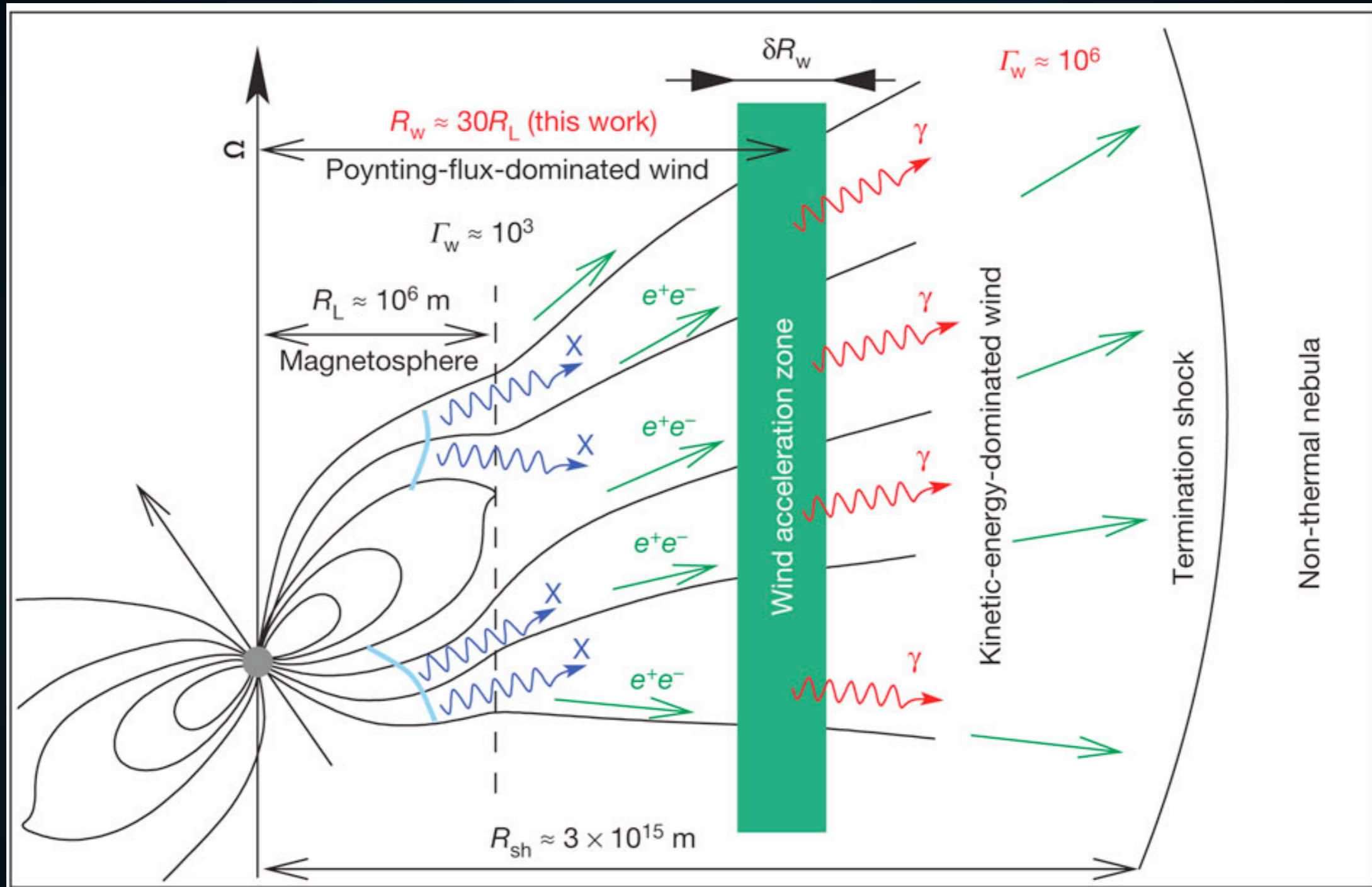


# PULSARS AS ASTROPHYSICAL ACCELERATORS

- ▶ radio beam
- ▶ gamma-ray beam
- ▶  $e^+e^-$  acceleration in pulsar magnetosphere
- ▶  $e^+e^-$  acceleration at termination shock



# PRODUCTION OF ELECTRON AND POSITRON PAIRS



- ▶ Final  $e^+e^-$  spectrum is model dependent.
- ▶ Understanding this is important for MSPs.



## ENERGY LOSSES ARE DOMINATED BY THE ISM

- It is not energetically possible for Geminga to produce the magnetic field or ISRF that these electrons interact with.

$$U = \frac{1}{8\pi} B^2 = \frac{(10 \mu\text{G})^2}{8\pi}$$
$$= 4 \times 10^{-12} \frac{\text{erg}}{\text{cm}^3}$$
$$\int_0^{10 \text{ pc}} U dV = 5 \times 10^{47} \text{ erg}$$
$$\hookrightarrow \text{Magnetic Flux} \approx 5 \times 10^{38} \frac{\text{erg}}{\text{s}}$$

$$\text{ISRF} = 1 \frac{\text{eV}}{\text{cm}^3}$$
$$\int \text{ISRF} dV = 8 \times 10^{47} \text{ erg}$$
$$\hookrightarrow \text{Flux} = 8 \times 10^{38} \frac{\text{erg}}{\text{s}}$$

- We can use typical ISM values ( $5 \mu\text{G}$ ;  $1 \text{ eV cm}^{-3}$ ) to characterize interactions.
- Nearly equal energy to synchrotron and ICS.

# X-RAY PWN DETECTIONS

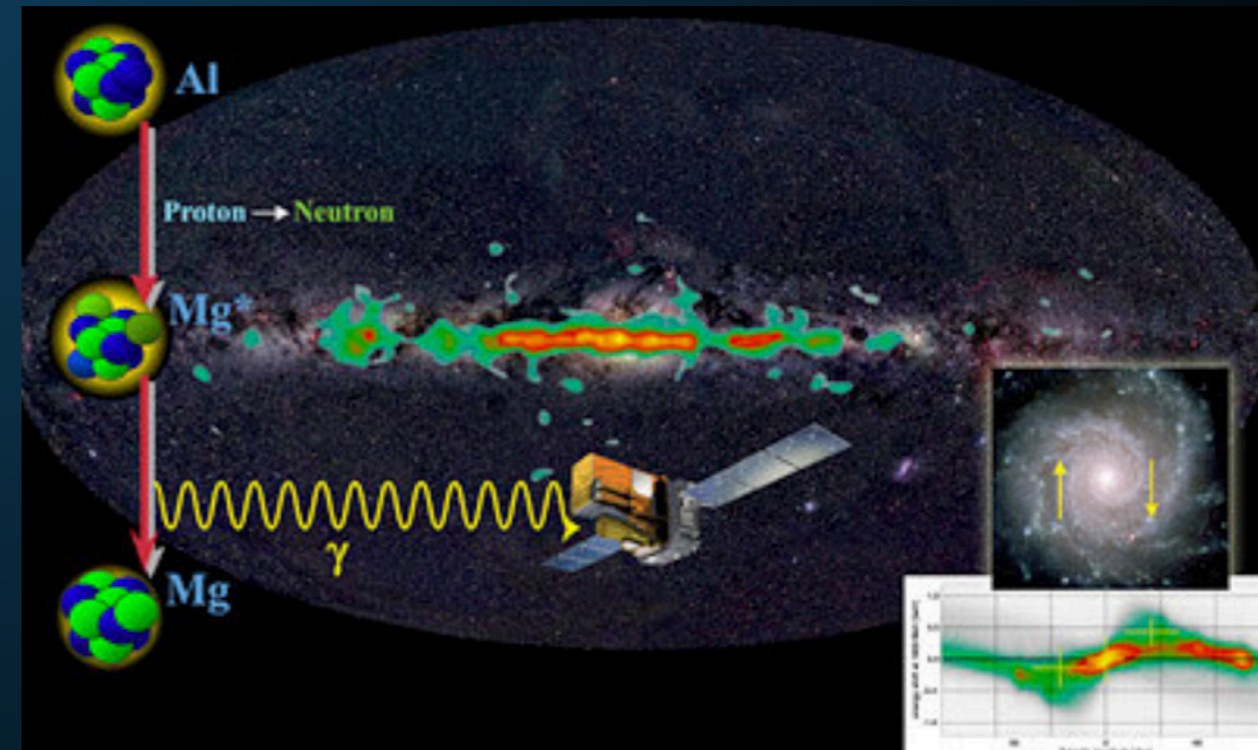
PWNe With No Detected Pulsar						
Gname	other name(s)	R	X	Q	G	
G0.13-0.11					?	notes
G0.9+0.1					N	notes
G7.4-2.0	GeV J1809-2327, Tazzie				Y	notes
G16.7+0.1					N	notes
G18.5-0.4	GeV J1825-1310, Eel				Y	notes
G20.0-0.2					N	notes
G24.7+0.6					N	notes
G27.8+0.6					N	notes
G39.2-0.3	3C 396				Y	notes
G63.7+1.1					N	notes
G74.9+1.2	CTB 87				Y	notes
G119.5+10.2	CTA 1				Y	notes
G189.1+3.0	IC 443				?	notes
G279.8-35.8	B0453-685				N	notes
G291.0-0.1	MSH 11-62				Y	notes
G293.8+0.6					N	notes
G313.3+0.1	Rabbit				Y	notes
G318.9+0.4					N	notes
G322.5-0.1					N	notes
G326.3-1.8	MSH 15-56				N	notes
G327.1-1.1					N	notes
G328.4+0.2	MSH 15-57				N	notes
G358.6-17.2	RX J1856.5-3754	N	N		N	notes
G359.89-0.08					Y	notes

▶ X-Ray PWN have detected only ~6 of these 37 systems.

# GEMINGA ISN'T SPECIAL

$$f \sim \frac{N_{\text{region}} \times \frac{4\pi}{3} r_{\text{region}}^3}{\pi R_{\text{MW}}^2 \times 2z_{\text{MW}}}$$
$$\sim 0.25 \times \left( \frac{r_{\text{region}}}{100 \text{ pc}} \right)^3 \left( \frac{\dot{N}_{\text{SN}}}{0.03 \text{ yr}^{-1}} \right) \left( \frac{\tau_{\text{region}}}{10^6 \text{ yr}} \right) \left( \frac{20 \text{ kpc}}{R_{\text{MW}}} \right)^2 \left( \frac{200 \text{ pc}}{z_{\text{MW}}} \right)$$

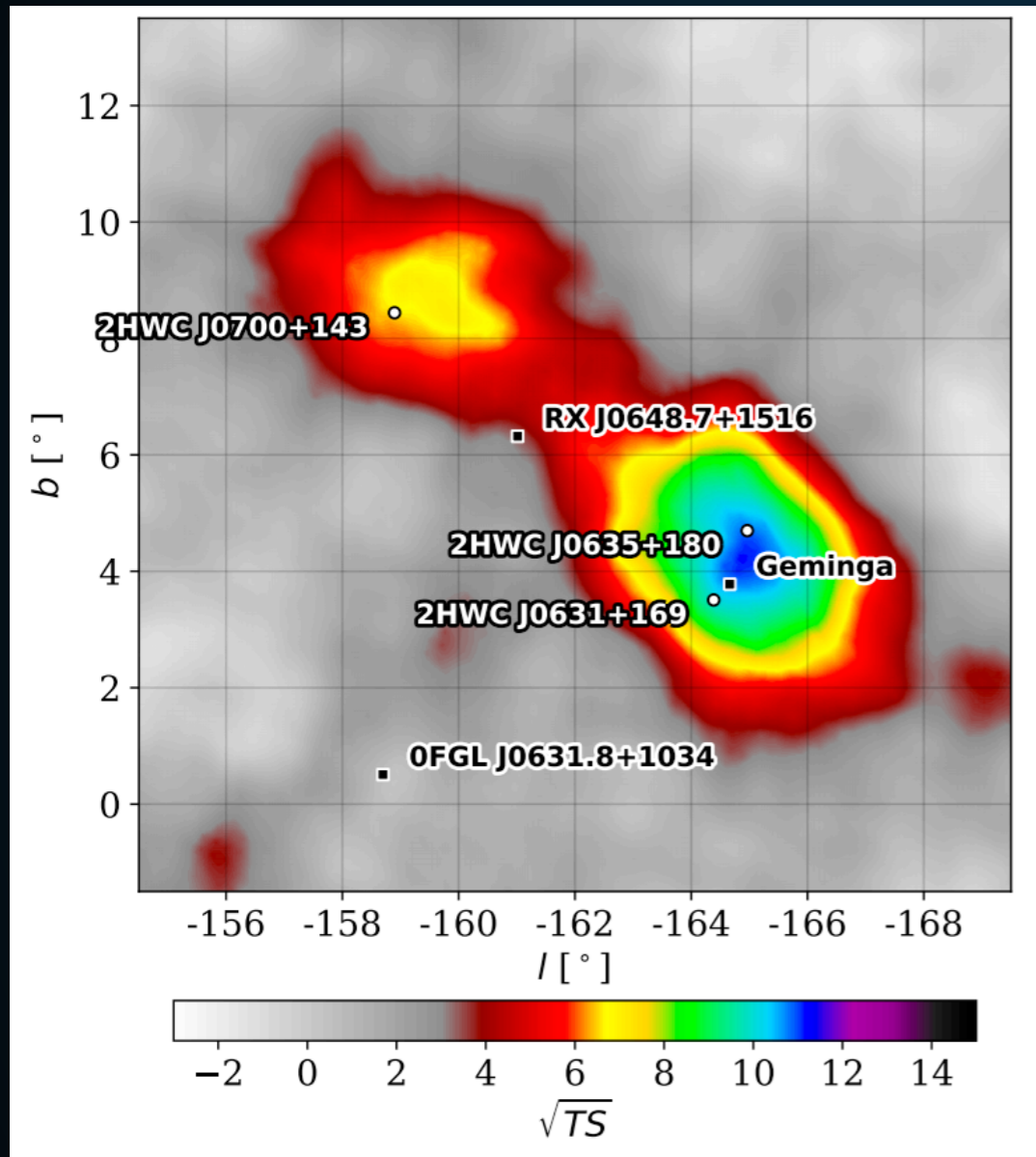
- Galactic Supernova rate  $\sim 0.02 \text{ yr}^{-1}$
- If each supernova (and natal pulsar) produces a large diffusion region, the diffusion constant should be low everywhere.
- Only alternative is that a very unique event produced the local bubble.





# TWO CONTRASTING OBSERVABLES

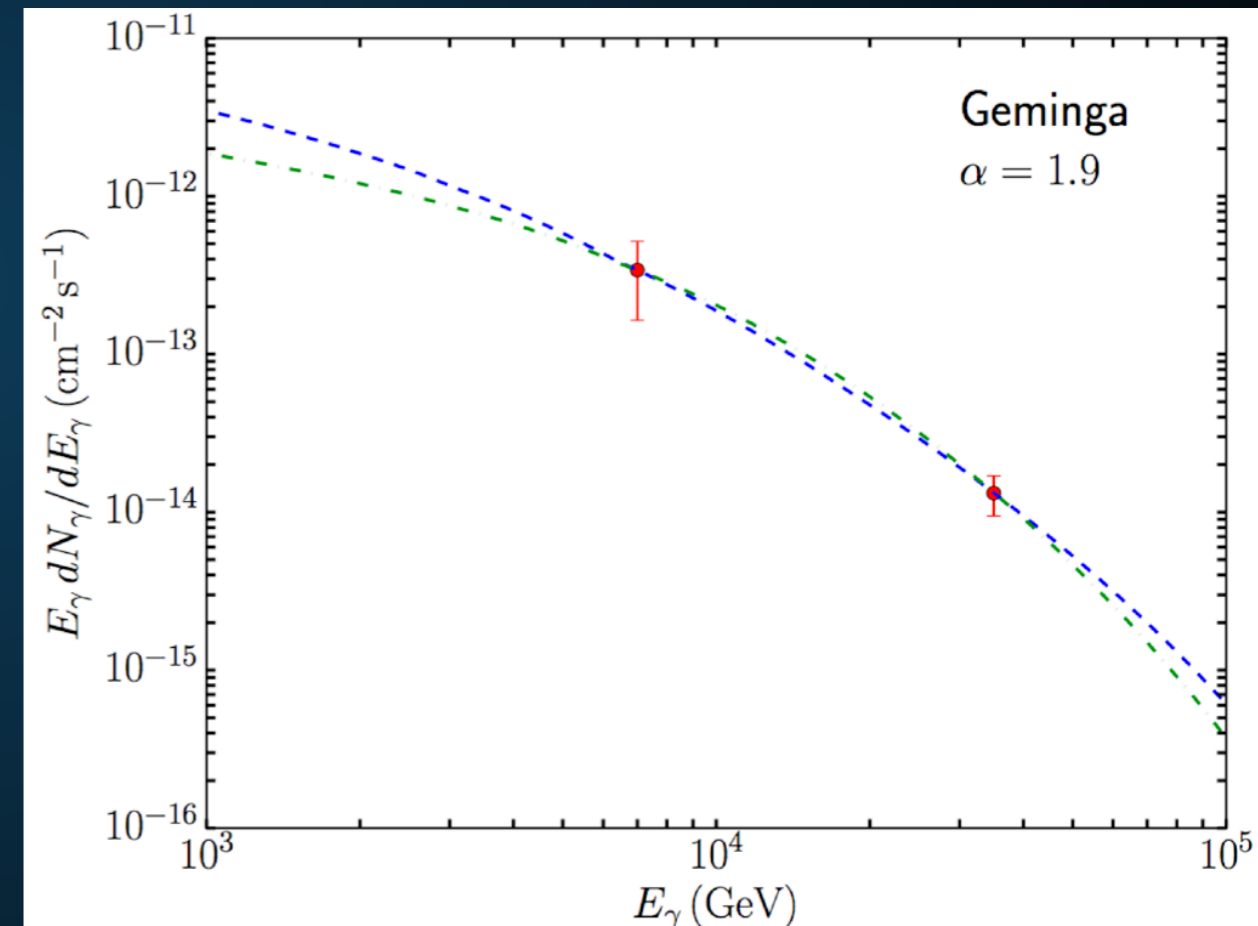
## Geminga is Bright



Indicative of significant  
electron cooling

## Geminga has a hard-spectrum

Name	Tested radius [°]	Index	$F_7 \times 10^{15}$ [ $\text{TeV}^{-1} \text{cm}^{-2} \text{s}^{-1}$ ]	TeVCat
2HWC J0631+169	-	$-2.57 \pm 0.15$	$6.7 \pm 1.5$	Geminga
"	2.0	$-2.23 \pm 0.08$	$48.7 \pm 6.9$	Geminga
2HWC J0635+180	-	$-2.56 \pm 0.16$	$6.5 \pm 1.5$	Geminga



Indicative of minimal  
electron cooling

## TOTAL POWER OF TEV HALOS

---

- ▶ **Measured Geminga flux translates to an intensity:**

$$2.86 \times 10^{31} \text{ erg s}^{-1} \text{ at 7 TeV}$$

- ▶ **For the best-fit spectrum, this requires an  $e^+e^-$  injection:**

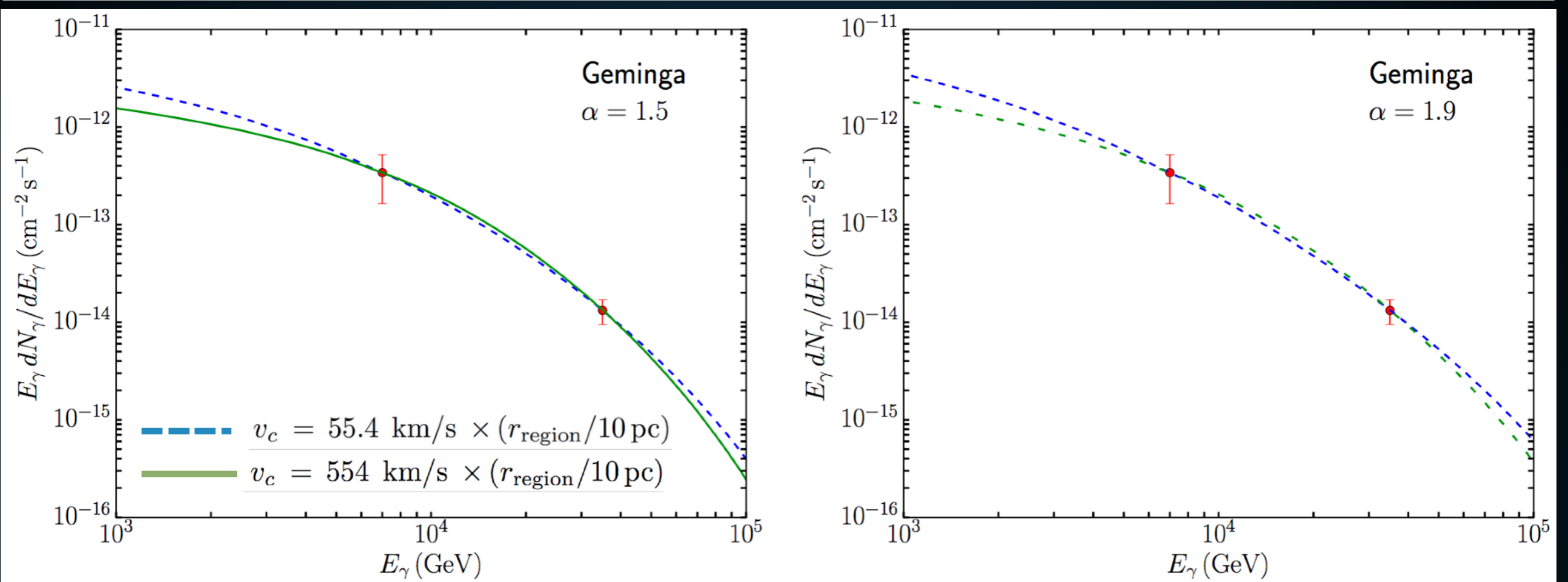
$$3.8 \times 10^{33} \text{ erg s}^{-1}$$

- ▶ **Total Spindown Power of Geminga is:**

$$3.4 \times 10^{34} \text{ erg s}^{-1}$$

- ▶ **Roughly 10% conversion efficiency to  $e^+e^-$  !**

# GEMINGA SPECTRUM INDICATIVE OF CONVECTION



- ▶ However, Bohmian diffusion is incompatible with the gamma-ray spectrum.
- ▶ If low-energy electrons are cooled, the spectrum at 7 TeV should be significantly softer.

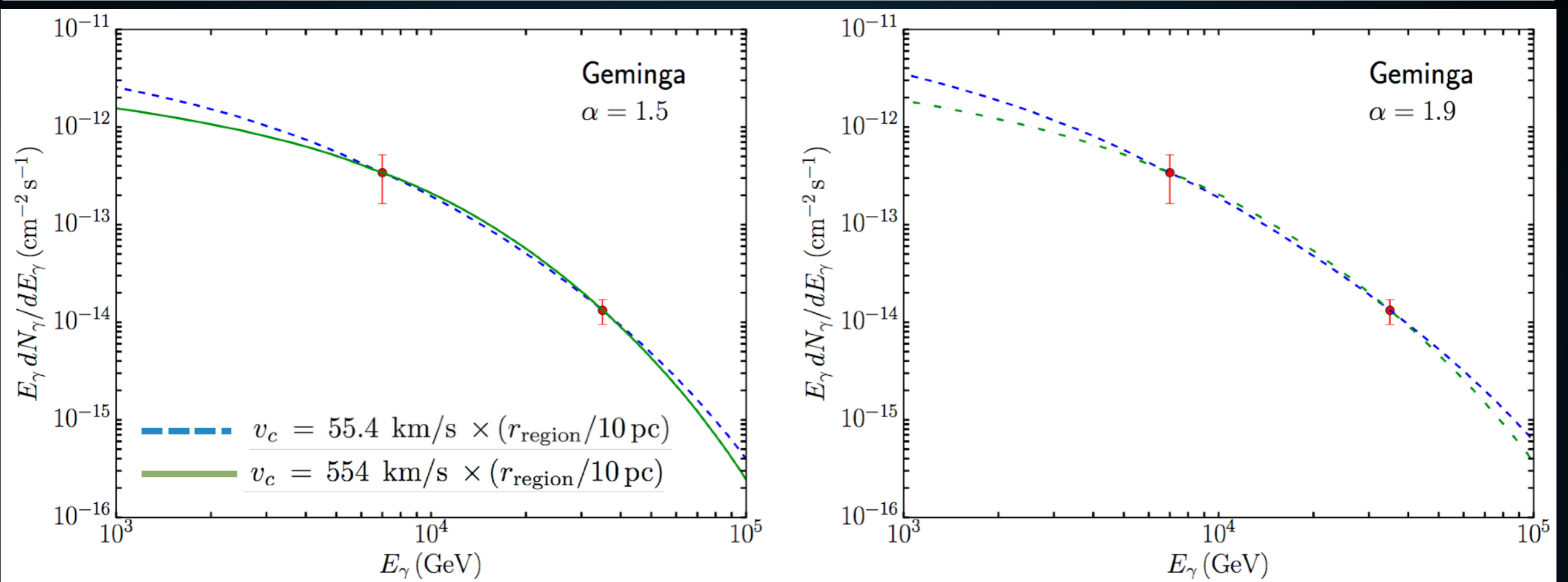


## AN UPPER LIMIT ON THE TEV HALO SIZE

---

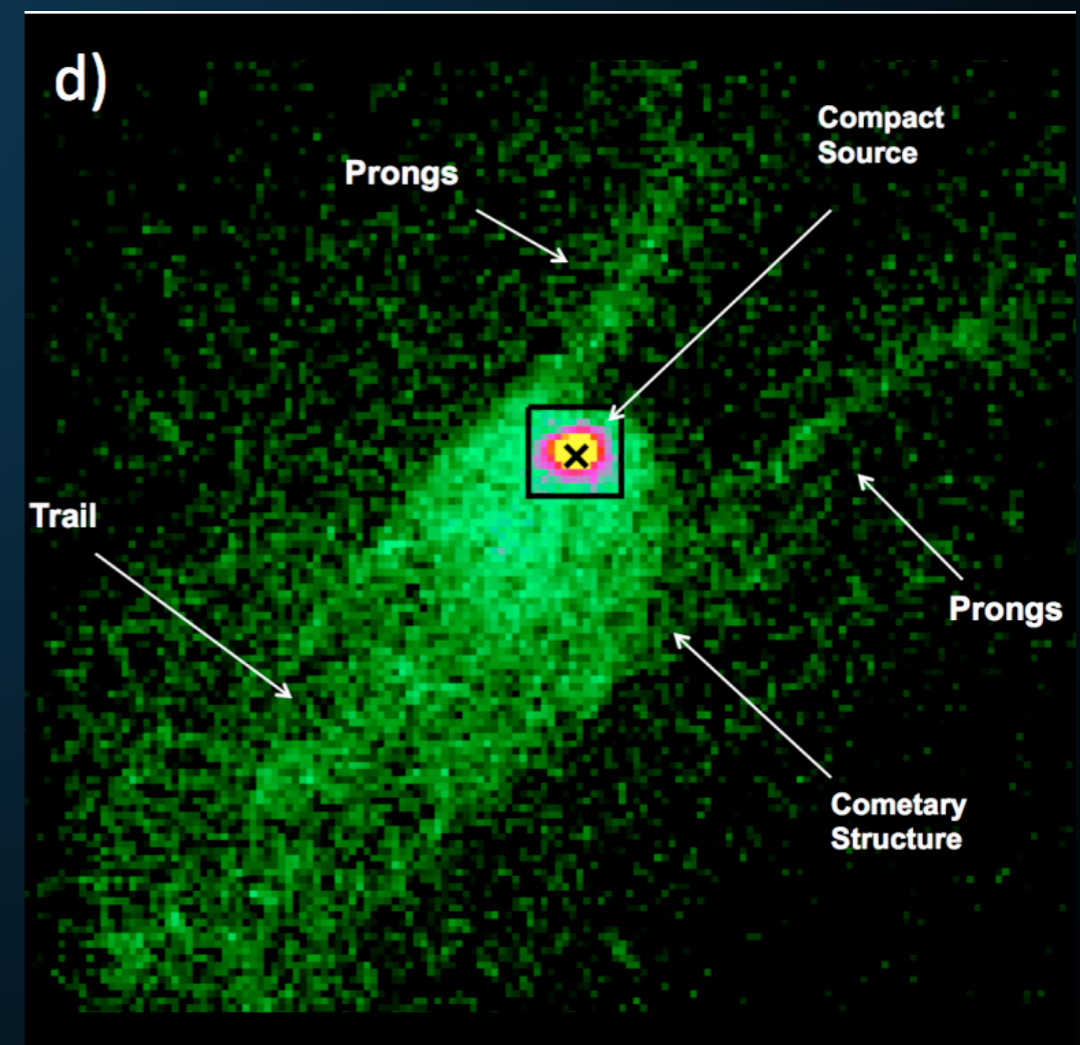
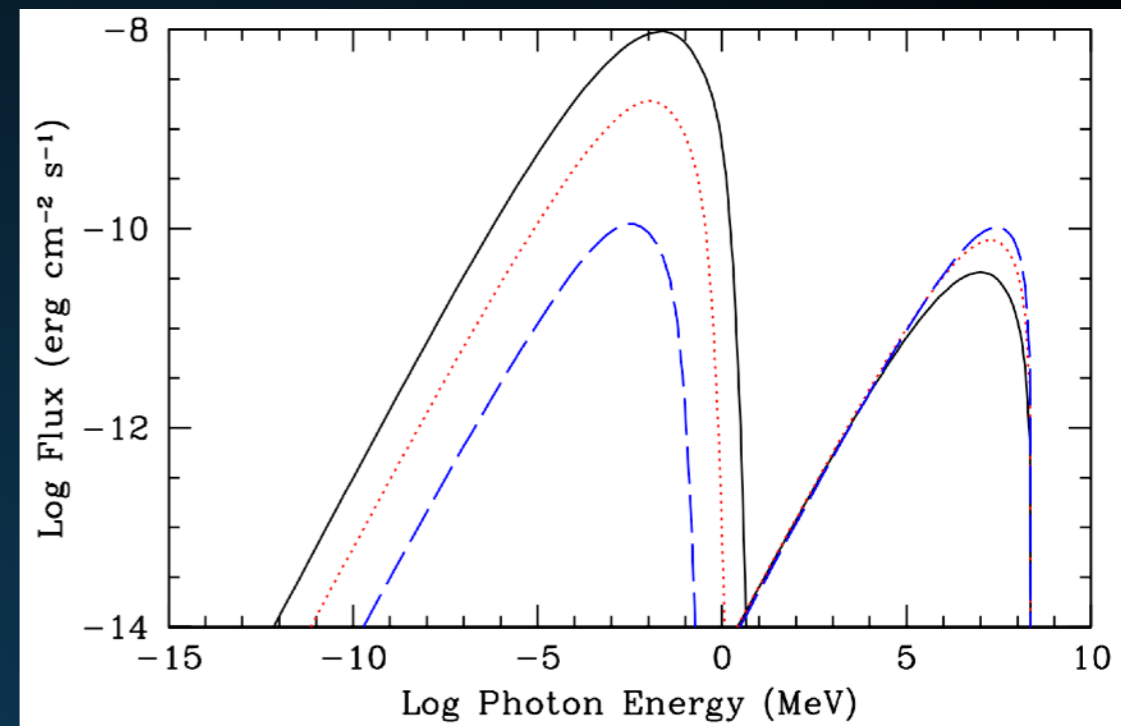
- ▶ **These arguments only set a lower limit on the TeV halo size.**
- ▶ **What if TeV halos are much larger, but the TeV electrons die at  $\sim 10$  pc?**
- ▶ **Will need to answer this question on the population level.**

# GEMINGA SPECTRUM INDICATIVE OF CONVECTION



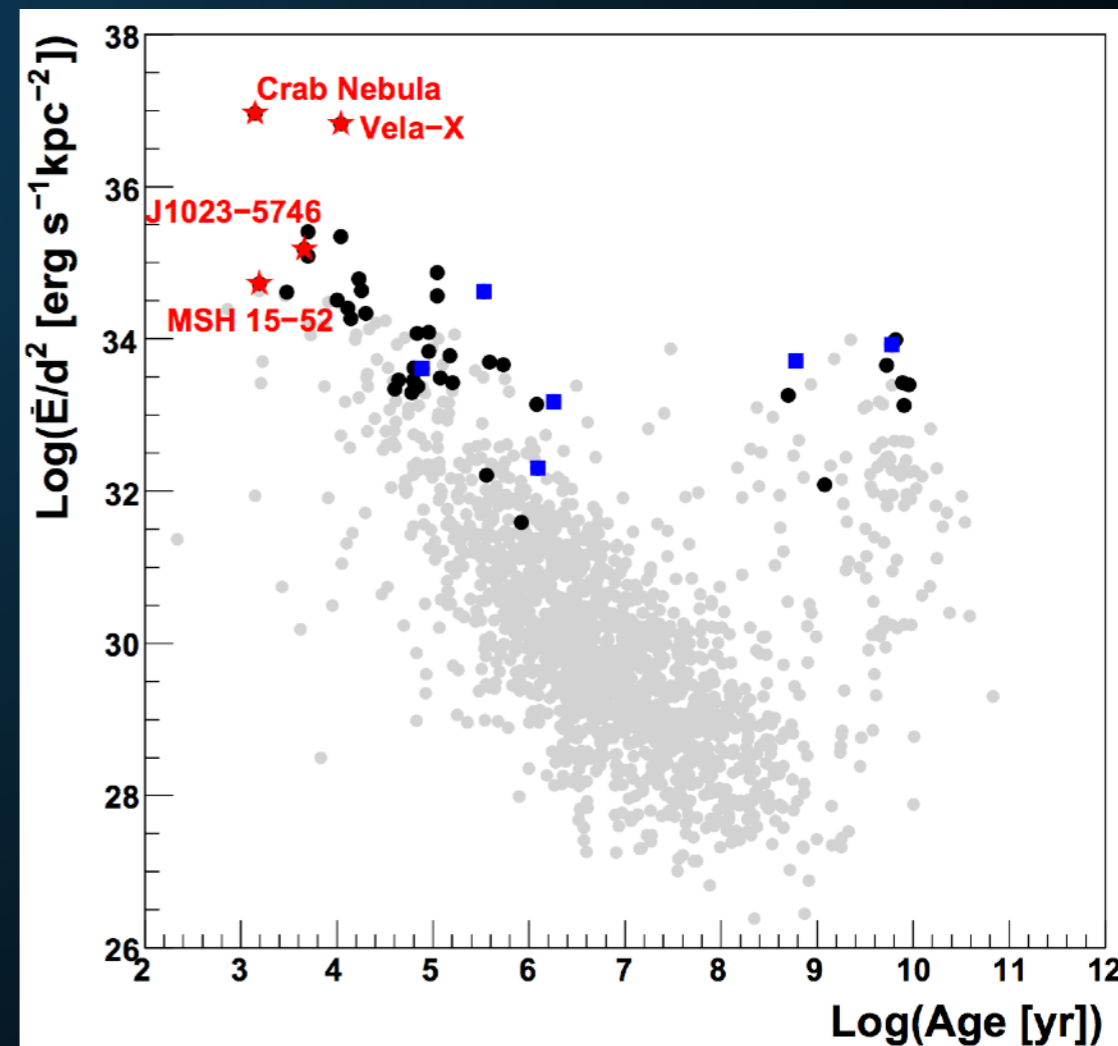
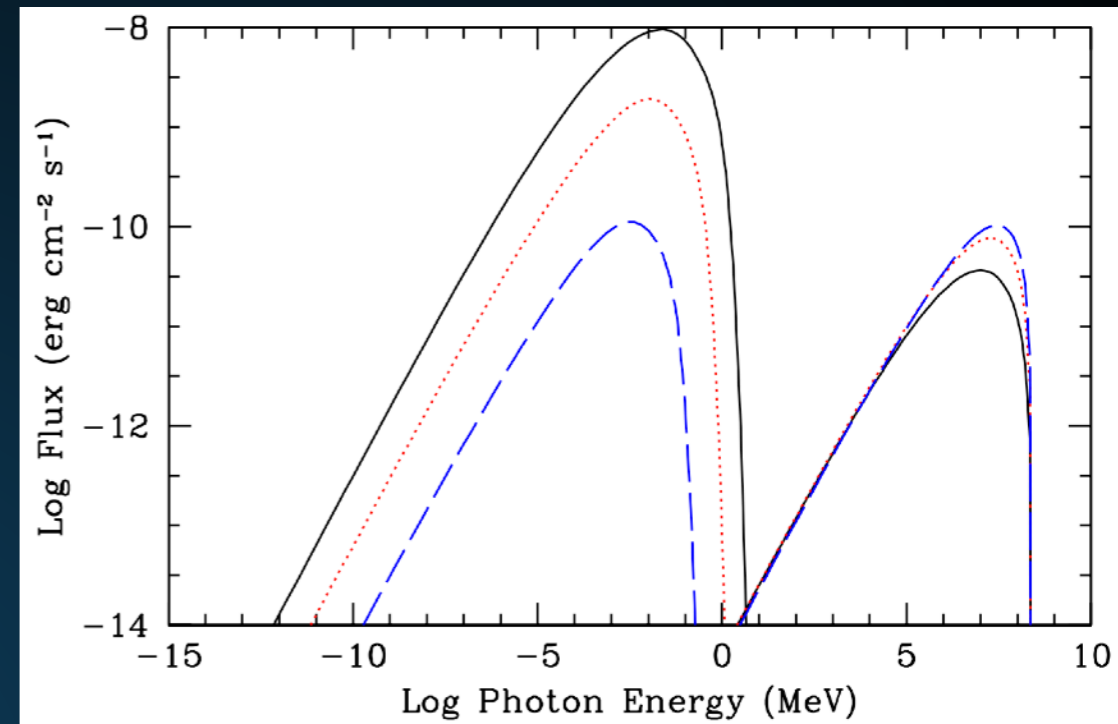
- ▶ Geminga spectrum is fit better with convective models.
- ▶ Energy-independent diffusion provides identical results
- ▶ Best-fit spectral-index ( $-2.23 \pm 0.08$ ) prefers high convection

- ▶ **Cooling dominated by  $20 \mu\text{G}$  magnetic field.**
- ▶ **Energy loss time:  $\sim 40$  years**
- ▶ **Distance Traveled:  $\sim 6$  pc for standard diffusion constant. Real diffusion must be slower.**
- ▶ **The spectrum changes as a function of distance and time.**

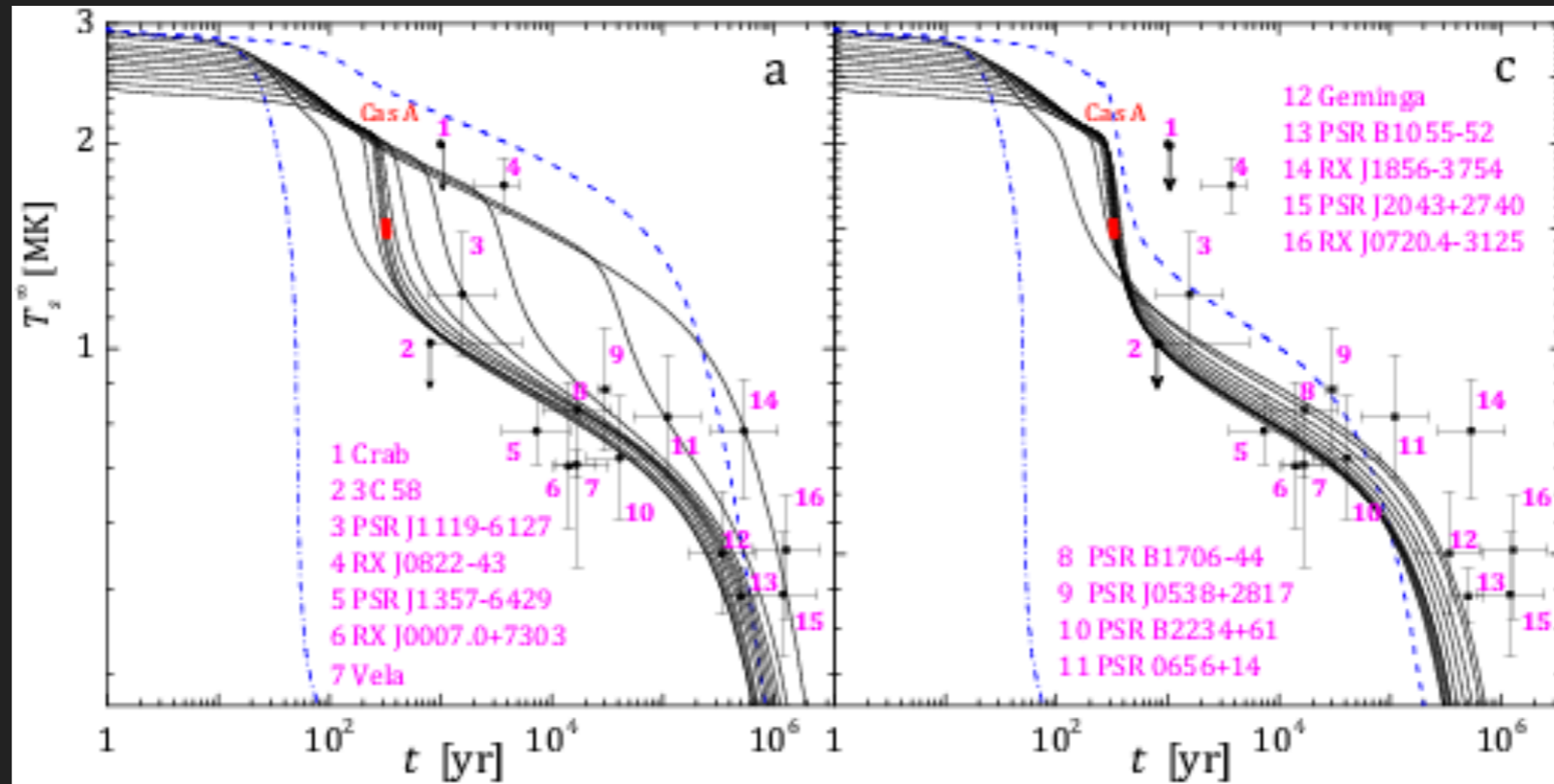




- ▶ **Gamma-Ray produced through ICS should accompany synchrotron emission.**
- ▶ **Synchrotron observations imply very hard GeV gamma-ray spectrum.**
- ▶ **Conclusively prove leptonic nature of emission.**

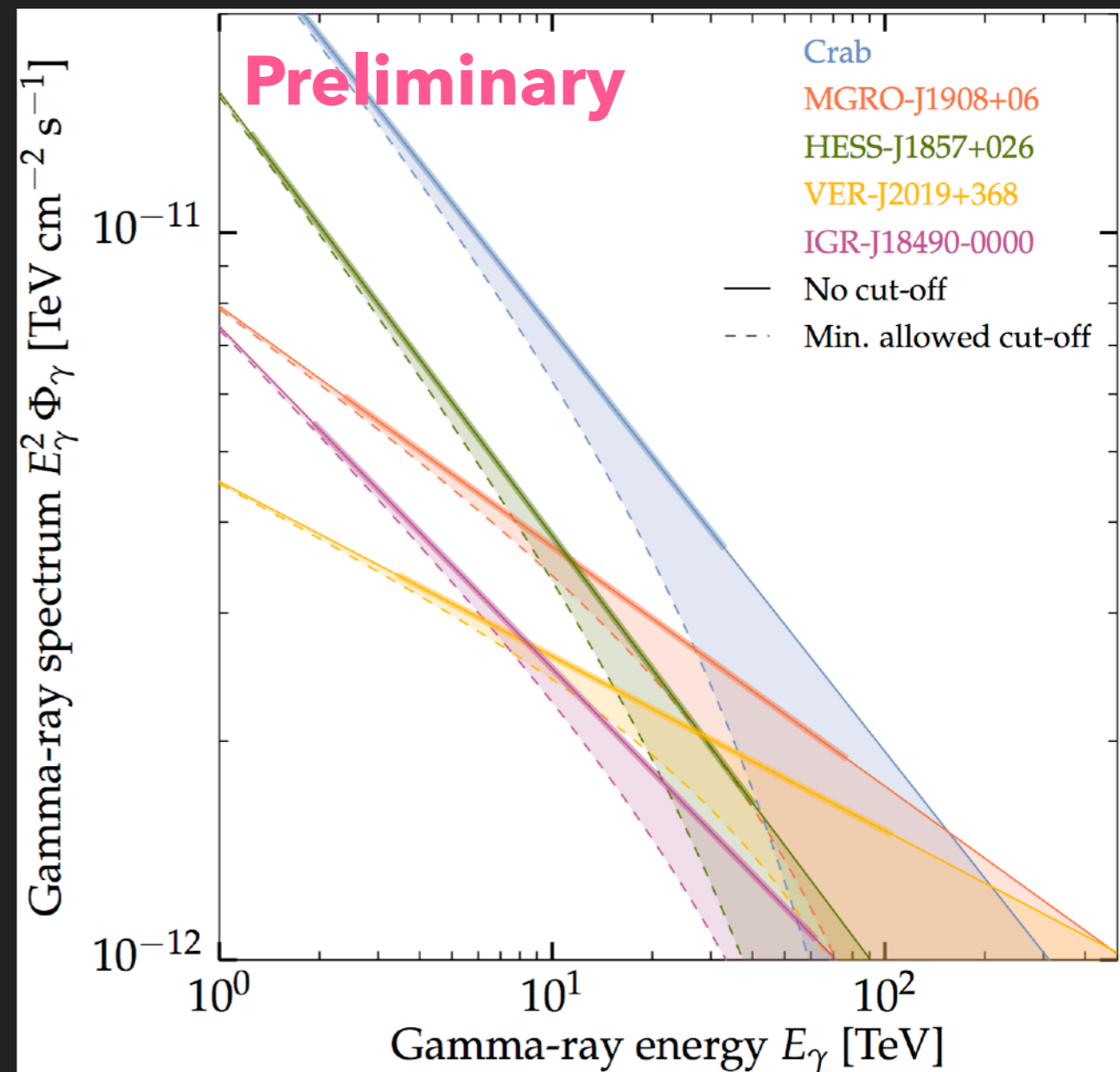


# THERMAL PULSAR EMISSION

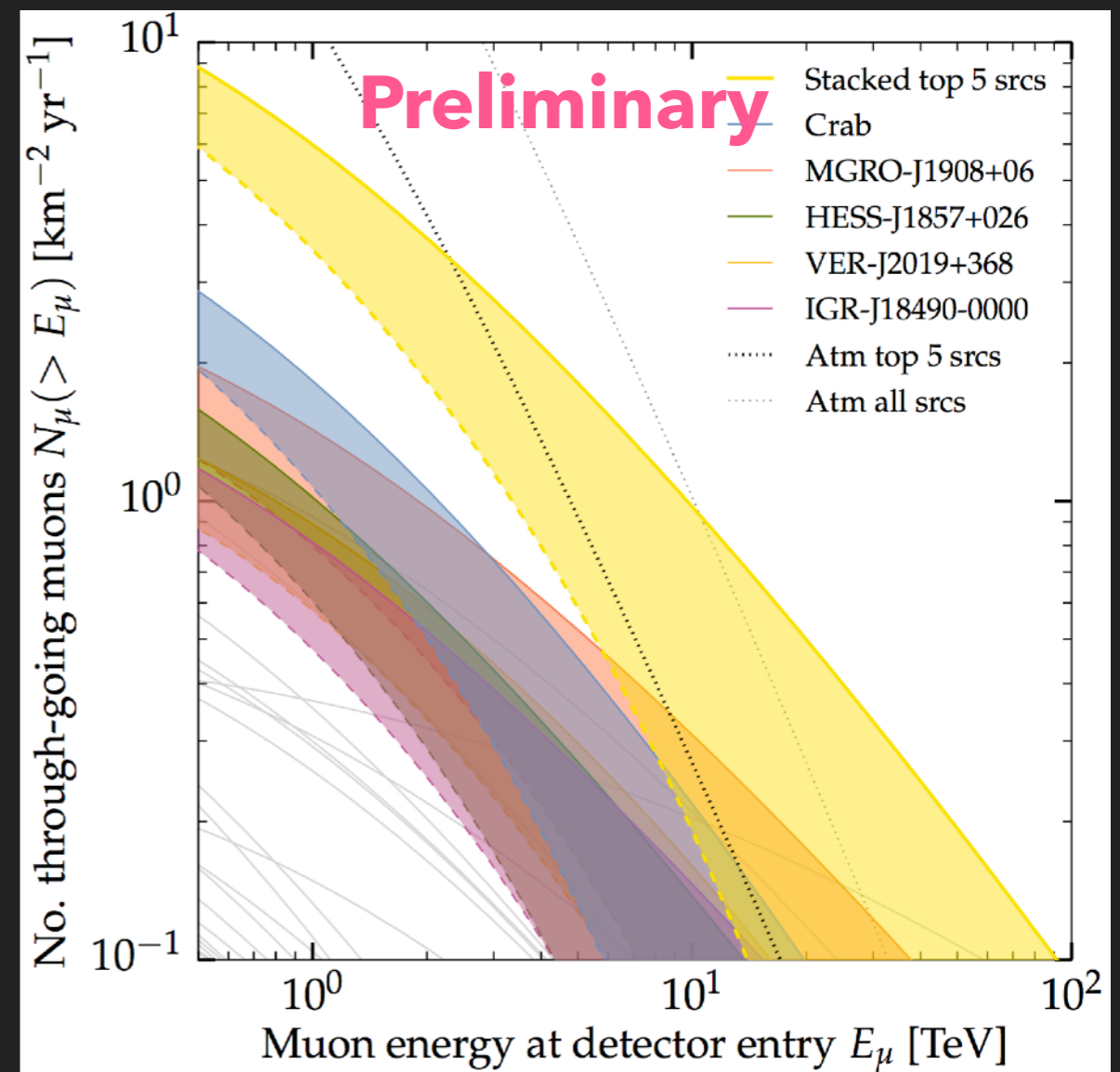
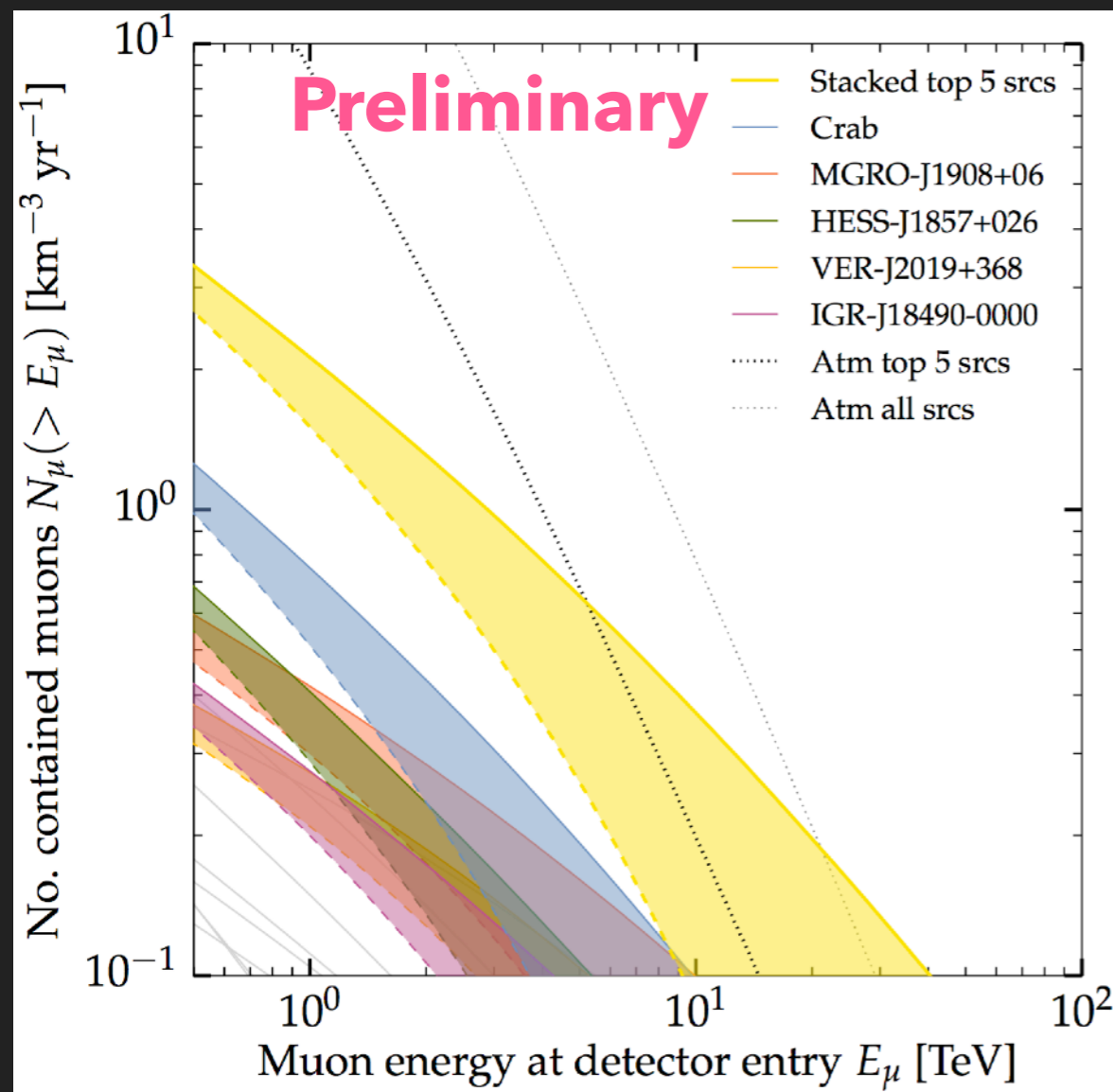


- ▶ Hot neutron stars can also be observed via their isotropic thermal emission.
- ▶ X-Ray observations can be sensitive to  $\sim 2$  kpc for  $10^6$  K NS.
- ▶ Cooler NS extremely hard to see.
- ▶ Could potentially detect a system which has recently ceased producing TeV particles.

- ▶ **HAWC sources are potential IceCube neutrino sources.**
- ▶ **Spectral measurements of HAWC sources are imperative to calculating the expected neutrino flux.**
- ▶ **Here we produce an analysis taking into account a 20% uncertainty in total flux, as well as spectral uncertainty due to an exponential cutoff.**

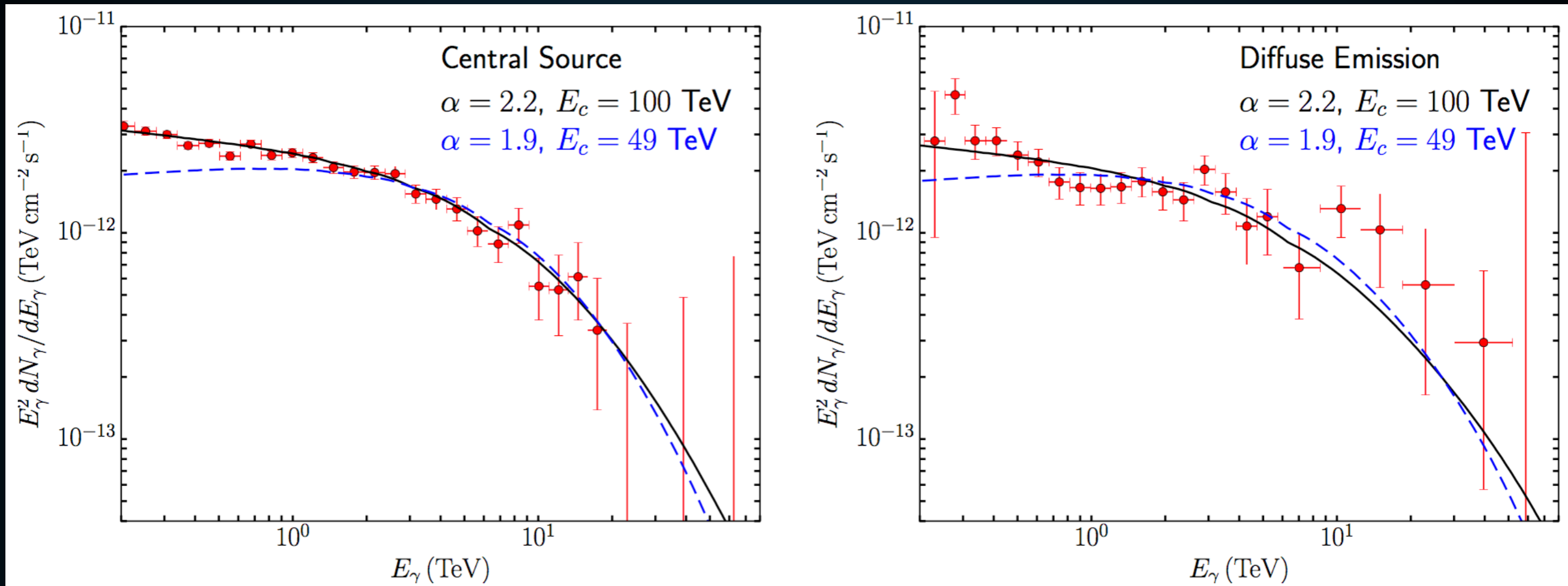






- ▶ If these sources are hadronic, their stacked neutrino flux is detectable in current IceCube data.
- ▶ Alternatively, can place a strong constraint on the hadronic fraction of the brightest HAWC sources.

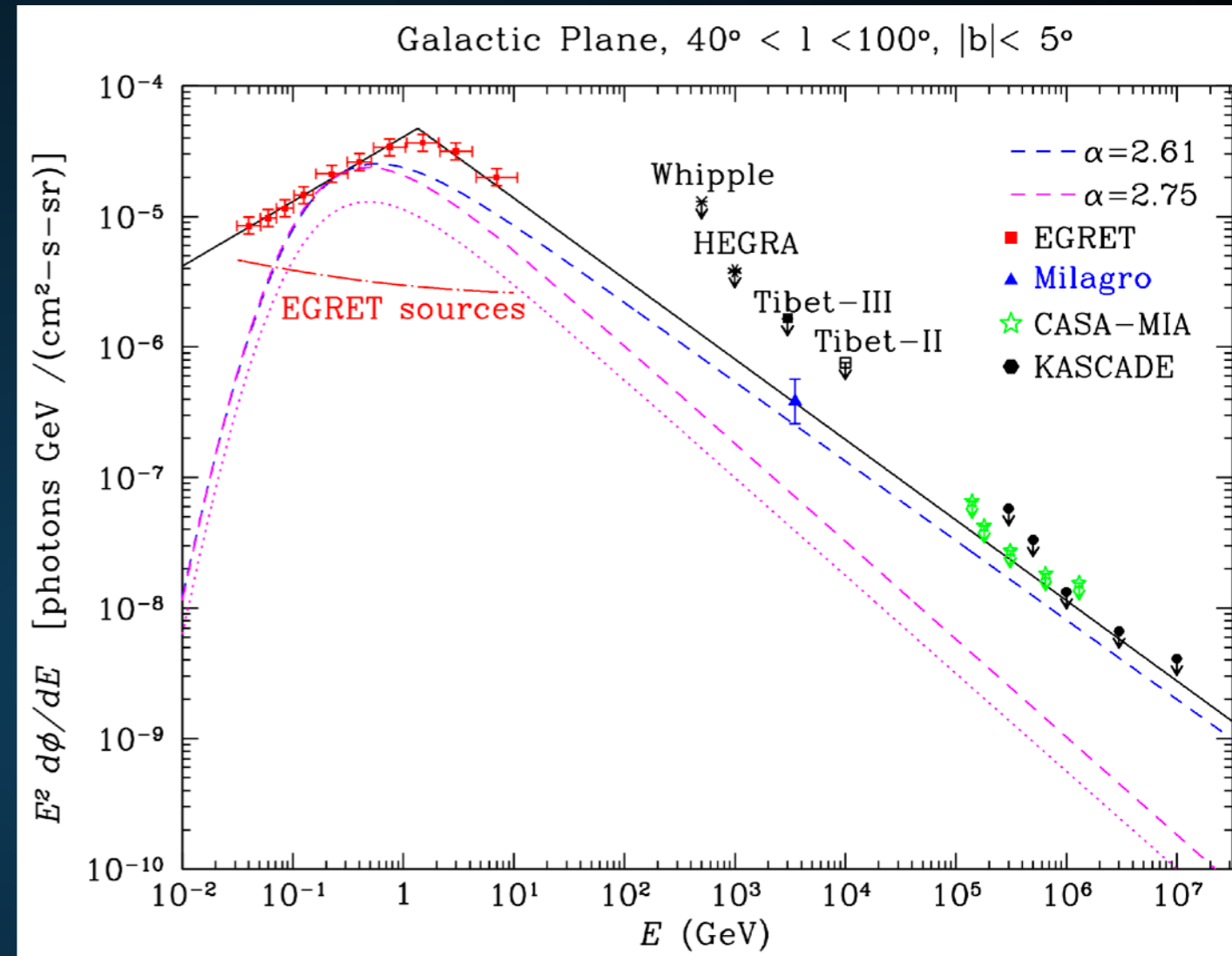
# TeV HALOS PRODUCE THE PEVATRON SPECTRUM



- ▶ The TeV halo spectrum from Geminga naturally reproduces the HESS observations.
- ▶ Slightly softer spectra preferred.
  - ▶ Some evidence that Geminga spectrum is particularly hard.
  - ▶ Hadronic diffuse background contamination?

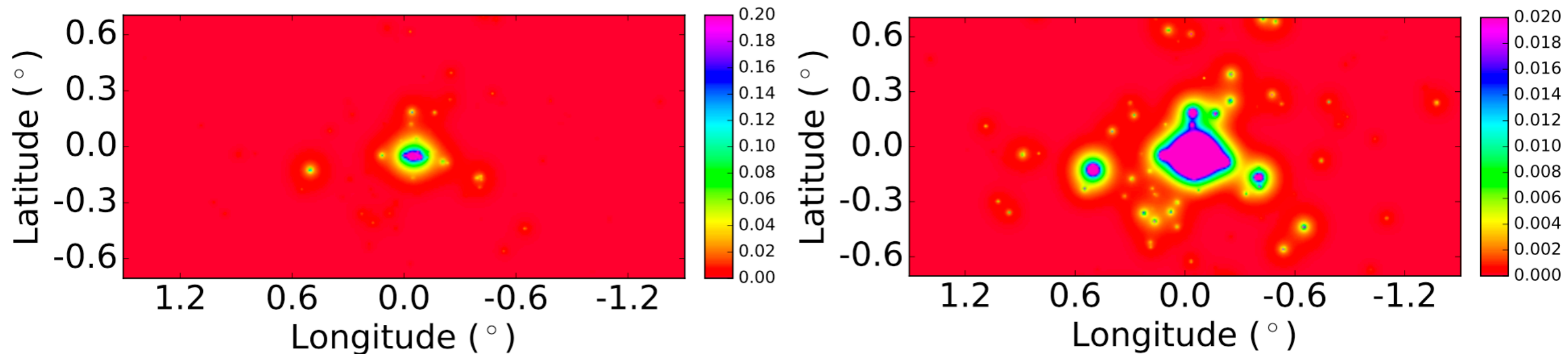
- **Milagro detects bright diffuse TeV emission along the Galactic plane.**

- **Difficult to explain with pion decay, due to steeply falling local hadronic CR spectrum.**



- **Can harden gamma-ray emission to some extent using radially dependent diffusion constants (1504.00227).**

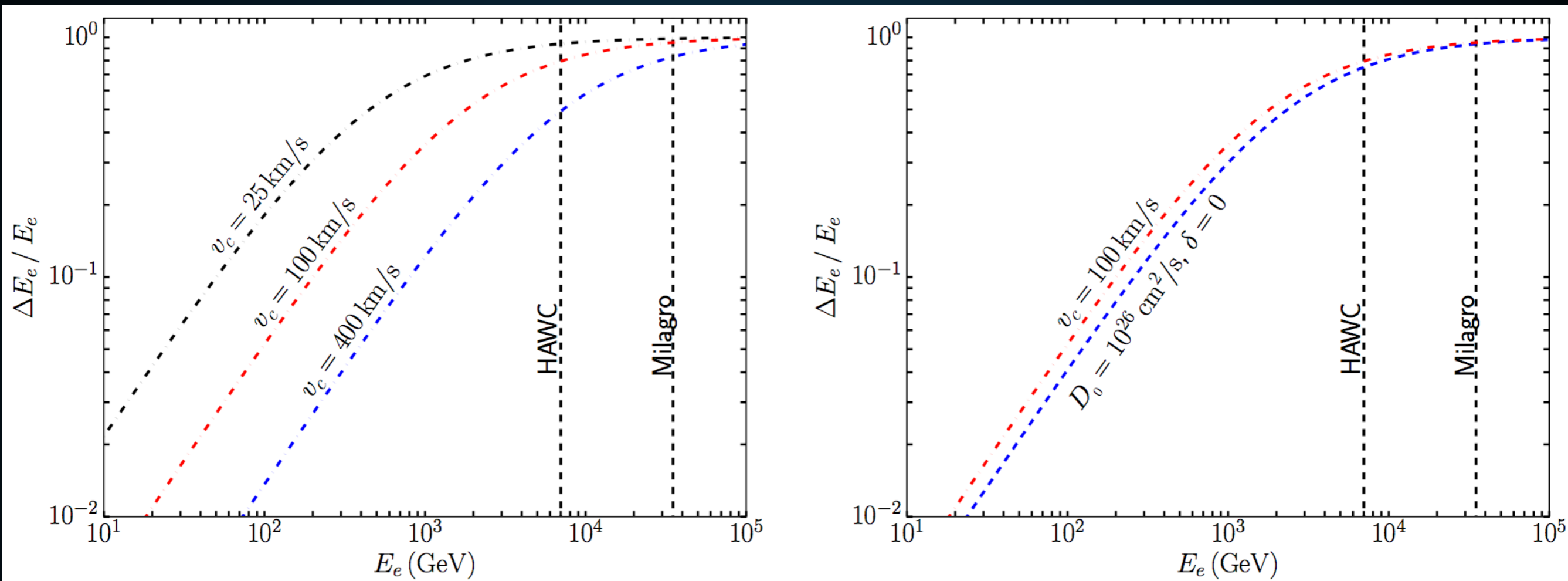




- **Significant star (pulsar) formation in the Galactic center**
- **Pulsars formed in the central parsec will be kicked into surrounding medium.**
- **Source of diffuse gamma-rays in the Galactic center.**

# WHAT ABOUT THE LOW-ENERGY ELECTRONS?

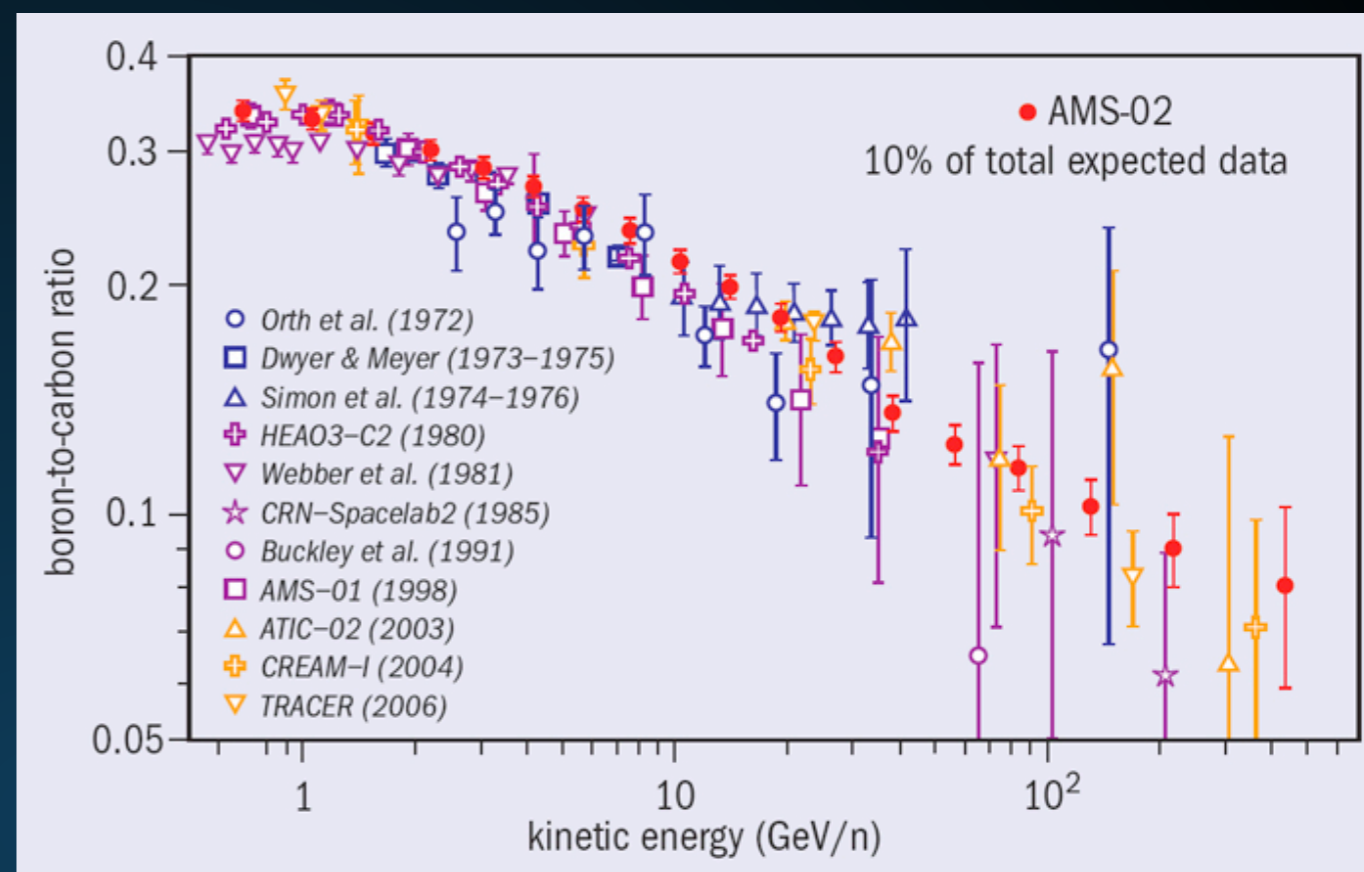
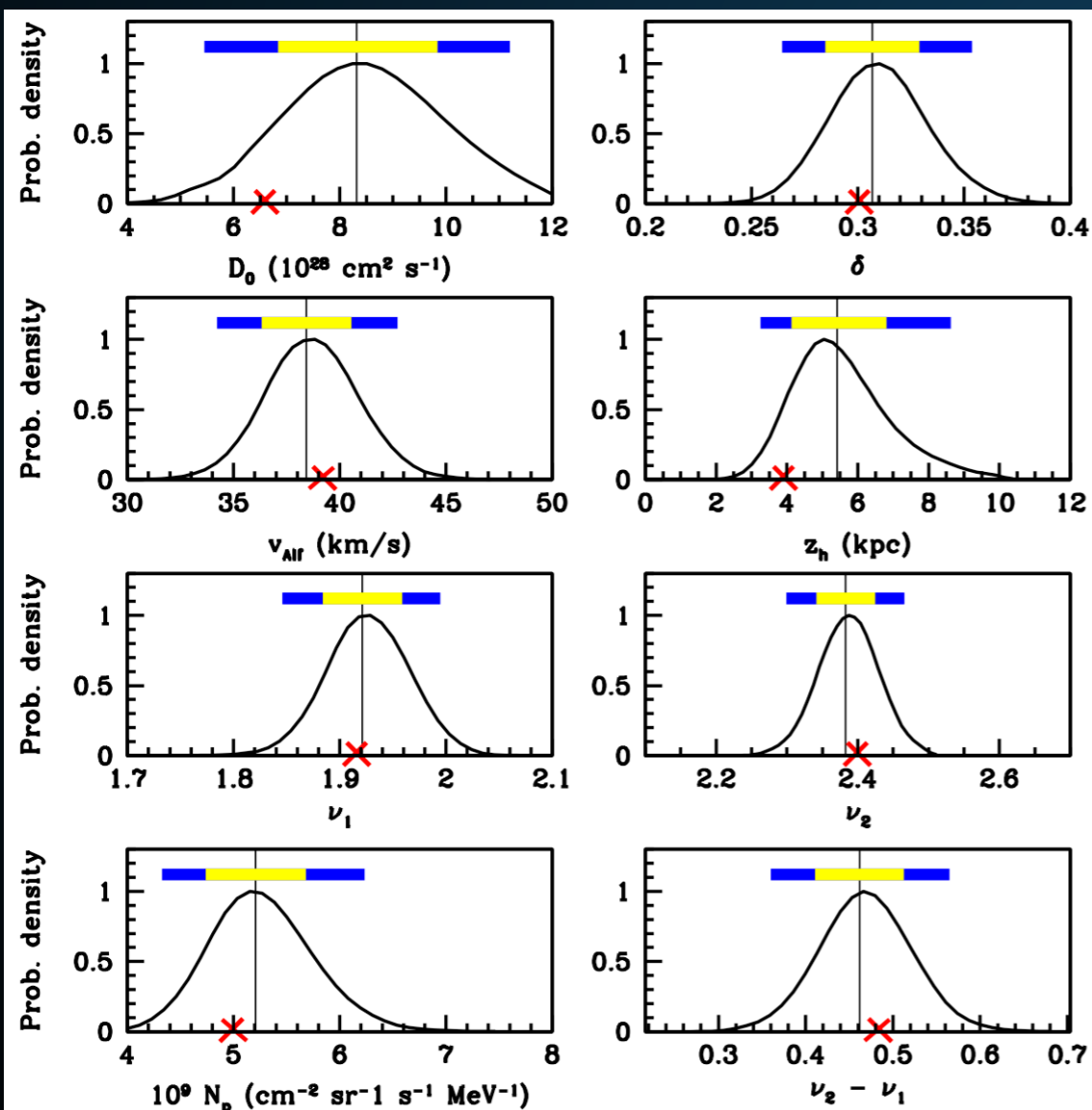
## Fraction of energy lost before Electrons Travel a constant distance



- **Low-energy electrons lose energy slower, must travel farther.**
- **This is true in both convective case (shown here) as well as most diffusive (e.g. Kolmogorov, Kraichnian) scenarios.**
- **Where do these electrons go?**

# EFFECT OF TEV HALOS ON ISM PROPAGATION

- Multiple cosmic-ray observations indicate that the average diffusion constant is  $\sim 5 \times 10^{28} \text{ cm}^2 \text{ s}^{-1}$

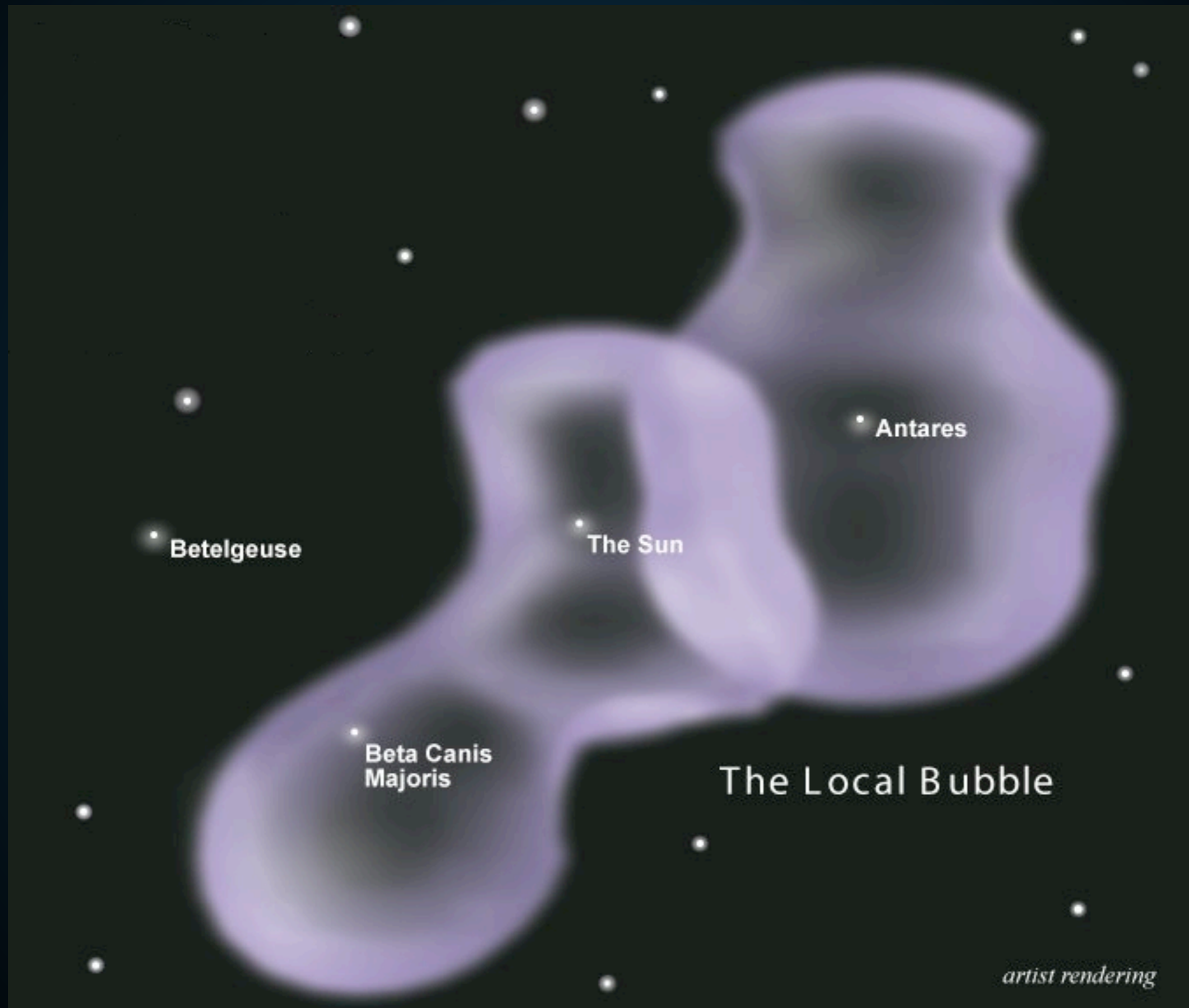


- Assume that diffusion reverts back to the standard case outside the TeV halo.
- Primary difference between our results and those from HAWC.



# CAN THE DIFFUSION CONSTANT BETWEEN GEMINGA AND US BE LOW?

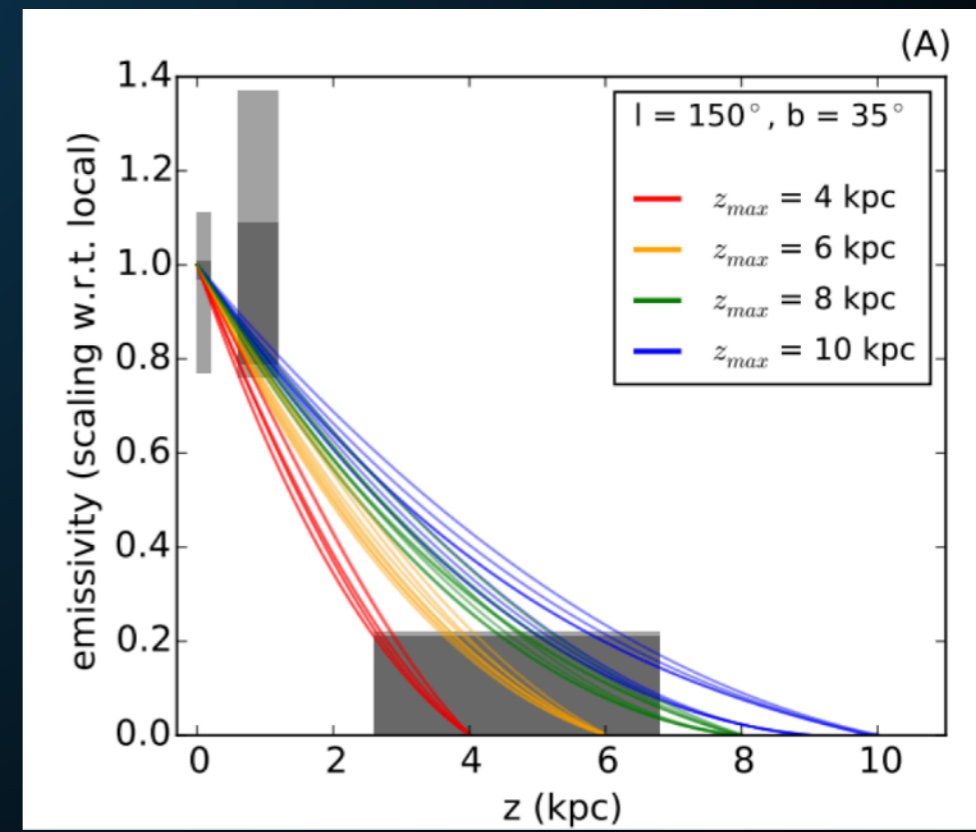
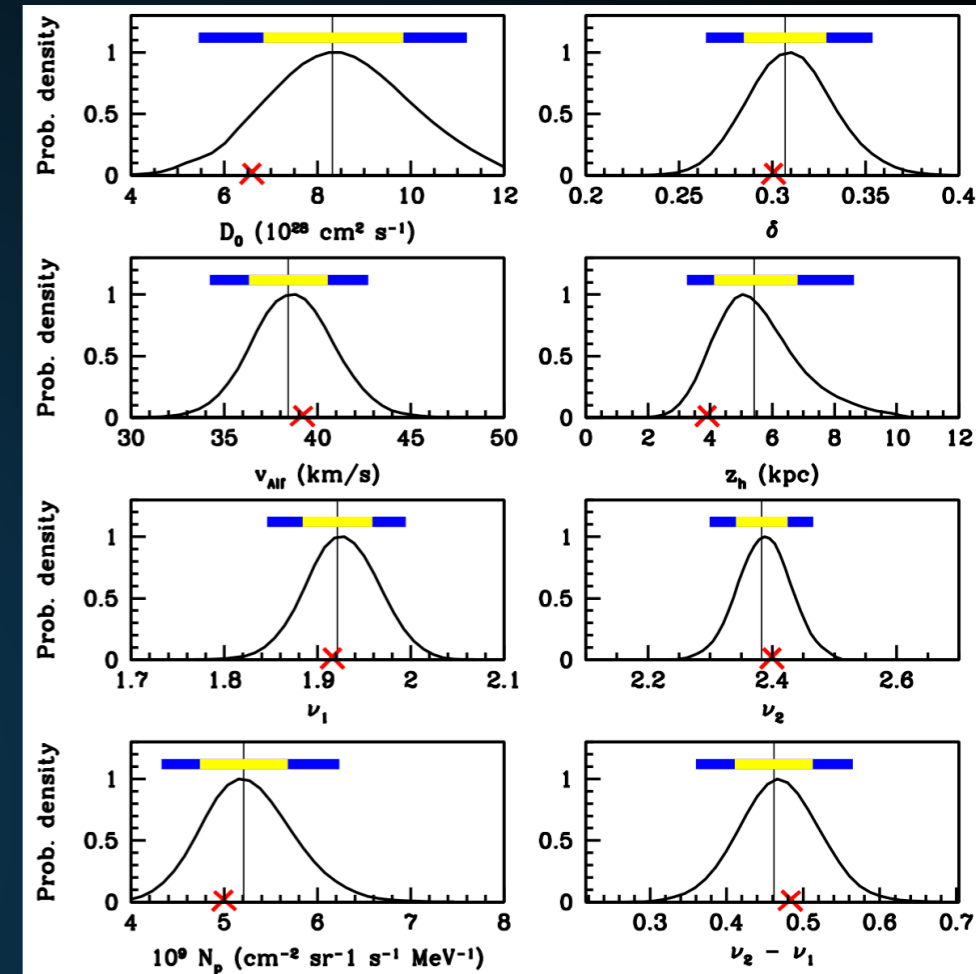
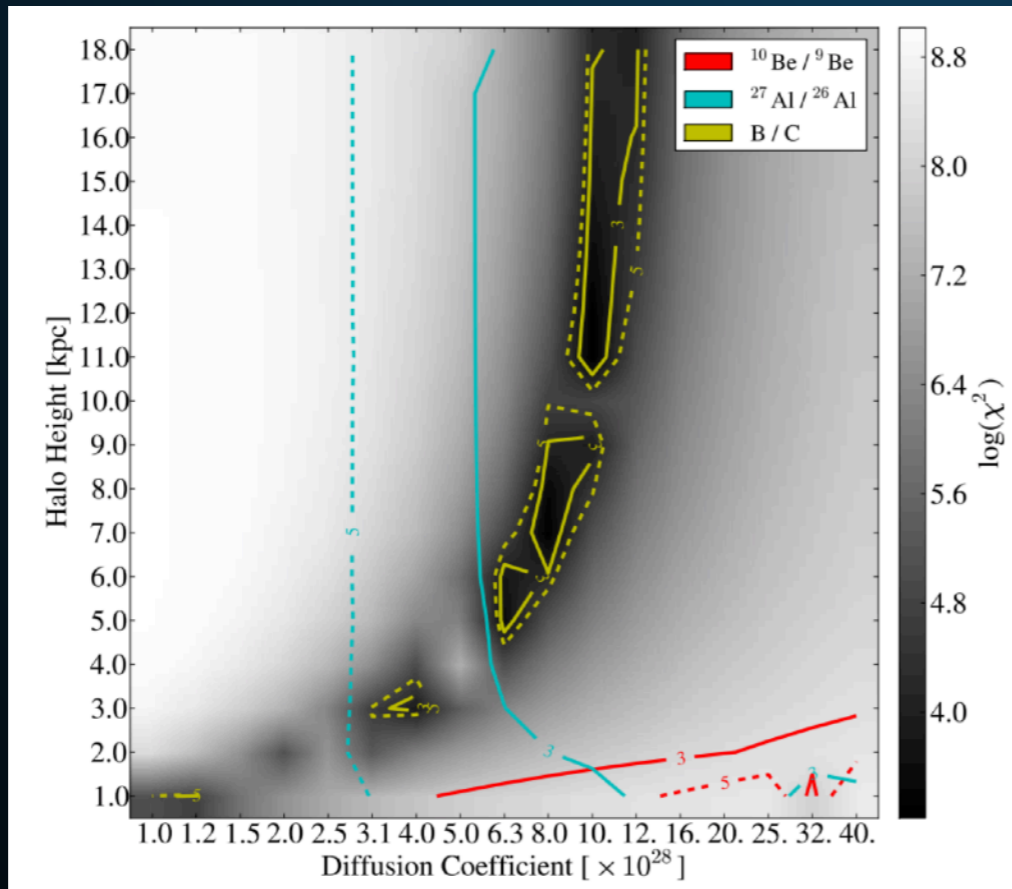
---

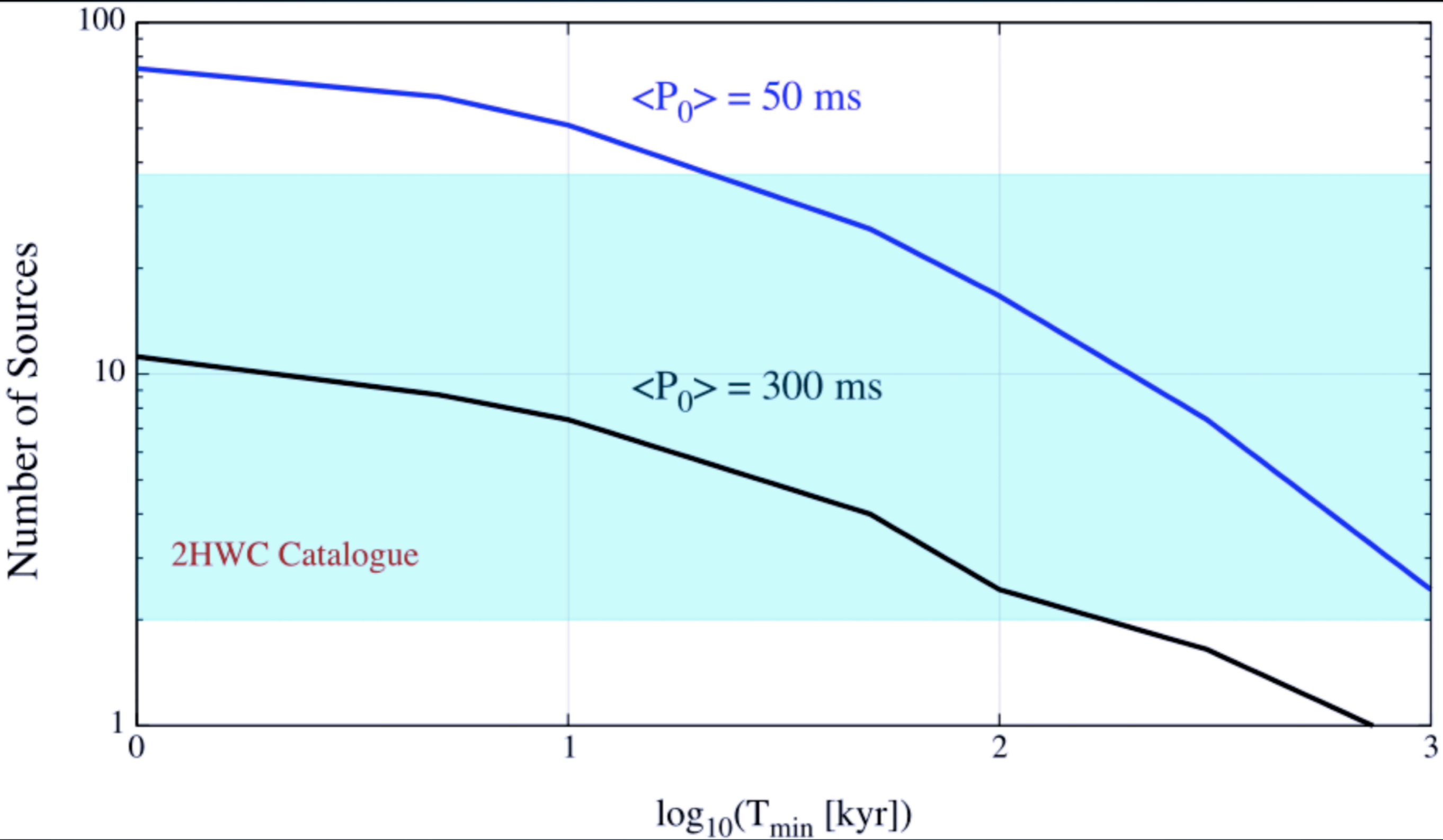


# SCENARIO 1: THE MILKY WAY DIFFUSION CONSTANT IS LOW

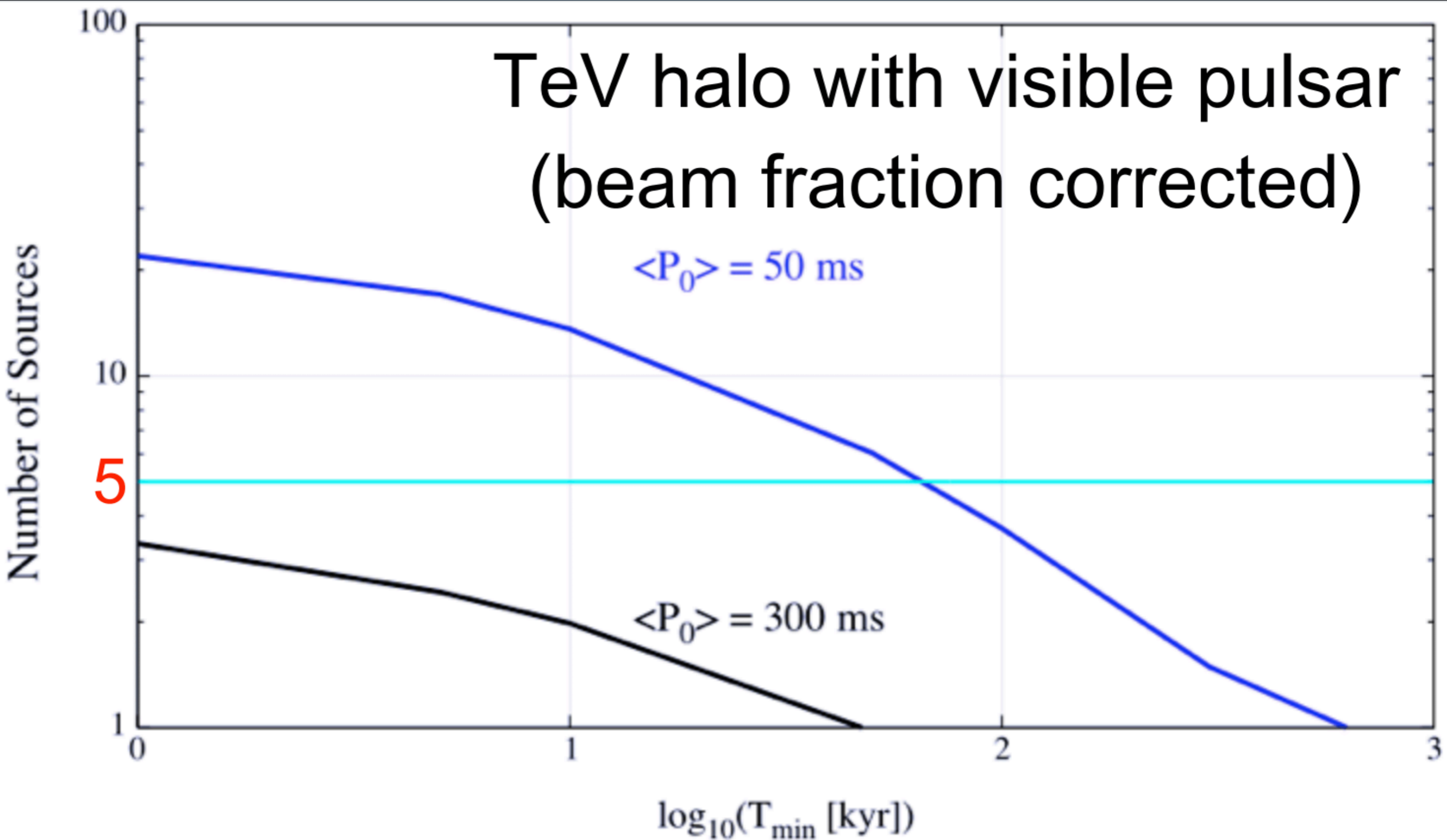
Cosmic-Ray primary to secondary ratios tell us about:

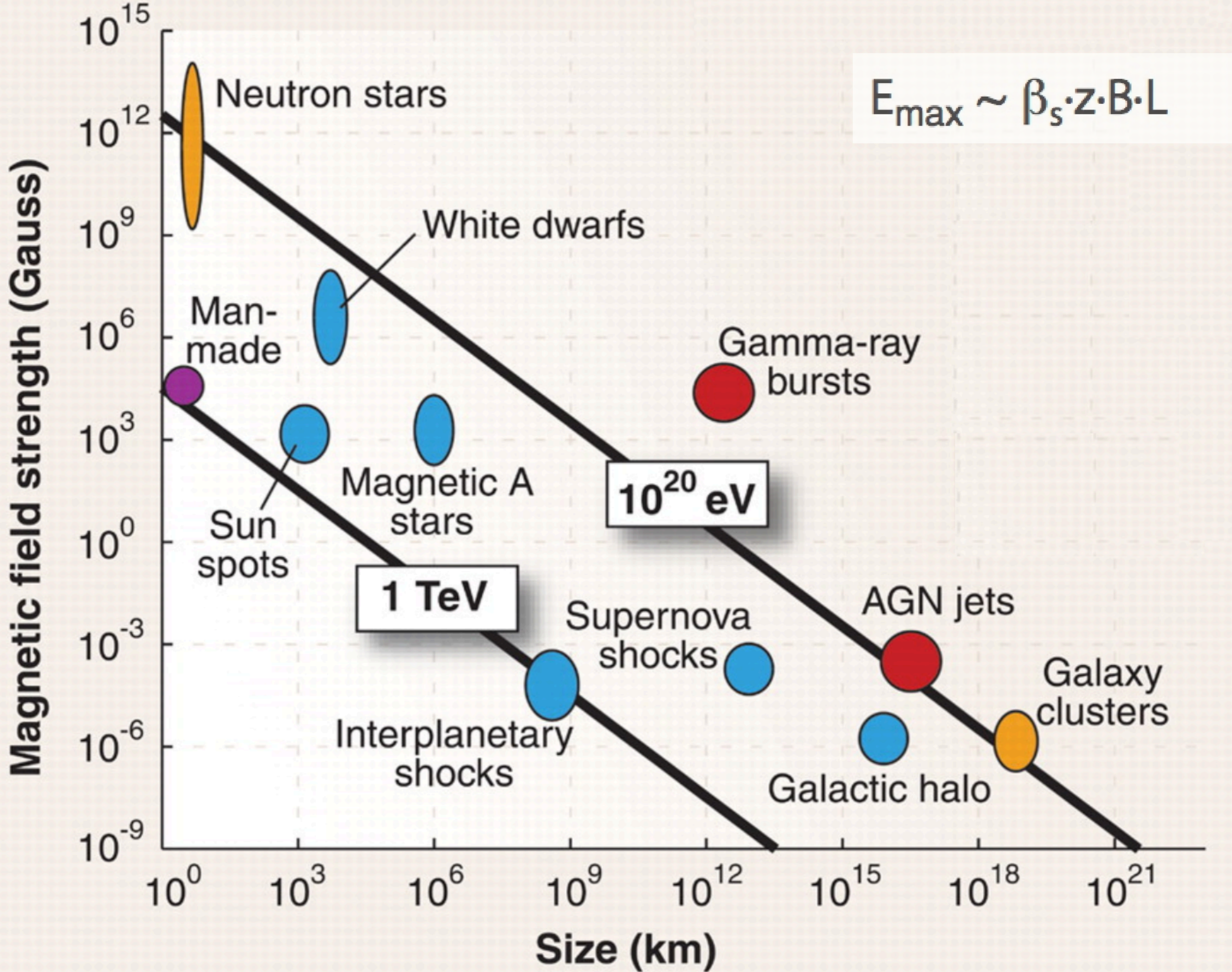
- The average grammage encountered by cosmic-rays before they escape the galaxy (e.g. B/C)
- The average time cosmic-rays are confined in the galaxy ( $^{10}\text{Be}/^9\text{Be}$ ).





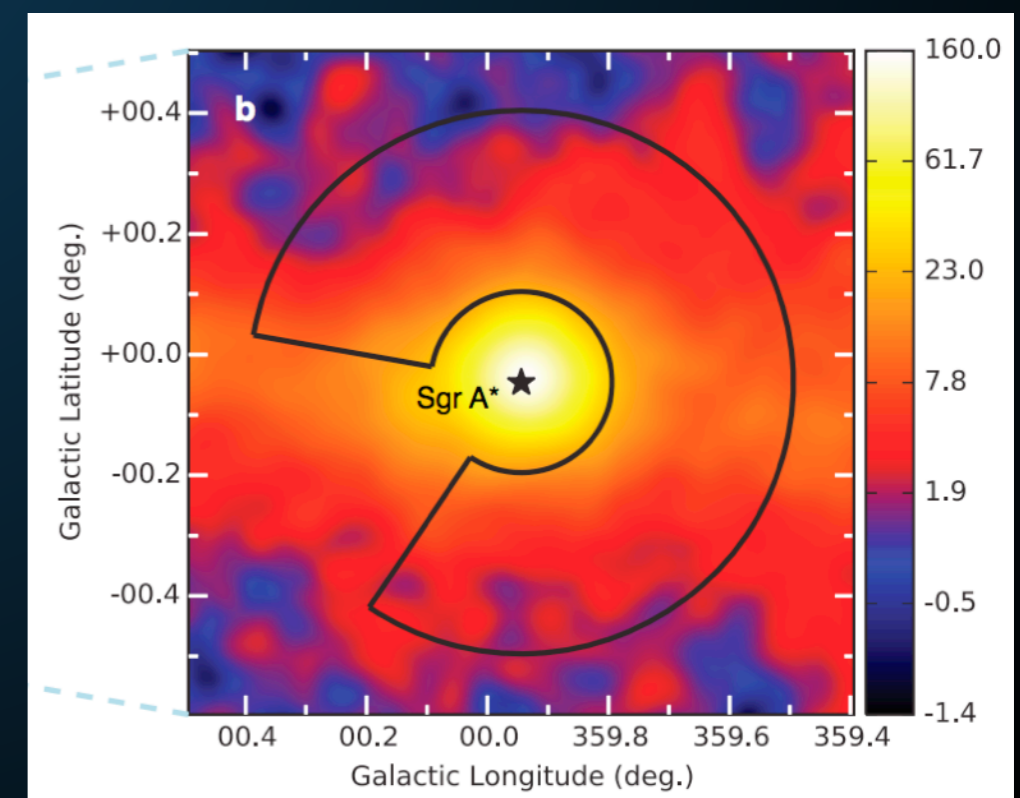
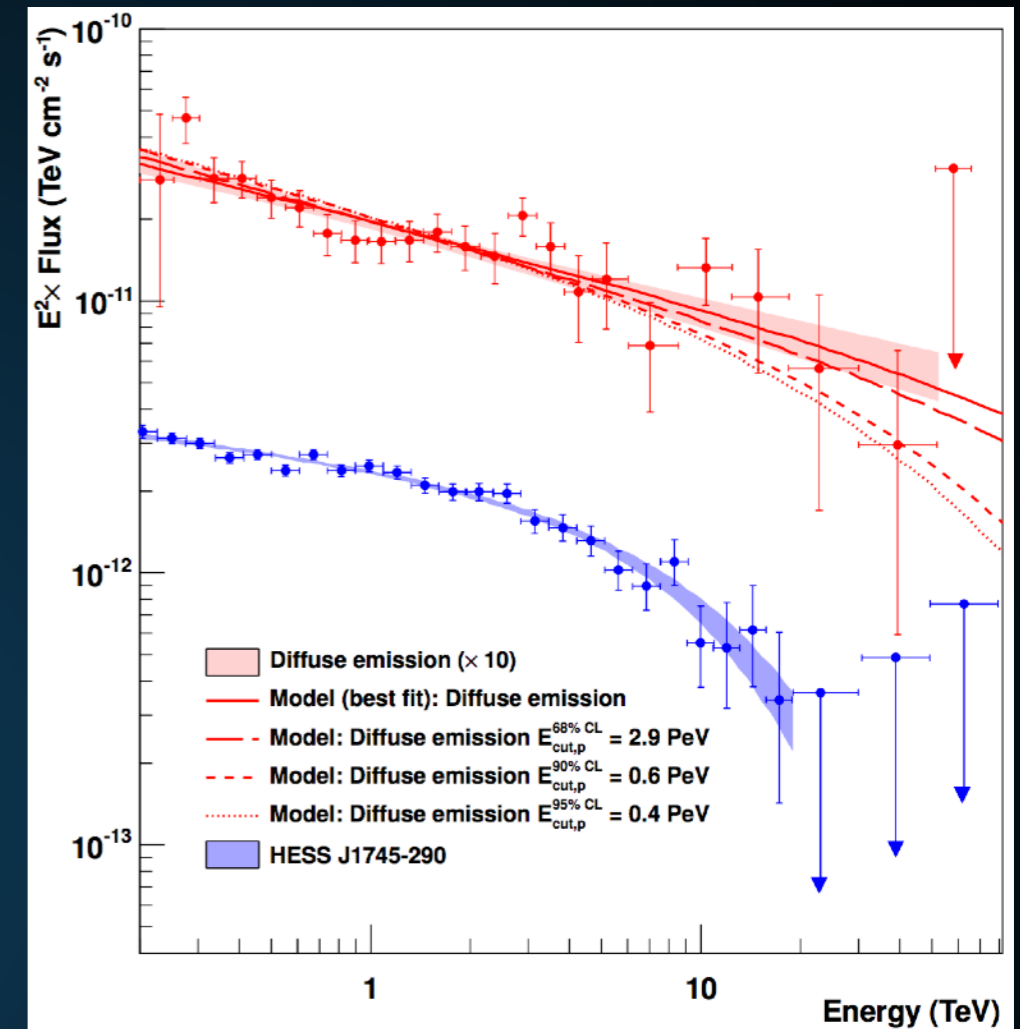






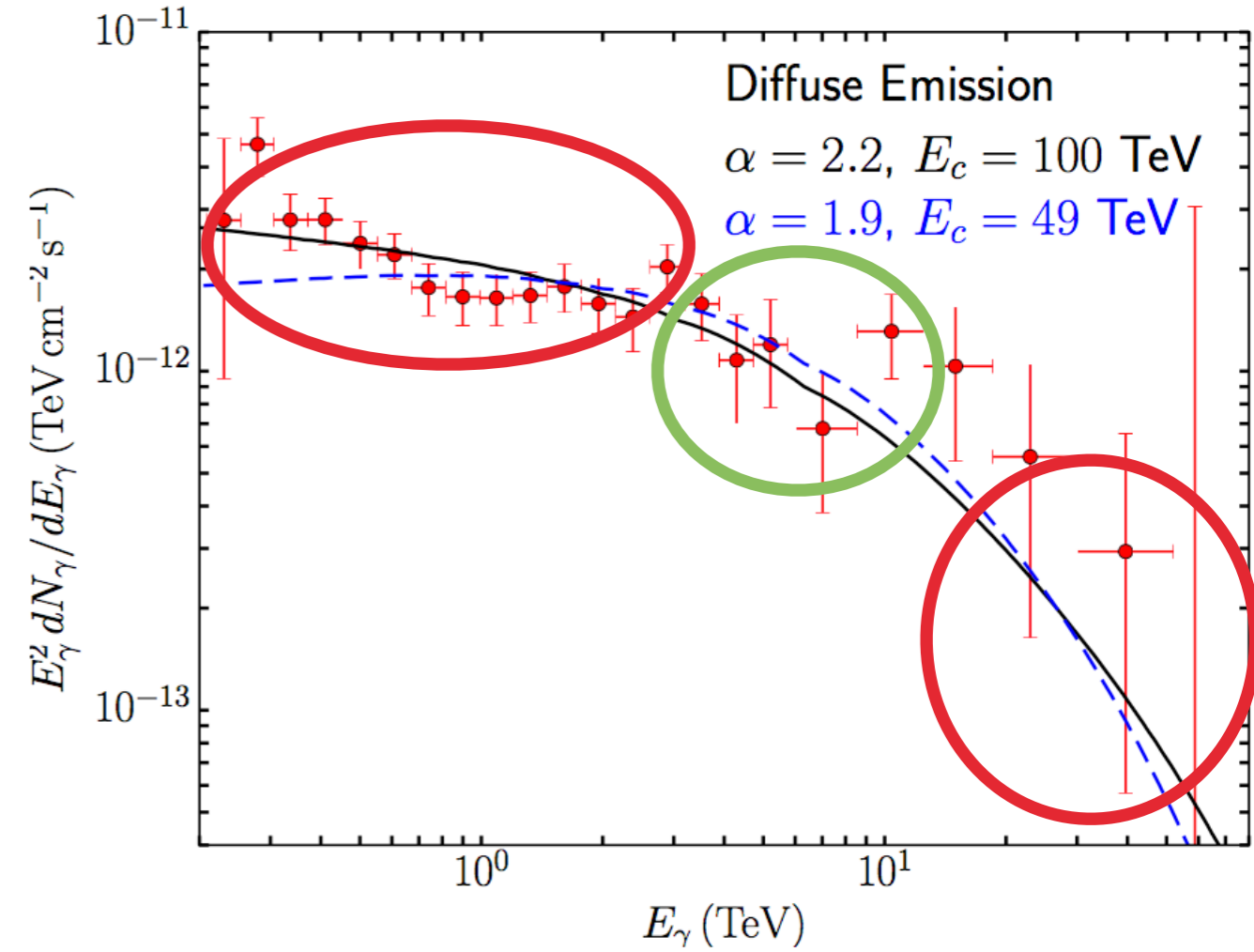
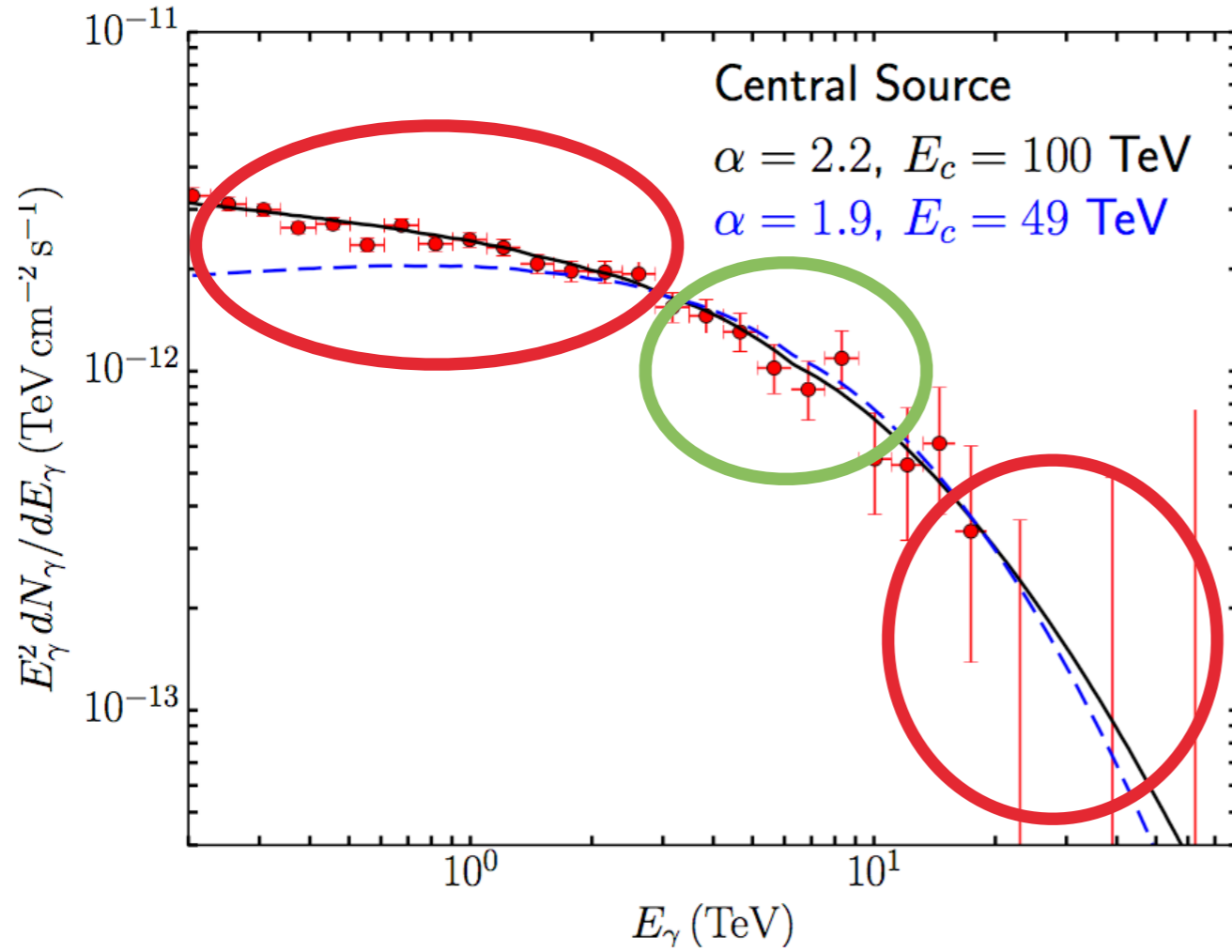


- **HESS observed diffuse ~50 TeV emission from the Galactic center.**
- **If this emission is hadronic, it indicates PeV particle acceleration in the GC**
- **Spherical symmetry hints at Galactic Center source.**





- TeV halos naturally explain the data!



# GEMINGA GAMMA-RAY SPECTRUM

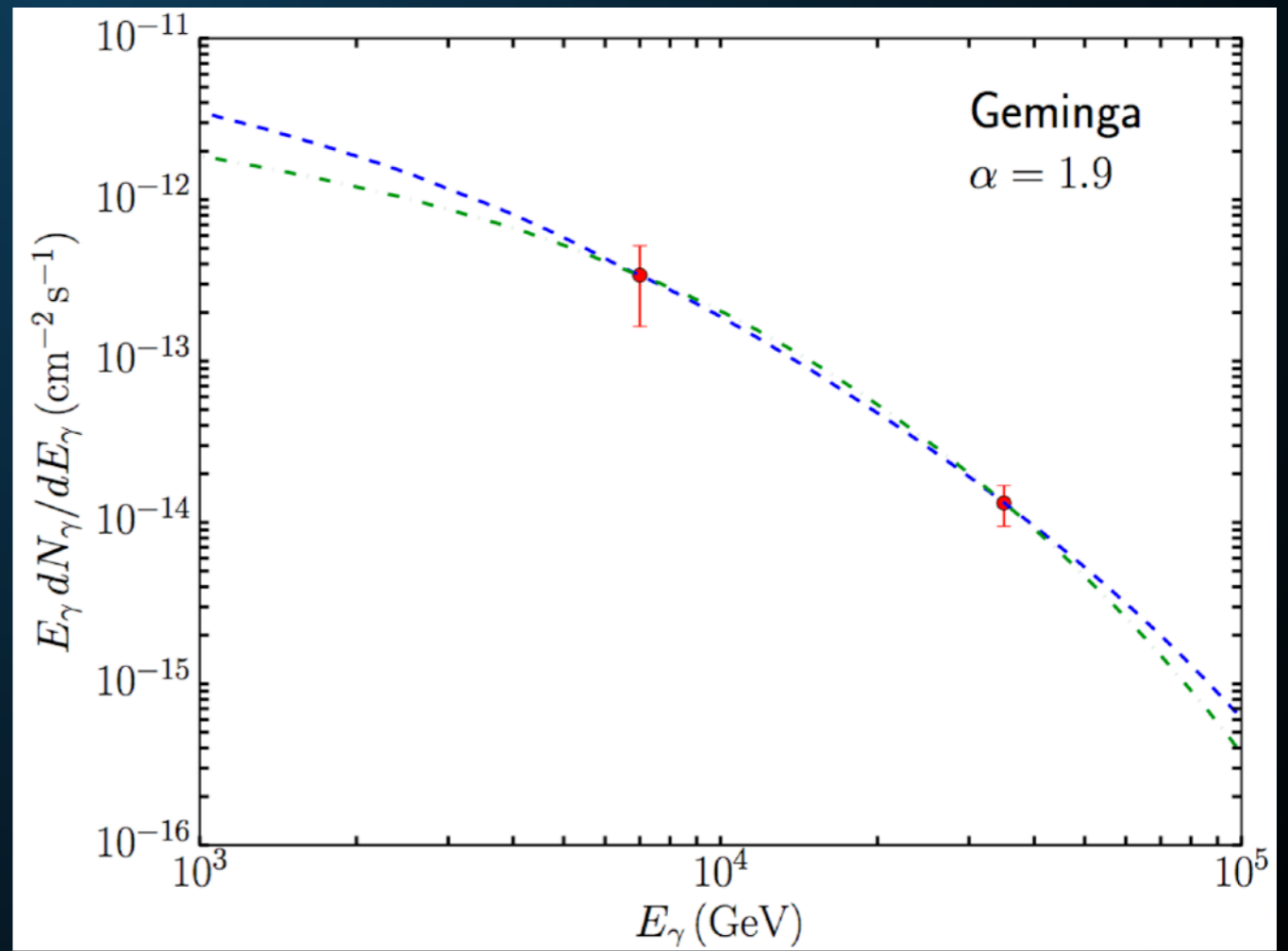
Name	Tested radius [ $^{\circ}$ ]	Index	$F_7 \times 10^{15}$ [ $\text{TeV}^{-1} \text{cm}^{-2} \text{s}^{-1}$ ]	TeVCat
2HWC J0631+169	-	$-2.57 \pm 0.15$	$6.7 \pm 1.5$	Geminga
”	2.0	$-2.23 \pm 0.08$	$48.7 \pm 6.9$	Geminga
2HWC J0635+180	-	$-2.56 \pm 0.16$	$6.5 \pm 1.5$	Geminga

- **We assume an electron injection spectrum following a power-law with an exponential cutoff.**

- **Best Fit:**

- $-1.9 < \alpha < -1.5$

- $E_{\text{cut}} \approx 50 \text{ TeV}$



---

**These conclusions stem merely from the  
existence of these sources.**

**So far - no modeling of what a TeV halo is...**



### Overview:

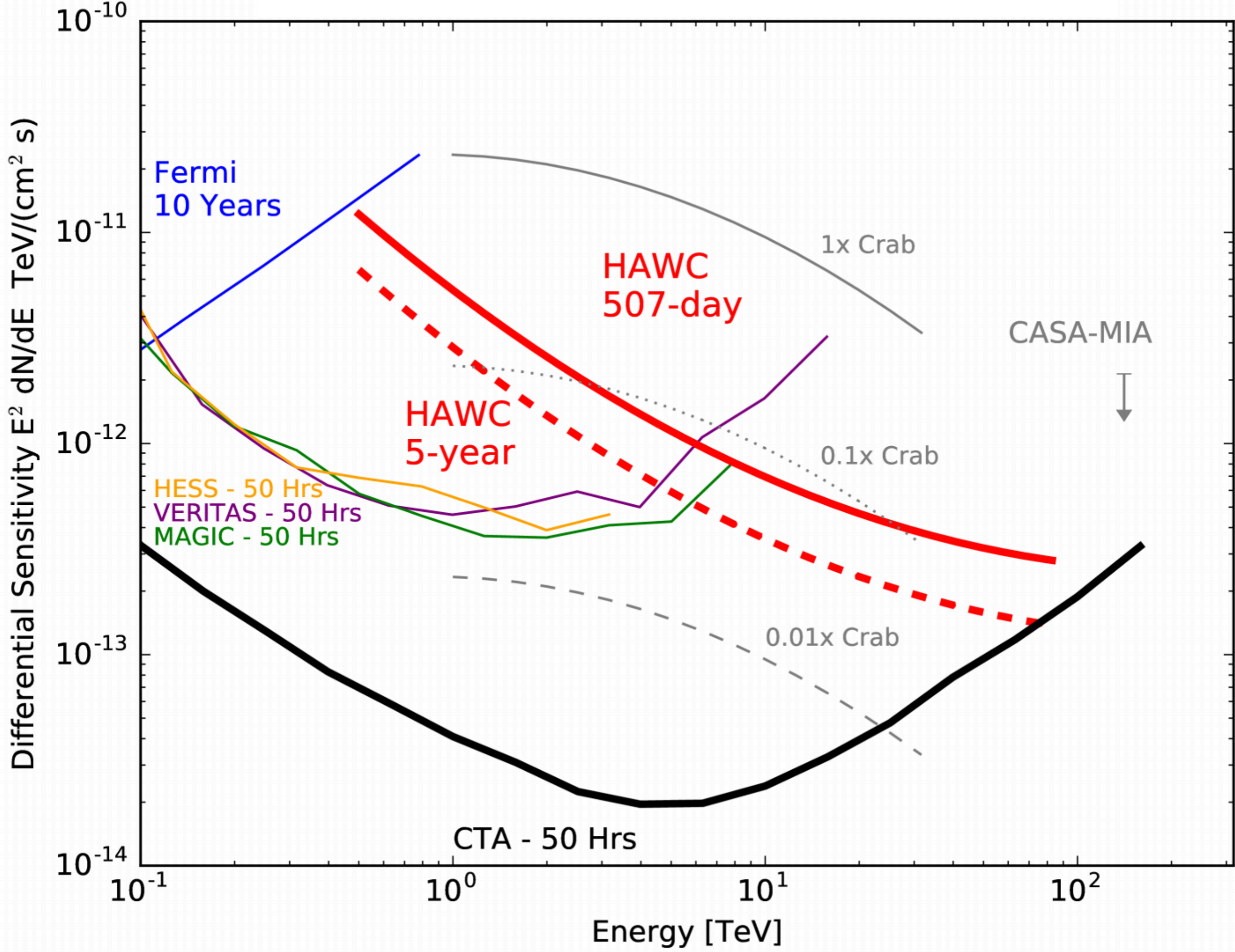
**Assume that pulsars convert an the same fraction of their spindown power to  $e^+e^-$  as Geminga.**

**Assume that the  $e^+e^-$  spectrum is the same as Geminga.**

Table 4 Candidate pulsar wind nebulae from the pre-selection.

HGPS name	ATNF name	$\lg \dot{E}$	$\tau_c$ (kyr)	$d$ (kpc)	PSR offset (pc)	$\Gamma$	$R_{\text{PWN}}$ (pc)	$L_{1-10 \text{ TeV}}$ ( $10^{33} \text{ erg s}^{-1}$ )
J1616–508 (1)	J1617–5055	37.20	8.13	6.82	< 26	$2.34 \pm 0.06$	$28 \pm 4$	$162 \pm 9$
J1023–575	J1023–5746	37.04	4.60	8.00	< 9	$2.36 \pm 0.05$	$23.2 \pm 1.2$	$67 \pm 5$
J1809–193 (1)	J1811–1925	36.81	23.3	5.00	$29 \pm 7$	$2.38 \pm 0.07$	$35 \pm 4$	$53 \pm 3$
J1857+026	J1856+0245	36.66	20.6	9.01	$21 \pm 6$	$2.57 \pm 0.06$	$41 \pm 9$	$118 \pm 13$
J1640–465	J1640–4631 (1)	36.64	3.35	12.8	< 20	$2.55 \pm 0.04$	$25 \pm 8$	$210 \pm 12$
J1641–462	J1640–4631 (2)	36.64	3.35	12.8	$50 \pm 5$	$2.50 \pm 0.11$	< 14	$17 \pm 4$
J1708–443	B1706–44	36.53	17.5	2.60	$17 \pm 3$	$2.17 \pm 0.08$	$12.7 \pm 1.4$	$6.6 \pm 0.9$
J1908+063	J1907+0602	36.45	19.5	3.21	$21 \pm 3$	$2.26 \pm 0.06$	$27.2 \pm 1.5$	$28 \pm 2$
J1018–589A	J1016–5857 (1)	36.41	21.0	8.00	$47.5 \pm 1.6$	$2.24 \pm 0.13$	< 4	$8.1 \pm 1.4$
J1018–589B	J1016–5857 (2)	36.41	21.0	8.00	$25 \pm 7$	$2.20 \pm 0.09$	$21 \pm 4$	$23 \pm 5$
J1804–216	B1800–21	36.34	15.8	4.40	$18 \pm 5$	$2.69 \pm 0.04$	$19 \pm 3$	$42.5 \pm 2.0$
J1809–193 (2)	J1809–1917	36.26	51.3	3.55	< 17	$2.38 \pm 0.07$	$25 \pm 3$	$26.9 \pm 1.5$
J1616–508 (2)	B1610–50	36.20	7.42	7.94	$60 \pm 7$	$2.34 \pm 0.06$	$32 \pm 5$	$220 \pm 12$
J1718–385	J1718–3825	36.11	89.5	3.60	$5.4 \pm 1.6$	$1.77 \pm 0.06$	$7.2 \pm 0.9$	$4.6 \pm 0.8$
J1026–582	J1028–5819	35.92	90.0	2.33	$9 \pm 2$	$1.81 \pm 0.10$	$5.3 \pm 1.6$	$1.7 \pm 0.5$
J1832–085	B1830–08 (1)	35.76	147	4.50	$23.3 \pm 1.5$	$2.38 \pm 0.14$	< 4	$1.7 \pm 0.4$
J1834–087	B1830–08 (2)	35.76	147	4.50	$32.3 \pm 1.9$	$2.61 \pm 0.07$	$17 \pm 3$	$25.8 \pm 2.0$
J1858+020	J1857+0143	35.65	71.0	5.75	$38 \pm 3$	$2.39 \pm 0.12$	$7.9 \pm 1.6$	$7.1 \pm 1.5$
J1745–303	B1742–30 (1)	33.93	546	0.200	$1.42 \pm 0.15$	$2.57 \pm 0.06$	$0.62 \pm 0.07$	$0.014 \pm 0.003$
J1746–308	B1742–30 (2)	33.93	546	0.200	< 1.1	$3.3 \pm 0.2$	$0.56 \pm 0.12$	$0.009 \pm 0.003$

- **HESS systems have a higher spin down power, but are more distant.**



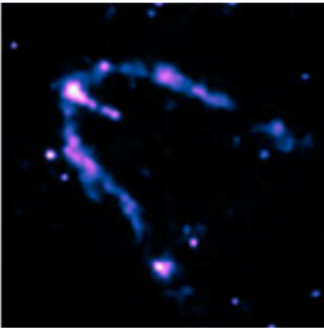


- **The energy loss timescale in the ISM ( $5 \mu\text{G}$ ;  $1 \text{ eV cm}^{-3}$ ) is approximately:**

$$\tau_{\text{loss}} \approx 2 \times 10^4 \text{ yr} \left( \frac{10 \text{ TeV}}{E_e} \right)$$

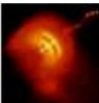
- **In the ISM ( $D_0 = 5 \times 10^{28} \text{ cm}^2\text{s}^{-1}$   $\delta=0.33$ ), this implies a radial extent of  $\sim 250 \text{ pc}$ .**

Geminga / Distance to Earth

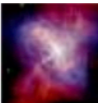


815.4 light years


People also search for



Vela Pulsar  
958.9 light years



Crab Pulsar  
7,175 light years



RX J1856.5-3754  
400 light years

Feedback

Geminga 🔗

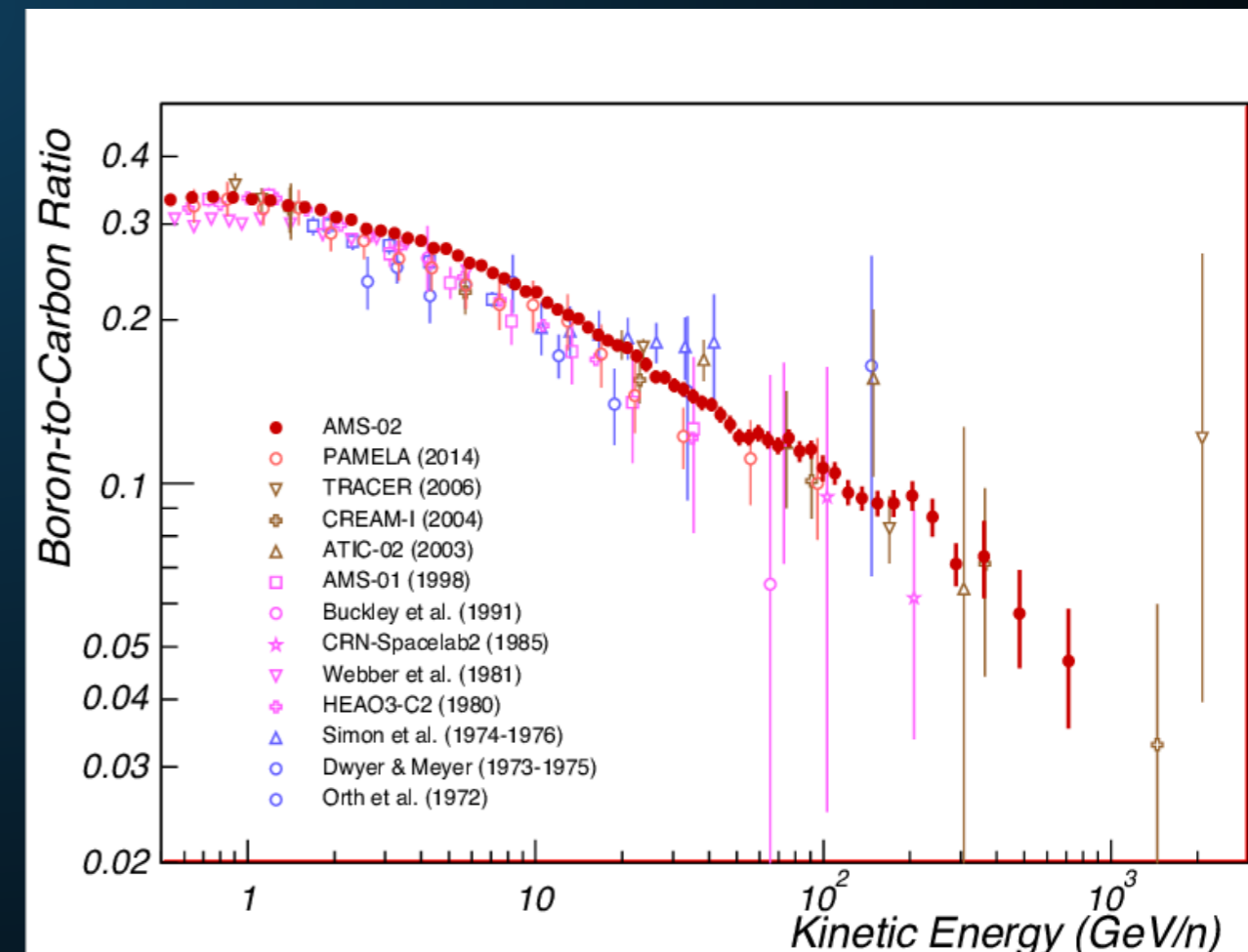
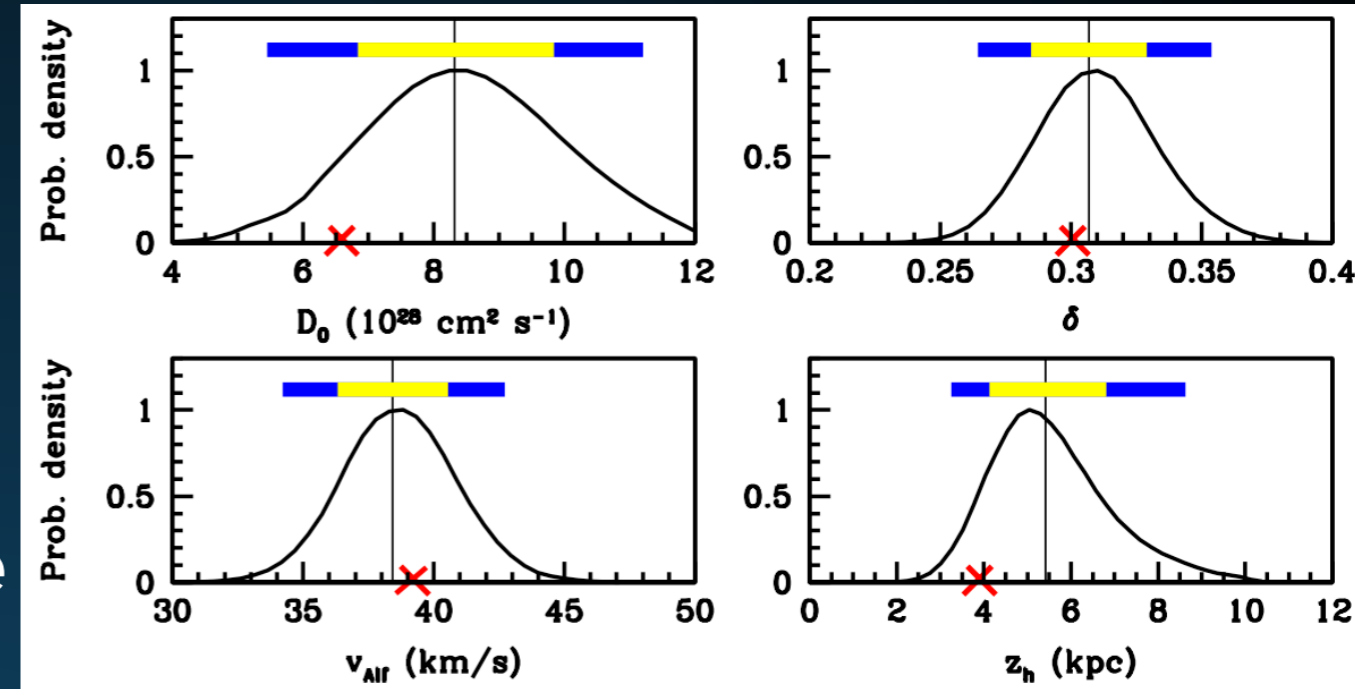
Star

Geminga is a neutron star approximately 250 parsecs from the Sun in the constellation Gemini. Its name, attributed by its discoverer Giovanni Bignami, is both a contraction of Gemini gamma-ray source, and a transcription of the words gh'è minga, meaning "it's not there" in the Milanese dialect of Lombard. [Wikipedia](#)

**Distance to Earth:** 815.4 light years  
**Magnitude:** 25.5  
**Constellation:** Gemini  
**Apparent magnitude (V):** 25.5  
**Right ascension:** 06<sup>h</sup> 33<sup>m</sup> 54.15<sup>s</sup>  
**Declination:** +17° 46' 12.9"

Feedback

- **Cosmic-Ray primary to secondary ratios tell us about:**
  - **The average grammage encountered by cosmic-rays before they escape the galaxy (e.g. B/C)**
  - **The average time cosmic-rays propagate before they escape (eg.  $^{10}\text{Be}/^9\text{Be}$ ).**

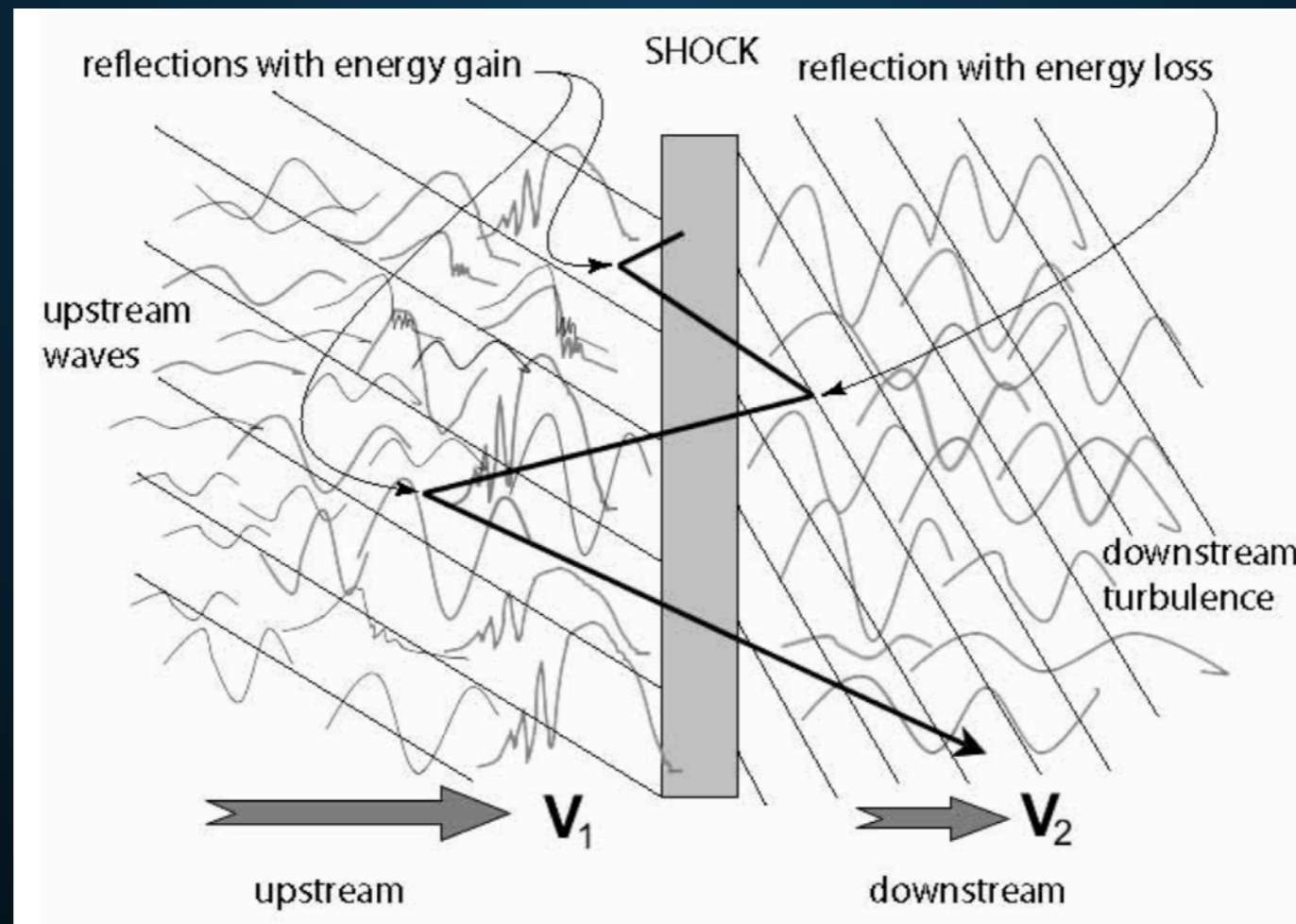


# COSMIC-RAY ACCELERATION AND PROPAGATION



Start with a source of relativistic cosmic-rays

- **Supernova Explosions**
- **Supernova Remnants**
- **Shocks/Mergers**





# TeV HALOS - AN EMPIRICAL MODEL

$$\phi_{\text{TeV halo}} = \left( \frac{\dot{E}_{\text{psr}}}{\dot{E}_{\text{Geminga}}} \right) \left( \frac{d_{\text{Geminga}}^2}{d_{\text{psr}}^2} \right) \phi_{\text{Geminga}}$$

$$\theta_{\text{TeV halo}} = \left( \frac{d_{\text{Geminga}}}{d_{\text{psr}}} \right) \theta_{\text{Geminga}}$$

Name	Tested radius	Index	$F_7 \times 10^{15}$	TeVCat
	[°]		[TeV <sup>-1</sup> cm <sup>-2</sup> s <sup>-1</sup> ]	
2HWC J0631+169	-	-2.57 ± 0.15	6.7 ± 1.5	Geminga
"	2.0	-2.23 ± 0.08	48.7 ± 6.9	Geminga
2HWC J0635+180	-	-2.56 ± 0.16	6.5 ± 1.5	Geminga

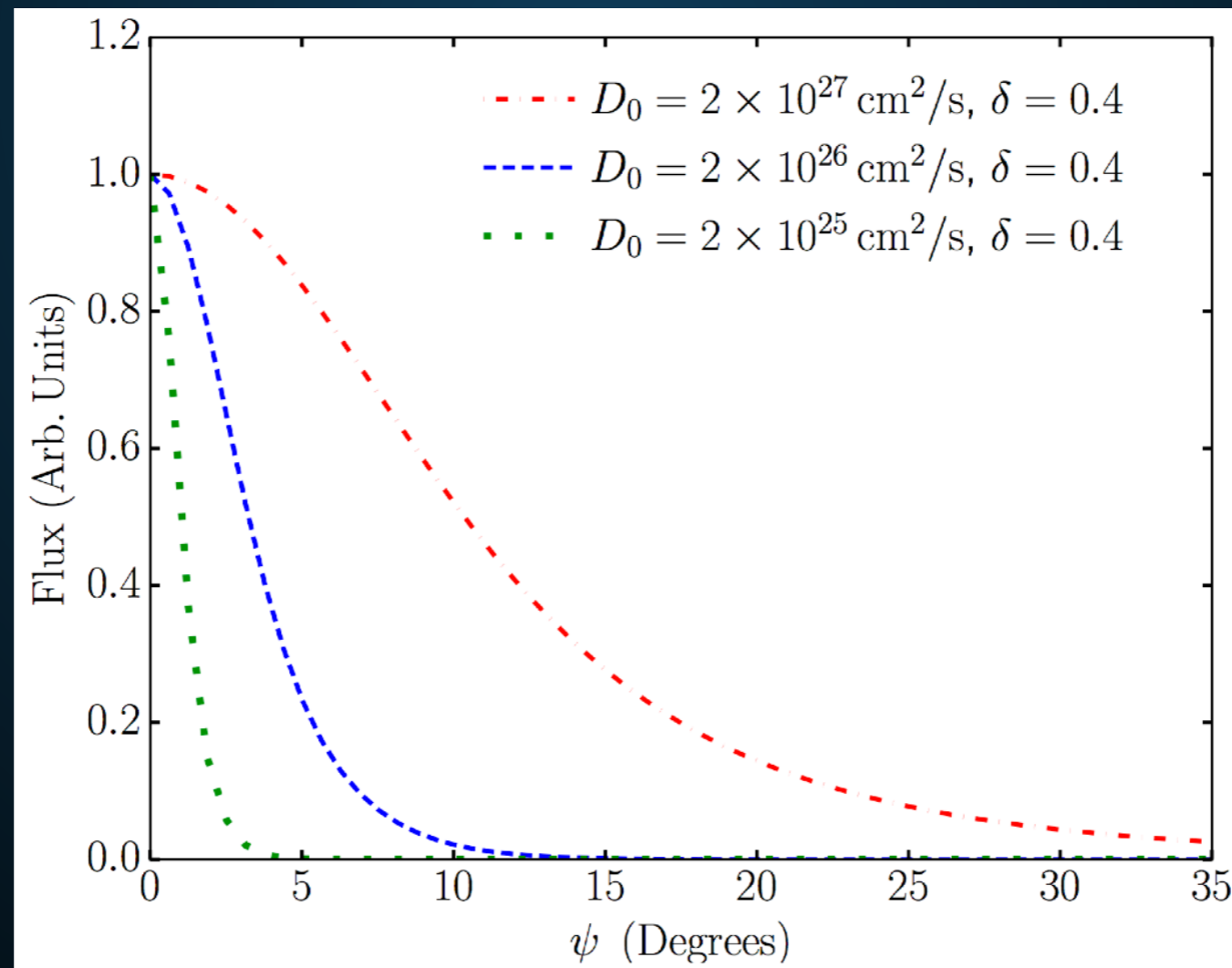
- **Assume that every pulsar converts an equivalent fraction of its spin down power into gamma-rays, with the same spectrum as Geminga.**

**Note: Using Monogem would increase fluxes by nearly a factor of 2.**

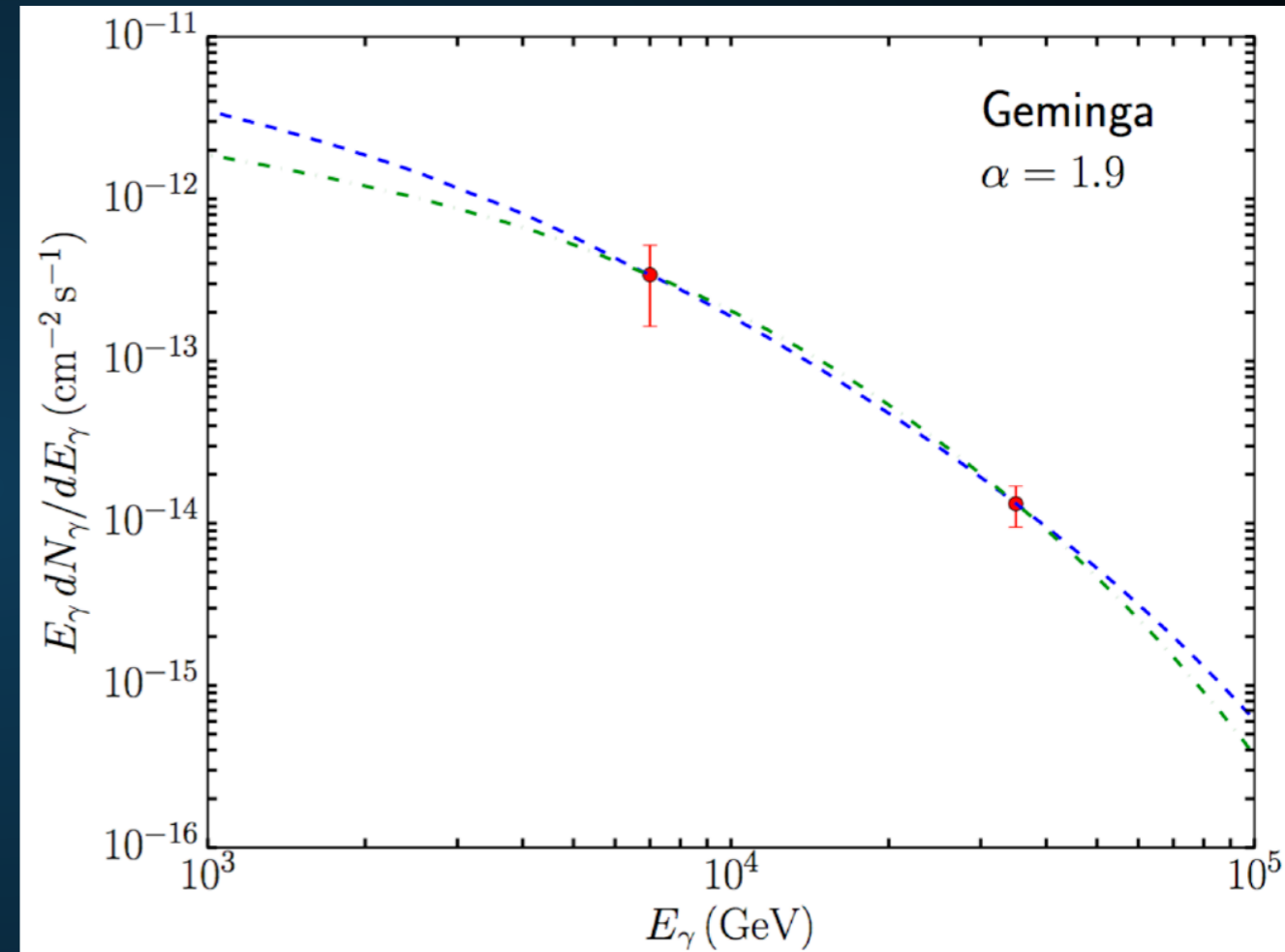
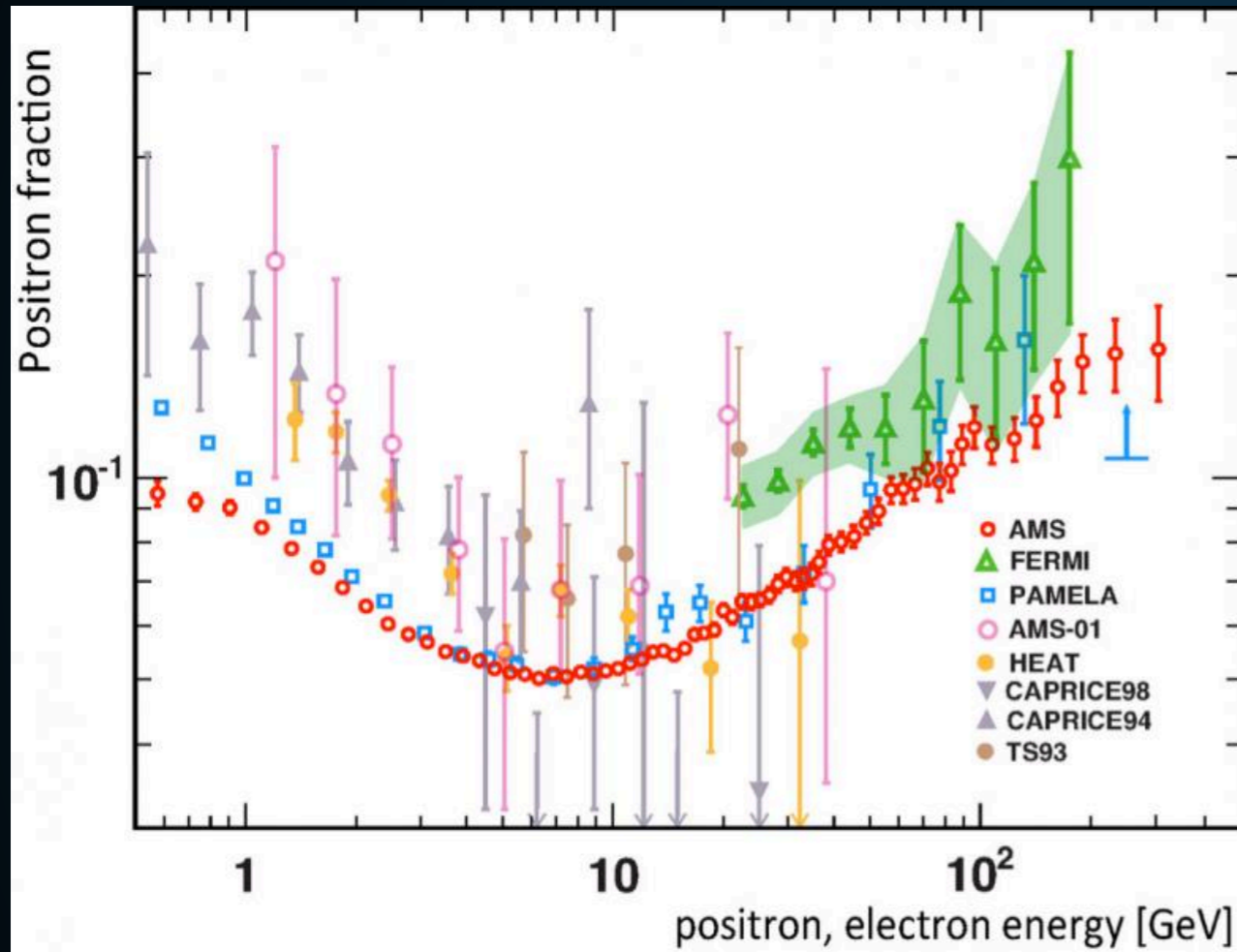
- The energy loss timescale in the ISM ( $5 \mu\text{G}$ ;  $1 \text{ eV cm}^{-3}$ ) is:

$$\tau_{\text{loss}} \approx 2 \times 10^4 \text{ yr} \left( \frac{10 \text{ TeV}}{E_e} \right)$$

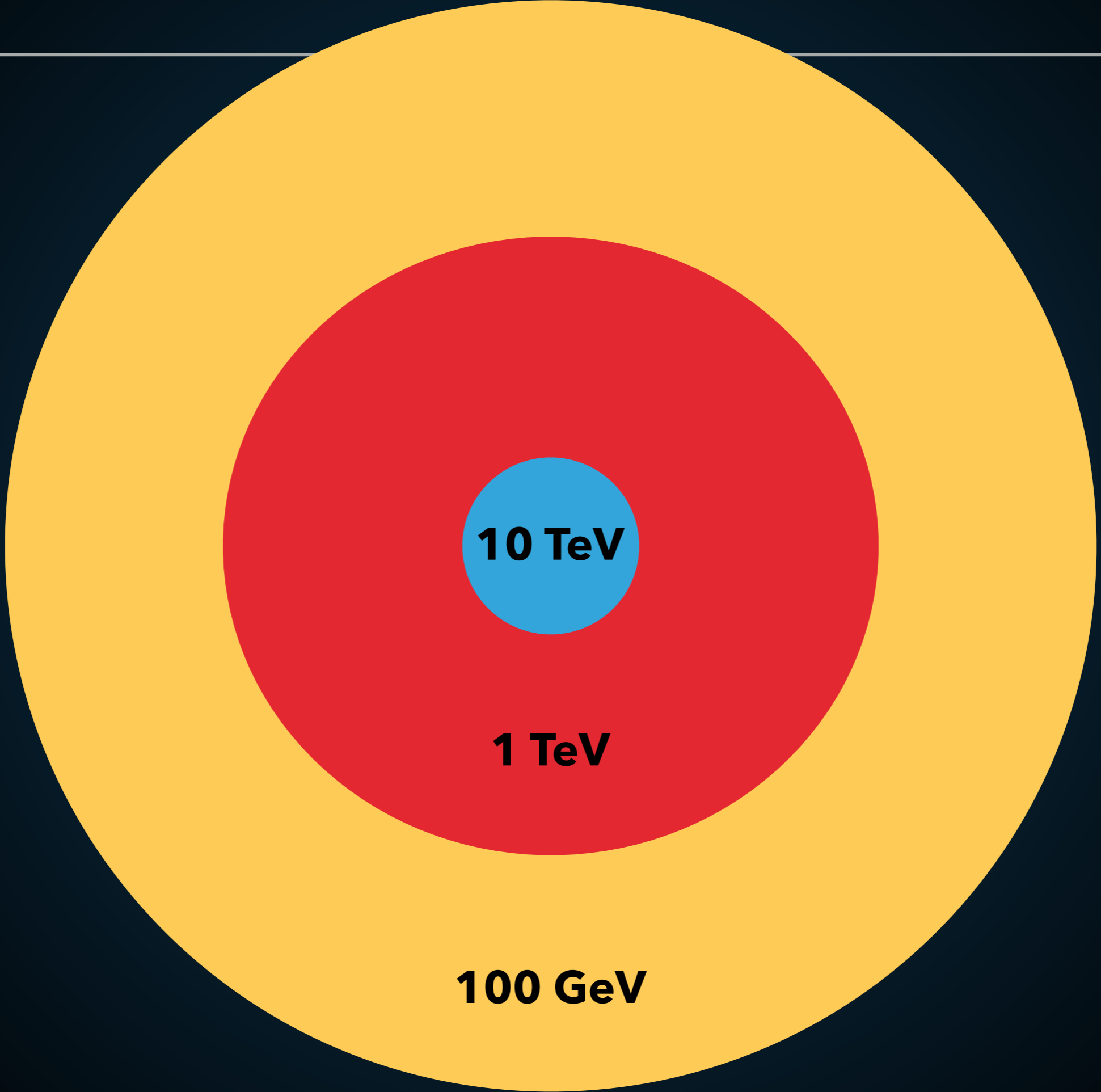
- Can calculate the profile for different diffusion constants:



# LOW-ENERGY COSMIC-RAY DIFFUSION







**10 TeV**

**1 TeV**

**100 GeV**